

Washington University in St. Louis
Washington University Open Scholarship

All Theses and Dissertations (ETDs)

1-1-2012

Taspase1 is a Non-oncogene Mediator of Tumorigenesis and Maintenance

David Chen

Washington University in St. Louis

Follow this and additional works at: <https://openscholarship.wustl.edu/etd>

Recommended Citation

Chen, David, "Taspase1 is a Non-oncogene Mediator of Tumorigenesis and Maintenance" (2012). *All Theses and Dissertations (ETDs)*. 563.

<https://openscholarship.wustl.edu/etd/563>

This Dissertation is brought to you for free and open access by Washington University Open Scholarship. It has been accepted for inclusion in All Theses and Dissertations (ETDs) by an authorized administrator of Washington University Open Scholarship. For more information, please contact digital@wumail.wustl.edu.

WASHINGTON UNIVERSITY IN ST. LOUIS

Division of Biology and Biomedical Sciences

Molecular Cell Biology

Dissertation Examination Committee:

James Hsieh, Chair

Emily Cheng

Stuart Kornfeld

Gerry Linette

Daniel Link

David Piwnica-Worms

Taspase1 is a Non-oncogene Mediator of Tumorigenesis and Maintenance

by

David Yuan-Sou Chen

A dissertation presented to the
Graduate School of Arts and Sciences
of Washington University in
partial fulfillment of the
requirements for the degree
of Doctor of Philosophy

May 2012

Saint Louis, Missouri

ABSTRACT OF THE DISSERTATION

Taspase1 is a non-oncogene mediator of tumorigenesis and maintenance

by

David Yuan-Sou Chen

Doctor of Philosophy in Biology and Biomedical Sciences

Molecular Cell Biology

Washington University in St. Louis, 2012

Asst. Professor James Hsieh, Chairperson

The clinical success of oncogene-targeted therapies substantiates the continued reliance of certain cancers upon the continued function of apical oncogenes involved in its genesis—a phenomenon known as “oncogene addiction.” Though this shift from non-targeted, cytotoxic therapies offers new hope to patients, resistance to oncogene inactivation often remains an eventuality, and it is clear that further investigation is required to more effectively battle cancer using alternative therapeutic targets. Our studies on Taspase1 (threonine aspartase 1) reveal its role in coordinating cellular proliferation and apoptosis in cancer. Loss of Taspase1 by shRNA-mediated knockdown decreased cellular proliferation in a diverse set of cancer cell lines, including glioblastoma, melanoma, lung, breast, colon, and prostate, as well as increased sensitivity to death stimuli in melanoma and glioblastoma. Taspase1 loss impedes proliferation via up-regulation of the Cyclin dependent kinase inhibitor p27 and destabilizes the anti-apoptotic BCL-2 family member MCL-1. Decreased levels of MCL-1 in glioblastoma and melanoma due to Taspase1 loss sensitizes these cells to a variety of apoptotic stimuli, including anoikis, DNA damaging agents etoposide and doxorubicin, and to a targeted inhibitor of BCL-2 family proteins, ABT-737. We found that Taspase1 is over-expressed in multiple primary human tumors, including glioblastoma and melanoma, suggesting that Taspase1 is relevant to tumorigenesis in humans and that its inhibition could be clinically useful.

In vitro examination of tumorigenic clones selected by their ability to form colonies in soft agar revealed an increase in Taspase1 expression compared to the unselected pool of MEFs

transduced by defined oncogenes, suggesting an increased reliance on Taspase1 in the process of tumorigenic transformation. Yet, we demonstrate that Taspase1 is not an oncogene, and therefore, Taspase1 better fits a new class of cancer targets—the subordinate cellular machinery of oncogene-driven processes. Dependence on this machinery was recently termed “non-oncogene addiction.” Taspase1 loss can sensitize cancer cells to both cytotoxic agents as well as oncogene-targeted agents, suggesting that inhibition of the non-oncogene addiction protease Taspase1 can complement traditional therapies.

Through high throughput screening, we have identified a noncompetitive, small molecule inhibitor of Taspase1, named TASPIN-1, which inhibits Taspase1 in vitro and in cell culture. Murine fibroblasts treated with TASPIN-1 exhibit decreased proliferative capacity, while also demonstrating molecular characteristics similar to those observed with the acute, genetic loss of Taspase1. TASPIN-1 treatment exerts specific cytotoxicity in human breast cancer and glioblastoma cells that have high expression of Taspase1. Additionally, TASPIN-1 treated mice bearing U251 human glioblastoma xenografts exhibit tumor regression while the mice tolerated short term treatment relatively well. This suggests that pharmacological inhibition of Taspase1 is of potential therapeutic benefit in the treatment of cancer patients.

ACKNOWLEDGEMENTS

I would like to express my greatest thanks and appreciation to my thesis advisor James Hsieh for his advice and support over the years and for all the effort spent in preparing me for what is to come. His is an example from which I hope to continue learning. I would also like to thank the great scientists on my thesis committee—Stuart Kornfeld, Emily Cheng, Gerry Linette, Dan Link, and David Piwnica-Worms—who continually challenged me to view problems from different perspectives, for always being critical but encouraging, and for being generous with their time and advice. In particular, I would like to thank Emily Cheng for her guidance on the cell death aspects of my project.

Our work relies on the gracious help of our collaborators, including Matthew Bogyo and colleagues of Stanford University for their work on peptide inhibitors of Taspase1, Bob Shoemaker and the NCI Developmental Therapeutics Program for their work with small molecule high throughput screening, and David Piwnica-Worms and colleagues for their advice and help with bioluminescence imaging. I would like to thank them and all of the support staff with whom I worked. Special thanks to the Medical Scientist Program at Washington University for their tremendous administrative and financial support—the Program is responsible for making Washington University an exceptional environment for physician-scientist training. Thanks also to the Hematology departmental training grant as well as the ACS and NCI for their financial support through my thesis advisor.

I appreciate the collegiality of the members of the Hsieh and Cheng labs, including Han Liu for his help with MCL-1 degradation studies, Shugaku Takeda for generating cDNA for qRT-PCR studies, and Todd Westergard teaching me how to work with mice. My friends and colleagues in the lab have buoyed me through the years, often in the form of late-night dinners and coffee breaks. I am grateful that Hyungjin Kim, Ho-Chou Tu, and Shugaku Takeda have been part of my lab family from day one. Their support, as well as from Brian Van Tine, Gary Wang, Greg

Bean, and Todd Westergard, was indispensable to finishing this work. Finally, I would like to thank my parents James and Claire, my sister Connie, my partner Patricia, and all of my friends for their enduring encouragement, good humor, and faith in hard work. They are the anchor in my life.

TABLE OF CONTENTS

Abstract	ii
Acknowledgements	iv
List of figures and tables	viii
Chapter 1: Oncogenes, Tumor Suppression, and Taspase1	
1.1 Cancer is a balance between oncogene signaling and suppressed tumor suppression...	2
1.2 Addiction to oncogene signaling pathways	8
1.3 Taspase1 is an evolutionarily conserved threonine protease required for proper embryonic development and execution of the cell cycle	12
Chapter 2: Taspase1 is a non-oncogene addiction protease that coordinates cancer cell proliferation and apoptosis	
2.1 Introduction	19
2.2 Taspase1 is required for tumor maintenance in vitro	22
2.3 Taspase1 is not an oncogene	23
2.4 Taspase1 is required for inhibition of human cancer cell proliferation	23
2.5 Requirement for Taspase1 in anoikis resistance	25
2.6 Taspase1 deficiency results in decreased MCL-1 level and increased sensitivity to chemotherapeutic agents and ABT-737	25
2.7 Taspase1 regulates the protein half-life of MCL-1	27
2.8 Taspase1 is over-expressed in primary human GBM and melanoma tissues and its deficiency disrupts tumor growth in a xenograft model	28
2.9 Discussion	29
2.10 Methods and materials	33
2.11 Figures	38

Chapter 3: Taspase1 inhibitors: rational design and small molecule high throughput screening	
3.1 Taspase1 is an evolutionarily conserved threonine protease important in tumorigenesis and tumor maintenance	57
3.2 Rational design of peptidomimetic inhibitors for Taspase1	59
3.3 A cell based dual-fluorescence reporter screen identifies NSC48300/TASPIN-1 as a potent inhibitor of Taspase1 in vitro and in vivo	63
3.4 FRET-based screening reveals further leads for Taspase1 inhibitors	71
3.5 Methods and materials	72
3.6 Figures	75
Chapter 4: Therapeutic implications of Taspase1 non-oncogene addiction and proposed future studies	
4.1 Future directions: in vitro studies	94
4.2 Future directions: in vivo studies	101
4.3 Therapeutic implications of non-oncogene addiction and Taspase1 inhibition	106
4.4 Figures	111
References	120
Curriculum Vitae	132

LIST OF FIGURES AND TABLES

Chapter 1

Figure	1	Taspase1 regulates the cell cycle through proteolysis of its substrate MLL	18
--------	---	--	----

Chapter 2

Figure	2.1	Taspase1 is required for the maintenance of MYC-RAS ^{G12V} transformed mouse embryonic fibroblasts (MEFs)	38
Figure	2.2	Taspase1 is not a classical oncogene	39
Figure	2.3	Taspase1 is required for the proliferation of human cancer cells	40
Figure	2.4	Deficiency of Taspase1 results in increased anoikis and reversion of the transformed phenotype in SK-MEL-2 melanoma and U251 glioblastoma cells	41
Figure	2.5	Taspase1 deficiency de-stabilizes MCL-1 protein and sensitizes U251 glioblastoma cells to cell death stimuli	42
Figure	2.6	Taspase1 is over-expressed in human glioblastoma and is required for for U251 glioblastoma maintenance in vivo	43
Figure	2.7	Taspase1 over-expression in NIH/3T3 and primary MEFs	44
Figure	2.8	Taspase1 loss using two, independent sh-RNAs impedes proliferation in SK-MEL-2 and U251	45
Figure	2.9	Cell cycle analysis of human cancer cell lines with Taspase1 deficiency	46
Figure	2.10	Analysis of p27 ^{KIP1} regulation in U251 with Taspase1 deficiency	47
Figure	2.11	Models for the core apoptotic pathway and its interaction with Taspase1	48
Figure	2.12	Analysis of SK-MEL-2 sensitivity to cell death with Taspase1 deficiency	49
Figure	2.13	MCL-1 level is not stabilized by GSK3-β inhibition in Taspase1-deficient cells	50
Figure	2.14	Taspase1 levels in U251 glioblastoma xenografts	51
Figure	2.15	Examination of Taspase1 expression in human glioblastoma	52
Figure	2.16	Demonstration of the specificity of Taspase1 immunohistochemistry	53
Figure	2.17	Examination of Taspase1 expression in melanoma	54
Table	2.1	Mutation status of sequenced genes in the NCI60 cancer cell lines used in this study	55

Chapter 3

Figure	3.1	Structural characteristics of Taspase1 and its substrates	75
Figure	3.2	Assessing Taspase1 inhibition I—the in vitro cleavage assay	76
Figure	3.3	Assessing Taspase1 inhibition II—the cell-based screening assay	77
Figure	3.4	Assessing Taspase1 inhibition III—the FRET based kinetics assay	78
Figure	3.5	HTI-9 is a competitive inhibitor of Taspase1 and cooperates with non-competitive inhibitor NSC48300/TASPIN-1	79
Figure	3.6	Proof of principle in rational design of peptide inhibitors of Taspase1	80
Figure	3.7	The vinyl sulfone yzm18 is a reversible inhibitor of Taspase1	81
Figure	3.8	The vinyl sulfone yzm18 is not a potent inhibitor of Taspase1 in vivo	82

Figure 3.9	An in vitro screen identifies NSC48300/TASPIN-1 as a potent bioactive inhibitor of Taspase1	83
Figure 3.10	Structural features of TASPIN-1 define its Taspase1 inhibitory activity	84
Figure 3.11	NSC48300/TASPIN-1 is a non-competitive inhibitor of Taspase1	85
Figure 3.12	Molecular consequences of genetic loss of Taspase1	86
Figure 3.13	TASPIN-1 treatment recapitulates the Taspase1-null phenotype	87
Figure 3.14	TASPIN-1 sensitivity is correlated with relative Taspase1 expression level in breast cancer cell lines	88
Figure 3.15	TASPIN-1 sensitivity is correlated with relative Taspase1 expression level in brain cancer cell lines	89
Figure 3.16	Breast cancer cell lines expressing higher Taspase1 are more sensitive to Taspase1 loss.	90
Figure 3.17	Glioblastoma xenografts respond to TASPIN-1 treatment in vivo	91
Figure 3.18	Tyrphostins are potent inhibitors of Taspase1 in vitro	92
Chapter 4		
Figure 4.1	Taspase1 coordinates proliferation and apoptosis through its regulation of Cyclin-dependent kinase inhibitors (CDKIs), Cyclins, and MCL-1	111
Figure 4.2	Primary MEFs are not sensitized to cell with Taspase1 deficiency	112
Figure 4.3	Transformed clones up-regulate Taspase1 expression	113
Figure 4.4	Taspase1 expression is up-regulated in subsets of blood tumors	114
Figure 4.5	Taspase1 is over-expressed in human breast cancer	115
Figure 4.6	Taspase1 is over-expressed in human colon cancer	116
Figure 4.7	Taspase1 is highly expressed in human melanoma	117
Figure 4.8	A murine model for Taspase1-dependence in CML blast crisis	118
Table 4.1	Promoter analysis pipeline analysis of the Taspase1 promoter	119

Chapter 1

Oncogenesis, tumor suppression, and Taspase1

- 1.1 Cancer is a balance between oncogene signaling and suppressed tumor suppression
- 1.2 Addiction to oncogene signaling pathways in cancer
- 1.3 Taspase1 is an evolutionarily conserved threonine protease required for proper embryonic development and cellular proliferation

1.1 Cancer is a balance between oncogene signaling and suppressed tumor suppression

Cancer phenotypes codified

Cancer is a phenotypic manifestation of genetic and epigenetic alterations that are adaptive for the cell but maladaptive, ultimately, for the host. Cellular alterations that give rise to cancer are multitudinous, particularly between cancers of different tissue origins but also within the same cancer subtype. Despite the diversity of molecular alterations, the phenotypic expression of malignancy has been codified into discrete hallmarks, including the ability to propagate independent of growth factor signaling, resistance against cell death, limitless replicative potential, insensitivity to growth-inhibitory signals, sustained angiogenesis, and metastasis (Hanahan and Weinberg, 2000). It seems, then, that the common goal of these traits, whether intrinsic to the cancer cell or extrinsic, lies in support for the continued potential for deregulated growth and survival of cancer, except in metastasis. Though successful metastasis—from migration from the primary tumor to intravasation and survival in the blood, extravasation, and survival in the end organ—is not of *prima facie* benefit to the malignant cell, the fact is that at terminal stage, cancers typically exhibit metastatic character. One might hypothesize, then, that the ability to metastasize is merely an incidental manifestation of alterations that were selected for on the basis that they are critical to tumor growth. Recent evidence suggests that this is indeed the case in breast cell lines which depend on a set of genes to support tumor growth as well as vascular remodeling (Gupta et al., 2007). It is increasingly clear that the common theme to these phenotypic hallmarks of cancer, then, is the molecular alterations that underlie them. These alterations are typically classified in two groups—genetic or epigenetic changes in certain genes drive various aspects of oncogenic processes, while the loss or alteration of function of other genes required for cellular homeostasis facilitates the oncogenic transformation processes. These genes are known as oncogenes and tumor suppressors, respectively, and they are of critical importance to tumorigenesis and tumor maintenance. Yet, this body of work demonstrates that Taspase1, which is not an oncogene, is also of critical importance to tumor maintenance.

Experimental determination of oncogenic potential

The genetic origins of cancer had been postulated by Theodore Boveri in conclusions drawn from his work on sea urchins:

A malignant tumor cell is—and here again I take up the ideas of Hansemann—a cell with a specific abnormal chromosome constitution. (Harris, 2008)

And of proto-oncogenes:

However, the hypothesis that there are chromosomes that stimulate cell multiplication is also compatible with our proposal. In this view, cell division would take place when the operation of the stimulatory region of the chromatin, normally too weak, is enhanced by some active agent. The unrestrained proliferation of malignant tumour cells would then be due to a permanent excess of these stimulatory chromosomes. (Harris, 2008)

Though these ideas were introduced in 1914, they had remarkable bearing on the ensuing discovery of oncogenes, illuminated by much work done in retroviral oncogenesis, which was subsequently extended to cellular oncogenes (Bishop, 1983). Many other oncogenes were identified through a combination of retroviral insertional mutagenesis as well as transfection of tumor-derived DNA into the immortalized murine fibroblast line NIH/3T3. This, notably, led to the discovery of the human *RAS* oncogene from bladder cancer (Shih and Weinberg, 1982), formally linking the previous retroviral oncogene work with the establishment of human cellular oncogenes (Der et al., 1982; Parada et al., 1982; Santos et al., 1982). The importance of oncogenic *RAS* was substantiated by later findings that human tumors bear *RAS* mutations primarily in codons 12, 13, or 61, rendering its GTPase ability constitutively active. *RAS* was found to be mutated in a wide spectrum of cancers, with the highest frequency in exocrine pancreas (80% bear *KRAS* mutations), though many other tumor types also exhibit a high frequency of *RAS* mutation,

including lung, colon, and thyroid adenocarcinoma, as well as NRAS mutations in myeloid leukemias (Bos, 1989).

RAS was found to be regulated by upstream factors like receptor tyrosine kinases, which are known to be oncogenes as well, including the epidermal growth factor receptor (Kamata and Feramisco, 1984; Mulcahy et al., 1985) and the related HER2/neu. Both receptors were defined as oncogenes by their ability to cause morphological transformation of NIH/3T3 cells as well as their ability to confer anchorage independent growth to these cells in soft agar assays and tumor formation when allografted in immunodeficient mice (Di Fiore et al., 1987; Hudziak et al., 1987; Velu et al., 1987) . In these studies, soft agar growth correlated well with tumor formation upon injection into mice likely because soft agar growth reflects many of the growth and survival advantages acquired in the transformation process. This includes the ability to survive independently of signals provided by ligation of homotypic and heterotypic adhesion receptors, without which typically initiates a physiological death stimulus known as anoikis (Frisch and Francis, 1994). Such a strong correlation—that soft agar growth always correlates with in vivo tumor growth—from a seemingly simple assay belies the complexity of oncogene signaling and the transformed phenotype. Indeed, RAS provides signals to regulate cellular proliferation, death and survival, protein translation, and cellular motility through its multiple effector pathways RAF, RAL-GDS and PI3K (Downward, 2003; Malumbres and Barbacid, 2003).

Despite the complexity of RAS signaling alone and the current knowledge that upstream growth factor signals regulate more proto-oncogenes than just RAS (for example, the phosphatidylinositol-3-kinase, PI3K, proto-oncogene), it has been shown that activated RAS alone cannot transform primary murine fibroblasts. Rather, at least two oncogenic changes are necessary for murine transformation. Additionally, these alterations must be complementary (Land et al., 1983), as RAS alone can interact with other oncogenic pathways, including the direct activation of the PI3K pathway (Rodriguez-Viciano et al., 1994; Sjolander et al., 1991).

RAS and MYC comprise one such pair of complementary oncogenes (Land et al., 1983). MYC is a strongly mitogenic oncogene and has a very short half-life, while co-expression of activated RAS can stabilize MYC levels. This results in MAPK dependent phosphorylation of MYC and subsequent E2F2-mediated transcription and Cyclin E/cdk2 activation, which leads ultimately to S-phase entry (Leone et al., 1997; Sears et al., 1999; Sears et al., 2000). Cooperation between MYC and RAS, however, extends beyond stabilization of MYC and enhanced proliferation driven by oncogenic RAS and MYC.

Oncogenes elicit tumor suppressive signals

Three key barriers to tumorigenesis are irreversible growth arrest (senescence), cell death, and differentiation. Deregulation of proto-oncogenes like MYC and RAS enhance the tumorigenic capabilities of the nascent cancer cell; however, tumor suppressive mechanisms can counteract aberrant, oncogenic signals. Ectopic expression of either MYC or activated RAS alone is not only unable to transform primary murine cells, the overwhelming oncogenic signaling is actually deleterious to cells. RAS over-expression induces p53 and p16^{INK4A} tumor suppressor expression and cellular senescence in vitro, and BRAF^{E600} expression in melanocytes induces senescence in vivo, as seen in growth-arrested benign nevi from patients (Michaloglou et al., 2005; Serrano et al., 1997). The degree to which tumor suppression is elicited seems to be dose-dependent. Increased MAPK/ERK signaling through RAF activation induces cell cycle arrest that depends on the expression of the Cyclin-dependent kinase inhibitor (CDKI) p21^{CIP1} (Woods et al., 1997). Titration of oncogenic RAS from a mammary specific promoter reveals that high levels of RAS signaling in vivo results in transient increases in proliferation in breast epithelium with an ensuing senescence that is dependent on the *INK4A/ARF* locus. Low level RAS signaling can escape p53 activation as well as activation of *INK4A/ARF* locus, while maintaining enhanced proliferation. Tumors formed by low-level RAS activation exhibited additional up-regulation of endogenous RAS as well as evasion of tumor suppressive signals, with p53 loss of heterozygosity and failure of *INK4A/ARF* induction (Sarkisian et al., 2007).

MYC expression, in normal cell cycle, is very tightly regulated as quiescent cells have undetectable MYC expression; however, upon mitogenic stimuli, MYC is transcribed and can promote S-phase entry by a variety of mechanisms, including directly activating Cyclin D2 and CDK4, activating CyclinE/ckd2, indirectly down-regulating p27^{KIP1}, and directly down-regulating p21^{CIP1} and p15^{INK4B} (Pelengaris et al., 2002a). Supraphysiological expression of MYC, however, is a potent inducer of apoptosis (Evan et al., 1992)—an effect which relies on the activation of the p53 pathway through p19^{ARF}-mediated stabilization, or the induction of pro-apoptotic BH3-only molecule BIM (Adhikary and Eilers, 2005). Deregulation of the p53 pathway, or mutation of residues in MYC that are required for BIM induction, facilitate MYC-induced lymphomagenesis (Eischen et al., 1999; Hemann et al., 2005). Expression of anti-apoptotic BCL-2 family members counteracts MYC-induced apoptosis in vitro and facilitates tumorigenesis in vivo (Beverly and Varmus, 2009; Fanidi et al., 1992; Pelengaris et al., 2002b).

Together, evasion of homeostatic tumor suppressor mechanisms as well as promotion of tumorigenic signaling is likely to form the basis for the cooperation of oncogenes in oncogene complementation or with tumor suppressor inactivation. Though RAS can serve to prevent apoptosis initiated by MYC over-expression through activation of PI3K/AKT (Kauffmann-Zeh et al., 1997), in the context of Cyclin D1, D2, and D3 triple deficiency, MYC and RAS are not able to efficiently complement each other, presumably because an important pro-mitogenic arm is lost. This suggests that prevention of apoptosis alone is not sufficient to generate tumors and highlights the necessary function of cooperating oncogenes to both disarm tumor suppressors as well as provide proliferative signals (Kozar et al., 2004).

Oncogene-induced tumor suppressive mechanisms, like apoptosis and senescence, act as a barrier for tumor evolution because these endpoints are achievable through the same oncogenic signals that drive tumorigenesis, depending on the context in which they occur (Lowe et al., 2004). Though there was little question whether apoptosis was a tumor suppressive mechanism, senescence was only more recently established as a *bona fide* antitumor mechanism in vivo

(Braig et al., 2005; Chen et al., 2005b; Michaloglou et al., 2005). That efficient tumorigenesis from oncogenes requires complementary deactivation of tumor suppressive pathways illuminates the intrinsic failsafe mechanisms that have evolved in multi-cellular organisms to maintain homeostasis. Indeed, it is these intrinsic failsafe mechanisms that we are attempting to engage when treating cancer.

Revealing the complexity of cancer

The scope of mutations characterized in cancers is rapidly increasing as we overcome technological hurdles. Massive sequencing projects have recently identified many mutations in various cancers. Exonic sequencing in lung cancer revealed more than 1,000 somatic mutations across 623 genes, with 26 occurring at high frequency (Ding et al., 2008). Subsequent efforts to look globally at mutations encompassed the entire genome in samples from patients with leukemia as well as in human cancer cell lines. This has led to some interesting insights regarding the number of total mutations in cancer cells as well as how many are intragenic versus intergenic (Ding et al., 2010; Jones et al., 2008; Ley et al., 2008; Parsons et al., 2008; Pleasance et al., 2010a; Pleasance et al., 2010b). In the sequencing of cytogenetically normal M1 AML (~10% of all cases of AML), the number of mutations in gene coding regions that were non-synonymous and unique to the tumor was surprisingly few—10 mutations, of which the majority of genes had no described function in AML pathogenesis. Furthermore, not all of the mutated genes were detectably expressed in the tumor (Ley et al., 2008). However, the total tumor-specific single nucleotide variants (SNVs) in intergenic sequences was on the order of tens of thousands, and using normal skin as a control renders germline predisposition mutations virtually undetectable. Though studying the gene-coding mutations is likely to have the highest yield in the short term, these studies highlight the intricacy of how one determines which mutations drive oncogenesis and which ones are incidental; in short, it is possible that nongenic mutations play a critical role in tumorigenesis. These issues will likely be addressed as sequencing and analysis technologies advance, and when all mutations in all tumors can be catalogued.

With this unprecedented detail in resolving genetic mutations in cancer, it is increasingly clear that key drivers are still few within a tumor, at least those involved in gene coding regions, though the variety of possible drivers may be large between tumor types. Based on age and incidence statistics, it is estimated that common adenocarcinomas, including breast, colon, and prostate, require 5-7 rate limiting events, while hematological malignancies may require fewer changes (Stratton et al., 2009). Indeed, knowledge of oncogene and tumor suppressive functions has made it possible to rationally generate tumors with a minimal set of defined oncogenes in human cells (Hahn et al., 1999; Hahn and Weinberg, 2002). Concordantly, recent mutational analysis of gliomas suggests that three critical signaling pathways are typically altered in brain cancers, including receptor tyrosine kinases (RTKs) and the p53 and Rb tumor suppressor pathways (Network, 2008). With the implication that relatively few pathways are deregulated in each cancer type, and hence dependence on these limited pathways for the maintenance of tumor phenotypes, it seems that targeting one or a few of these pathways would be an effective way to kill cancers.

1.2 Addiction to oncogene signaling pathways in cancer

Persistent oncogenic signaling is required for maintenance of tumor phenotypes

The initial discovery of oncogenes spurred a wave of continued discovery of important factors involved in the initiation of tumorigenesis. The prescient words of J. Michael Bishop indicated that

...cellular oncogenes are involved in tumorigenesis, whatever its proximal cause.

Some of these genes may serve to initiate the genesis of tumors, some to sustain the final neoplastic phenotype, some may serve either purpose in different contexts. Cellular oncogenes appear not to be tumorigenic in their native state; they must either be activated to abnormal levels of expression, or mutated so as to change some aspect of their function (Bishop, 1983).

At the time it had not been demonstrated that propagation of the tumor required persistent oncogenic signaling. Since then, however, it has been demonstrated that in various contexts, cancers depend on the continued function of apical oncogenes—a phenomenon termed “oncogene addiction” (Weinstein, 2002). The earliest evidence of oncogene addiction involved the targeted inhibition of the ERBB2 receptor tyrosine kinase in breast cancer. Antisense oligonucleotide-mediated down-regulation of ERBB2 inhibited proliferation in breast cancer cell lines that had amplified ERBB2, but not in cell lines that lacked this amplification (Colomer et al., 1994). Subsequent studies in pancreatic cancer cell lines demonstrated the dependence of the tumor upon mutated KRAS, while cancer cells that did not have KRAS mutations were insensitive to KRAS depletion (Aoki et al., 1997). These *in vitro* studies suggested that the specific sensitivity of tumors to the loss of mutant or amplified oncogenes reflected a dependence on the evolutionary history of the tumor—that the tumor was still dependent on the oncogene that drove its genesis.

Murine models were generated to demonstrate this phenomenon *in vivo*. MYC activation in the skin caused features of cancer, including hyperplasia, dysplasia, and angiogenesis, resulting in a papillomatosis at around three weeks post-induction. Cessation of MYC induction, however, caused full regression of skin lesions (Pelengaris et al., 1999). A similar phenotype was observed in $p16^{\text{INK4A-/-}}$ mice with activated RAS expression in the skin. Melanomas developed after a period of RAS induction but depended on continued expression to maintain the tumor, as withdrawal from RAS^{G12V} caused these tumors to regress (Chin et al., 1999). Similarly, withdrawal of MYC in MYC-driven T-cell leukemia caused regression of the tumor with evidence of differentiation, growth arrest, and apoptosis (Felsher and Bishop, 1999).

The observed dependence of tumors to these oncogenes *in vivo* spurred the search for means of pharmacological inactivation of apical oncogenes, resulting in the development of inhibitors for multiple oncogenes, including HER2 (trastuzumab), BCR/ABL (imatinib), EGFR (gefitinib and

erlotinib), and VEGFR (sunitinib and sorafenib). These drugs represented a paradigm shift in cancer therapy, and hence cancer susceptibility to oncogene inactivation was dubbed the “Achilles heel” of cancer (Weinstein, 2002). Despite the successes of these therapies, none of these drugs represent a cure for the cancers that they treat. Because of the additional selection pressure from treatment, clones resistant to treatment emerge, whether it is by mutation of the targeted kinase (for example, drug resistance mutations that are frequently observed in BCR/ABL and EGFR in relapsed tumors), or whether tumor suppressive pathways, like p53, are inactivated, or whether the oncogene addiction shifts its burden to alternative oncogenes (Weinstein and Joe, 2008). Indeed, in a model of MYC-driven breast tumorigenesis, inactivation of MYC caused regression of tumors; however, tumors relapsed often bearing KRAS2 mutations, which are known to cooperate with MYC in tumorigenesis (Boxer et al., 2004). Similarly, in human tumors engineered from 293 kidney epithelial cells, RAS-induction caused rapid tumor formation that was reversible upon de-induction of RAS; however, tumor maintenance could be enforced by the activation of the PI3K pathway in the absence of RAS (Lim and Counter, 2005). These studies suggest that initiation of oncogenesis likely causes a rewiring of cellular circuitry that, even in the single oncogene MYC-driven tumors, retains many pre-malignant changes, making subsequent oncogenesis easily achievable. The plasticity of these pathways indicates that we must find alternative modalities to successfully eradicate cancers.

Latent tumor suppressor networks remain functional

One of these modalities relies, like oncogene addiction, on exploiting the evolutionary history of the tumor. In many tumors, inactivation of the tumor suppressors like p53 are critical to tumorigenesis since p53 responds to oncogenic stress by causing cell cycle arrest, differentiation, apoptosis, and senescence (Vousden and Lu, 2002). Roughly 50% of tumors inactivate p53 by mutation, thus compromising its tumor suppressive ability; however, whether the tumor suppressive effector pathways of p53 remain intact was not known until relatively recent reports demonstrating the effects of p53-restoration in vivo. Activation of p53 in E μ -MYC driven lymphoid tumors caused widespread apoptosis of lymphoma cells (Martins et al., 2006). Similarly,

autochthonous lymphomas—those spontaneously arising from p53-null mice—and sarcomas are sensitive to p53 re-introduction. Though lymphomas typically responded by initiating cell death, sarcomas underwent senescence, reflecting an underlying difference in the molecular circuitry between the different cancer types (Ventura et al., 2007). A third report also demonstrated a primarily senescence-mediated tumor suppression for transplanted RAS^{G12V}-induced liver tumors upon p53 reactivation (Xue et al., 2007).

Together, these studies suggest that though p53 is inactivated in the course of tumorigenesis, the simple re-introduction of p53 expression is enough to drive its tumor suppressive functions. This suggests that both the oncogenic signaling that drives p53 as well as the downstream effector mechanisms are largely intact and that re-activation of suppressed tumor suppressive programs is a tractable anti-cancer strategy.

Taspase1 regulates the expression of oncogenes and tumor suppressors

The clinical success of oncogene-inactivating therapies validates the biological concept of oncogene addiction, while re-introduction of tumor suppressors is a promising new avenue for the development of novel therapies. Indeed, antagonists of MDM2, an E3-ligase responsible for p53 degradation, have shown pre-clinical promise (Vassilev et al., 2004). Both oncogene addiction and tumor suppressor sensitivity are important therapeutic concepts, and at the outset of this present work, we established that Taspase1 regulates the expression of core cell cycle components Cyclin E as well as p16^{INK4A}, which are oncogenes and tumor suppressors, respectively (Takeda et al., 2006b). This uniquely places Taspase1 at the hub of both pathways. Whether Taspase1, is required for maintenance of tumors, and hence, whether Taspase1 could serve as a pharmacological target for cancer therapy, is the question we will address with this work.

1.3 Taspase1 is an evolutionarily conserved threonine protease required for proper embryonic development and execution of the cell cycle

The protease Taspase1 (*threonine aspartase 1*) is a threonine nucleophile endopeptidase composed nearly in its entirety of an asparaginase type II homology domain (Pfam PF01112). This family of enzymes includes L-asparaginase, which converts L-asparagine to L-aspartate by hydrolysis of the side chain amide bond. Interestingly, Taspase1 participates in proteolysis of the peptide bond following specific aspartate residues with the consensus peptide sequence QXD/GXDD, thereby initiating a new class of proteases harboring the asparaginase type II homology domain. Taspase1 is translated as a 420 amino acid, 50kDa proenzyme which undergoes auto-proteolytic maturation to generate 28kDa and 22kDa α and β subunits, respectively which form stable dimers and finally heterotetramers with enzymatic activity from the β -subunit N-terminal threonine nucleophile.

Taspase1 was purified as the enzyme responsible for processing the protein product of the human homologue of *Drosophila trithorax*, the mixed lineage leukemia (MLL) transcriptional regulator, which is proteolyzed at two distinct sites, generating 320kDa N-terminal and 180kDa C-terminal fragments. Proteolyzed MLL fragments form stable heterodimers which localize to the nucleus where MLL complexes maintain proper *Hox* gene expression (Hsieh et al., 2003a; Hsieh et al., 2003b; Yokoyama et al., 2002). MLL functionally antagonizes polycomb group proteins at *Hox* loci in order to properly define segmental identity. Though MLL is not known to have sequence-specific DNA binding capacity, it is able to associate with other transcription factors and regulate chromatin structure through histone methylation via its C-terminal SET domain as well as with other epigenetic marks, whether by intrinsic ability or by virtue of cooperation with co-activators or repressors (Milne et al., 2002). Targeted disruption of a single *MLL* allele in mice results in overt loss of segmental identity with bi-directional homeotic transformations, while bi-allelic loss results in mid-gestational embryonic lethality (Yu et al., 1995).

MLL is deregulated in blood cancers

Aside from its role in development, MLL is involved in at least 60 different in-frame translocations at chromosome 11, between its N-terminal 1400 amino acids and various translocation partners. These translocations typify certain hematological malignancies, particularly infant leukemias and leukemias secondary to treatment with DNA-damaging chemotherapies such as topoisomerase II inhibitors. It is estimated that up to 10% of blood disorders, including acute myeloid leukemia (AML), acute lymphocytic leukemia (ALL), biphenotypic leukemias, and myelodysplastic syndromes (MDS) harbor rearrangements of the *MLL* genomic locus, 11q23 (Dimartino and Cleary, 1999). The mechanism by which *MLL* rearrangements cause leukemia is a matter for debate, though it has been suggested that leukemogenesis depends on effector functions of the reciprocal translocation partner, which remain largely uncharacterized (Ayton and Cleary, 2001).

A common feature, however, between various MLL translocations is the retention of the first 1400 amino acids of MLL. Whether the oncogenic properties are due to MLL effector function, fusion partner gain of function, or haploinsufficiency of the translocation partner is unclear; however, in many fusions, the leukemogenic potential of MLL translocations depends on intact transactivation ability of the fusion protein. Surprisingly, an MLL- β -galactosidase fusion knock in promotes leukemic transformation, which complicates understanding the underlying mechanism as it deemphasizes the effector function of the fusion partner (Dobson et al., 2000).

Besides MLL translocations, two other forms of leukemogenic MLL alterations exist—partial tandem duplication (PTD) of MLL exons and PHD1 domain deletions in exon 8. Given that leukemias bearing these mutations form in the absence of MLL translocations suggests that alteration of MLL function is ultimately responsible for leukemogenesis (Ayton and Cleary, 2001), though other evidence suggests that translocation partners require the intact function of both MLL as well as the translocation partner (Slany et al., 1998).

Evidence from our lab indicates that stabilization of MLL in fusion proteins usurps a cell cycle-dependent, biphasic expression pattern of MLL seen in normal cells. MLL accumulates in G1/S and G2/M cell cycle phase boundaries and are tagged for proteasomal degradation in S-phase and mitosis by SCF^{SKP2} and APC^{CDC20}, respectively. Loss of this biphasic expression results in a G1/S phase block in the case of MLL deficiency, or an intra-S-phase block in MLL over-expression. Surprisingly, MLL leukemic fusions resulted in persistent, moderate expression of MLL and consequent deregulation of cell cycle checkpoints (Liu et al., 2007). This suggests that part of a unifying mechanism for MLL fusion-mediated leukemogenesis is the evasion of cell cycle checkpoints normally elicited by MLL deregulation.

Despite the importance of MLL in certain leukemias, Taspase1 regulated MLL cleavage may not have an important role in regulating the MLL fusion protein in leukemogenesis *per se*, since leukemic fusions do not retain the Taspase1 consensus cleavage site. However, Taspase1 may be of importance in MLL-fusion leukemias as a more general regulator of MLL function, particularly in cell cycle, as well as a regulator for functions subordinate to its other substrates.

Loss of Taspase1 disrupts MLL function in development and the cell cycle

Taspase1 knockout mice exhibit *homeotic* transformations consistent with aberrant segmental identification due to alteration of MLL function, including a broadened anterior arch of the atlas, posterior transformation of C7 cervical vertebra to T1, anterior transformation from T8 to T7, among others (Takeda et al., 2006b). MLL non-cleavage results in hypomorphic histone H3 lysine 4 (H3K4) histone methyltransferase activity, which negatively affects its transactivation capability. Additionally, non-cleavage of MLL may affect its target loci specificity as well as its ability to complex with key transcriptional co-regulators. Either of these mechanisms could be in operation in regulating *HOX* gene expression, as Taspase1 si-RNA mediated knockdown prevents the maintenance of the 3' *HOXA* group gene expression (Hsieh et al., 2003a). Importantly, though we illustrated the role of MLL proteolysis in developmental patterning, we

uncovered a distinct and important role for MLL proteolysis in regulation of the cell division cycle, specifically by regulating E2F-mediated Cyclin expression (Takeda et al., 2006b).

Taspase1 knockout mice in the mixed B6/129 background are typically postnatal lethal, but the rare survivors exhibit small body size and male infertility reminiscent of Cyclin D1 and Cyclin E knockout mice (Geng et al., 2003; Sicinski et al., 1995). Orderly progression through the cell cycle requires the concerted expression of Cyclins D, E, A, and B, which can be inhibited at various points by upstream Cyclin-dependent kinase inhibitors (CDKIs) p16^{INK4A}, p21^{CIP1}, p27^{KIP1}, and others (Figure 1). Taspase1-deficient murine embryonic fibroblasts (MEFs) exhibit delayed cell cycle entry as well as blunted expression of Cyclins E, A, and B. We demonstrated that decreased transactivation of Cyclin E was associated with decreased H3K4 methylation at its promoter, suggesting that the hypomorphic H3K4 methyltransferase activity from non-cleaved MLL might directly regulate Cyclin expression. We found that E2F family members, which are the known transcriptional regulators of Cyclin expression, interact with MLL, suggesting that E2F family transcription factors direct MLL to Cyclin promoters to promote their full expression. Taspase1 deficient MEFs also exhibited increased p16^{INK4A} expression, further compounding a cell cycle defect, as p16^{INK4A} sh-RNA knockdown could rescue, to some extent, the Taspase1-null proliferative defect (Takeda et al., 2006b).

The contributions of other Taspase1 substrates

To dissect the contribution of MLL non-cleavage to the Taspase1-null phenotype, knock-in mice bearing non-cleavable alleles (nc) of MLL1 and MLL2 were generated. MEFs from *MLL1^{nc/nc};MLL2^{nc/nc}* embryos exhibited a milder proliferative defect than *Taspase1^{-/-}* MEFs, suggesting that non-cleavage of other Taspase1 substrates may contribute to this defect.

The α/β subunit of general transcription factor TFIIA was shown to be proteolytically processed at a QVDG motif, though it was originally thought to be cleaved N-terminal to an aspartate residue a few positions downstream. It was later discovered that the protease responsible for cleavage

after the P1 aspartate was Taspase1 (Hoiby et al., 2004; Zhou et al., 2006). Similarly, a paralog of TFIIA, ALF, which is specifically expressed in the testis, is also proteolyzed at a site consistent with a consensus site for Taspase1 cleavage (Figure 4.1). Though the cleaved form of TFIIA is the predominant form in cells, the biological significance of this cleavage is still unclear. TFIIA has been shown to interact with TATA binding protein (TBP) and stabilize its interaction with DNA at core promoters, yet it is also known to be critical for basal and activated transcription at TATA-less promoters, suggesting a function beyond binding TBP (Hoiby et al., 2007).

Cleaved TFIIA $\alpha\beta$ is primed for ubiquitination and subsequent proteasomal degradation; yet, non-cleavage did not affect TFIIA interaction with TFIIA γ or its ability to associate with TBP or its ability to handle bulk transcription (Zhou et al., 2006). It has been postulated that cleavage helps to fine-tune expression levels of TFIIA, and it may be that the interactions between cleaved and un-cleaved forms of ALF and TFIIA with their respective cofactors increases the combinatorial diversity of their target promoter specificity or effector functions (Hoiby et al., 2007).

Taspase1 as a cancer therapeutic target

Taspase1 is highly expressed in nearly all tested cancer cell lines from various histological origins (Takeda et al., 2006b); moreover, Taspase1 is up-regulated in transformed clones MEFs selected through soft agar, including those initially transformed by E1A/RAS^{G12V}, MYC/RAS^{G12V}, and dominant negative p53 (DNP53)/RAS^{G12V} (Figure 4.3). Loss of Taspase1 renders MEFs resistant to transformation by the same oncogene pairs and causes a profound depression in proliferation rate in unadulterated MEFs compared to those that are Taspase1 wild type. Importantly, loss of Taspase1 results in the up-regulation of p16^{Ink4a} with accordant hypo-phosphorylation of pRb and down-regulation of Cyclins E, A, and B. Though the MLL-Cyclin axis is an important arm of Taspase1-orchestrated proliferation program, Cyclin D isoforms are largely unaffected by Taspase1 loss. This may not be altogether surprising since Cyclin D levels are tightly controlled, with a half-life of 25 minutes and critical sensitivity to extracellular signals, in a manner different from Cyclins E, A, and B (Sherr and Roberts, 1995) (Figure 1A). As p16^{Ink4A} can both hinder the

assembly of the regulatory Cyclin D subunit and its catalytic kinase counterparts CDK4 and CDK6 as well as inhibit CyclinD-CDK4/6 holoenzyme activity, the absence of Taspase1 may functionally inactivate Cyclin D by the de-repression (or the up-regulation) of p16^{INK4A}.

Though it is apparent that Taspase1 is critical to orchestrating normal cell cycle progression there is little known about the phenotypic output of Taspase1 deregulation in a disease context. We hypothesize that the severe, compound cell cycle defect created by Taspase1 loss strongly argues that Taspase1 is a good candidate for targeted molecular inactivation as an effective cancer therapy. The aim of this work will be address whether Taspase1 is critical to tumorigenesis and whether it subsequently bears responsibility for maintenance of established tumors. Answering these questions will be the first step in establishing Taspase1 as a molecular target for cancer therapy.

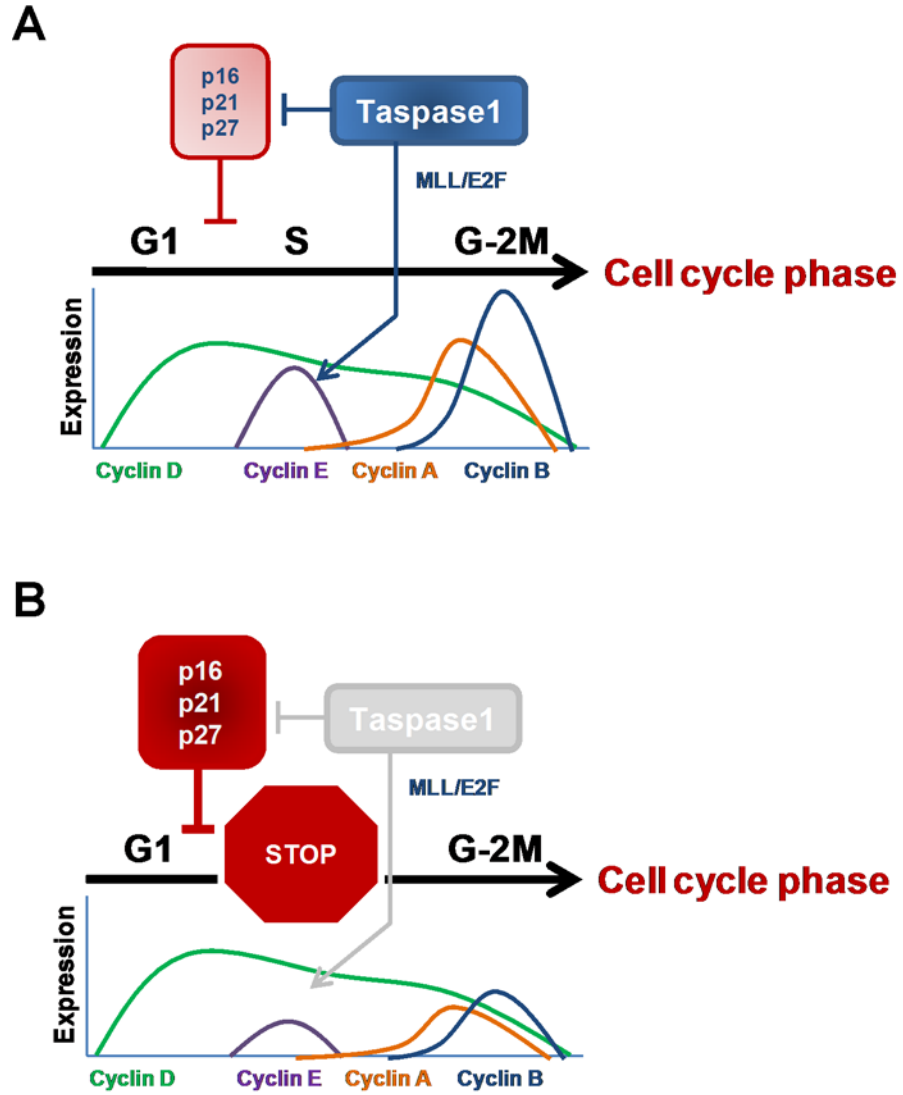


Figure 1. Taspase1 regulates the cell cycle through proteolysis of its substrate MLL

A, Orderly progression of the cell cycle requires Taspase1. **B,** Taspase1 deficiency can deregulate the cell cycle. Depiction of Cyclin levels is adapted from Figure 1 of Sherr, CJ, 1996.

Chapter 2

Taspase1 is a non-oncogene addiction protease that coordinates cancer cell proliferation and apoptosis

- 2.1 Introduction
- 2.2 Taspase1 is required for tumor maintenance in vitro
- 2.3 Taspase1 is not an oncogene
- 2.4 Taspase1 is required for inhibition of human cancer cell proliferation
- 2.5 Requirement for Taspase1 in anoikis resistance
- 2.6 Taspase1 deficiency results in decreased MCL-1 level and increased sensitivity to chemotherapeutic agents and ABT-737
- 2.7 Taspase1 regulates the protein half-life of MCL-1
- 2.8 Taspase1 is over-expressed in primary human GBM and melanoma tissues and its deficiency disrupts tumor growth in a xenograft mode
- 2.9 Discussion
- 2.10 Methods and materials
- 2.11 Figures

2.1. Introduction

Cancer is a state of disease that evolves over years of accumulating genetic and epigenetic abnormalities that confer an enhanced capacity to proliferate and evade apoptosis, eventually compromising the host (Hanahan and Weinberg, 2000; Vogelstein and Kinzler, 2004). Although cancers are the product of complex selection pressures, it has been shown that abrogation of certain apical oncogenes can effectively inhibit cancer cell growth and prolong patient survival—a phenomenon termed “oncogene addiction” (Weinstein and Joe, 2008). In accordance with this concept, molecularly targeted drugs have been developed and successfully utilized in treating cancer patients, exemplified by the use of imatinib for chronic myelogenous leukemia, erlotinib for lung cancer, and sunitinib for kidney cancer (Zhang et al., 2009). Despite these recent strides against cancer, most end-stage cancer patients still succumb to their diseases, highlighting the urgent need for novel anti-cancer therapeutic strategies. Recently, the “non-oncogene addiction” hypothesis was proposed based on the heavy reliance of cancer cells on certain non-oncogenes for their continuous growth and survival, which offers a new class of therapeutic targets that are not conventional oncogenes (Luo et al., 2009). Thus far, well-characterized non-oncogene addiction factors include the 26S proteasome, HSF1 (Dai et al., 2007a), and IRF4 (Shaffer et al., 2008), which handles the rapid protein turnover, mediates the stress response, and maintains expression of the MYC oncogene, respectively. The fact that the proteasome inhibitor bortezomib is effective against multiple myeloma in human patients substantiates this new anti-cancer therapeutic concept (Adams, 2004).

Uncontrolled proliferation and increased resistance to apoptosis are two cardinal features of cancer, and consequently, inhibiting cancer cell division and enhancing cancer cell death constitute two effective anti-cancer therapeutic strategies (Hanahan and Weinberg, 2000; Lowe et al., 2004). Cancer cell cycle is typified by constitutively activated Cyclin/CDK complexes, resulting from either over-expression of Cyclins or down-regulation of CDK inhibitors (CDKIs) that are oncogenes and tumor-suppressor genes, respectively (Besson et al., 2008; Sherr, 1996). By

analogy, impaired apoptosis in cancer cells can result from either up-regulation of anti-apoptotic (such as BCL-2, BCL-XL, and MCL-1) or down-regulation of pro-apoptotic BCL-2 family proteins (such as BAX, BAK, BIM, and PUMA) (Danial and Korsmeyer, 2004). Targeted anti-cancer drugs have been developed and are on clinical trials based on these frameworks, and hence continued elucidation of the molecular control of cancer cell proliferation and cell death should unveil new anti-cancer targets and offer novel treatment options.

Taspase1 (threonine aspartase 1) encodes a highly conserved 50kD α - β proenzyme which undergoes intramolecular autoproteolysis, generating a mature α 28/ β 22 heterodimeric protease that displays an overall $\alpha/\beta/\beta/\alpha$ structure (Hsieh et al., 2003a; Khan et al., 2005). *Taspase1* is the only protease within the family of enzymes that possesses an asparaginase_2 (PF01112) homology domain, while other members, including L-asparaginase and glycosylasparaginase, participate in the metabolism of asparagine and the ordered breakdown of N-linked glycoproteins, respectively (Hsieh et al., 2003a). *Taspase1*-mediated cleavage follows distinct aspartate residues of conserved QXD/GXDD motifs (Hsieh et al., 2003b), suggesting that *Taspase1* evolved from hydrolyzing asparagine and glycosylasparagine to cleaving polypeptides. The cloning of *Taspase1* founded a novel class of endopeptidases which utilizes the N-terminal threonine of mature β subunit to cleave protein substrates after P1 aspartate. *Taspase1* was initially purified as the protease which cleaves MLL to regulate *HOX* gene expression (Hsieh et al., 2003a). Subsequent studies identified additional *Taspase1* substrates, including MLL2, TFIIA α - β , ALF (TFIIA τ), and *Drosophila* HCF (dHCF) (Capotosti et al., 2007; Takeda et al., 2006b; Zhou et al., 2006). Collectively, all of the known *Taspase1* substrates are nuclear factors that control gene expression, suggesting that *Taspase1* cleaves nuclear factors to orchestrate genetic programs.

Our prior study of *Taspase1*^{-/-} mice uncovered a critical role of *Taspase1* in cell cycle control (Takeda et al., 2006b). In the absence of *Taspase1*, cell cycle is disrupted with decreased expression of *Cyclins*, including *E*, *A*, and *B*, and increased expression of CDK inhibitors (CDKIs),

including *p16*, *p21*, and *p27* (Takeda et al., 2006b). Hence, Taspase1 may play a permissive role in tumorigenesis, which is supported by the demonstrated resistance of *Taspase1*^{-/-} mouse embryonic fibroblasts (MEFs) to oncogenic transformation induced by MYC, RAS, DNp53, and E1A. Although the absence of Taspase1 poses a profound roadblock in cancer initiation (Takeda et al., 2006b), whether Taspase1 is required for cancer maintenance remains unknown. Here, we demonstrate that Taspase1 is required to maintain a full cancer phenotype and is over-expressed in primary human cancer tissues. Deficiency of Taspase1 in human cancer cells results in impaired proliferation and enhanced susceptibility to death stimuli. Taspase1 is not a classical oncogene, yet it enables expression of cancer characteristics; thus, it is better classified as a “non-oncogene addiction” protease. As proteases are ideal drug targets, small molecule inhibitors of Taspase1 may be developed for cancer therapy.

2.2 Taspase1 is required for efficient tumor maintenance in vitro

Our prior study demonstrated that *Taspase1*^{-/-} primary MEFs are defective in proliferation and thus resistant to in vitro transformation induced by well-characterized oncogene pairs including MYC-RAS^{G12V}, DNp53-RAS^{G12V}, and E1A-RAS^{G12V} (Takeda et al., 2006b). These data highlight a critical participation of Taspase1 in cancer initiation, whereas whether Taspase1 has any role in cancer maintenance remains unanswered. To address this question, we employed a tamoxifen-inducible cre-lox system that allows for a precisely controlled genomic deletion of the conditional “floxed” (*f*) *Taspase1* allele. Specifically, MYC-RAS-transformed *Rosa26-creERT;Taspase1f/-* (*R26-creERT;T1f/-*) and *R26-creERT;T1+/-* MEFs were treated with a 6-hour pulse of 500 nM 4-hydroxytamoxifen (4-OHT), which efficiently activated creERT fusion to excise the conditional allele of *Taspase1* (Figure 2.1A). Deletion of *Taspase1* in MYC-RAS transformed *R26-creERT;T1f/-* MEFs resulted in a profound proliferation block and disruption of colony formation on soft agar (Figure 2.1 B and C), indicating the requirement of Taspase1 for the proliferation of transformed cells. Of note, in agreement with the known toxicity of Cre recombinase in MEFs (Loonstra et al., 2001), the pulse activation of creERT in control, MYC-RAS transformed *R26-*

creERT;T1+/-, MEFs generated minor phenotypes in both assays (Figure 2.1 B and C). Taken together, our data support a permissive role of Taspase1 in cancer maintenance apart from cancer initiation.

2.3 Taspase1 is not an oncogene

To further define the role of Taspase1 in tumorigenesis, we asked whether Taspase1 functions as an oncogene. To directly assess the oncogenic potential of Taspase1, we employed two different sets of *in vitro* transformation assays that are commonly utilized to characterize newly discovered oncogenes. First, we stably introduced Taspase1 into NIH/3T3 cells by retrovirus-mediated gene transduction, and determined the ability of transduced NIH/3T3 cells to grow on soft agar. Taspase1-transduced NIH/3T3 cells were unable to produce discernible colonies on soft agar, whereas RAS^{G12V}, as a positive control, efficiently rendered anchorage-independent growth (Figure 2.2 A and Figure 2.7 A). Second, we tested the ability of Taspase1 to work in concert with RAS^{G12V}, MYC, or E1A to transform primary MEFs. Taspase1 was unable to complement respective oncogenes to induce colony growth on soft agar (Figure 2.2 B and Figure 2.7 B). Thus, Taspase1 appears not fit the criteria for a classical oncogene despite its requirement for cancer initiation and maintenance. The fact that Taspase1 is not an oncogene and yet enables oncogenesis suggests that Taspase1 is better classified as a “non-oncogene addiction” protease.

2.4 Taspase1 is required for inhibition of human cancer cell proliferation

Given the requirement of Taspase1 in murine oncogenesis *in vitro*, we chose a wide variety of human cancer cell lines from the well-characterized NCI-60 panel to study the role of Taspase1 in human carcinogenesis. Human melanoma (SK-MEL-2), glioblastoma (U251), colon (HT-29), ovary (OVCAR-3), lung (A549), prostate (PC3), and breast (MDA-MB-231) cancer cell lines, representing major tissue types of human solid cancers, were examined. The expression of Taspase1 in these cell lines was determined (Figure 2.3 A). Knockdown of Taspase1 in these

human cancer cell lines compromised their proliferative capacity but to a varying degree (Figure 2.3 B). Interestingly, cancer cell lines with higher Taspase1 levels appear to exhibit a more profound proliferation block upon knockdown of Taspase1 (Figure 2.3 B and Figure 2.8), lending support to the notion that Taspase1 is co-opted by oncogenes to enforce cancer characteristics. Increased Taspase1 expression in cancer cells likely reflects an inherently elevated dependence on Taspase1 for maintaining a full cancer phenotype. The molecular basis underlying the proliferation defect induced by the deficiency in Taspase1 was further interrogated with a primary focus on the regulation of Cyclin E, A, and CDKIs—known downstream targets of Taspase1 in the cell cycle control (Takeda et al., 2006b). Analyses of p16, p21, p27, Cyclin E2, and Cyclin A in these cancer cell lines revealed that the induction of p27 is most correlative with the growth inhibition induced by the Taspase1 loss (Figure 2.3 C). For example, PC-3 and MDA-MB-231 cells exhibited minimal growth inhibition upon Taspase1 knockdown, and no induction of p27 was observed in these Taspase1-knockdown cancer cells. Interestingly, p16 and p21 were induced in SK-MEL-2 and A549 cell lines, respectively though the role of p27 in inhibiting cancer cell cycle may dominate over p16 and p21 due to frequent deletions of the *p16/INK4A/p14ARF* locus, frequent mutation of p53, the upstream activator of p21, and the extremely rare incidence of p27 mutations in human cancers (Besson et al., 2008). Taspase1 regulation of p27 happens on a transcriptional as well as post-translational level (Figure 2.10).

Taspase1 activates the transcription of Cyclins through MLL proteolysis (Takeda et al., 2006b; Tyagi et al., 2007). However, we did not observe a reduction of Cyclin E2 or A expression in these cancer cell lines, suggesting that the Taspase1-MLL axis in regulating Cyclins may have been disrupted during the development of these cancers. Of note, analysis of known genetic mutations in oncogenes and tumor suppressors in these cancer cell lines did not identify a causal mutation explaining the Taspase1 dependence (Table 2.1), highlighting the potential, general application of Taspase1 inactivation to inhibit cancer cell growth.

2.5 Requirement for Taspase1 in anoikis resistance

As Taspase1 plays a critical role in sustaining cancer cell proliferation, we investigated whether Taspase1 is also involved in modulating cancer cell death—another principal mechanism often deregulated in tumorigenesis. Interestingly, Taspase1 deficiency resulted in a minor increase in spontaneous apoptosis in both SK-MEL-2 and U251—cells that express high levels of Taspase1 (Figure 2.4 A). The increase in spontaneous apoptosis due to Taspase1 deficiency suggests that Taspase1 governs a fundamental process in cellular survival and that deregulation of this process, in the absence of Taspase1, would sensitize these cell lines to further death stimuli. The initiation of cell death by detachment from its substrata is an important, physiological initiator of apoptosis, termed anoikis, and the cellular resistance to anoikis constitutes a primary determinant of metastatic potential. Accordingly, we determined whether the loss of Taspase1 in U251 and SK-MEL-2 would affect anoikis sensitivity. Taspase1 deficiency sensitized SK-MEL-2 and U251 cells to anoikis, which was not evident in other tested human cancer cell lines except to a lesser degree in A549 lung cancer cells (Figure 2.4 B). The degree to which Taspase1-sustained proliferation and enhanced anoikis resistance contribute to tumorigenesis was further interrogated with soft agar assays. The ability of cells to form colonies on soft agar is a stringent *in vitro* predictor of *in vivo* tumorigenicity as soft agar imitates tumor microenvironment and thereby simultaneously assesses cellular proliferation and anoikis resistance. Indeed, Taspase1 deficiency in SK-MEL-2 and U251 cancer cells resulted in reduced colonies on soft agar (Figure 2.4 C). Altogether, our data reveal a novel capacity of Taspase1 in regulating cell death in human cancers.

2.6 Taspase1 deficiency results in decreased MCL-1 level and increased sensitivity to chemotherapeutic agents and ABT-737.

Melanoma and glioblastoma multiforme (GBM) are two highly aggressive human cancers that portend dismal outcomes when presenting at advanced stages. Their increased sensitivity to

death upon Taspase1 knockdown prompted us to investigate the mechanism by which Taspase1 regulates apoptosis in these cancers. The BCL-2 family constitutes the core apoptotic machinery which operates at the mitochondrion, controlling cytochrome c release and caspase activation (Danial and Korsmeyer, 2004). The activator BH3-only molecules BID, BIM, and PUMA directly activate the apoptotic effectors BAX and BAK, whereas BCL-2, BCL-XL, and MCL-1 inhibit apoptosis by sequestering BH3s (Figure 2.11 A) (Cheng et al., 2001; Kim et al., 2006; Kim et al., 2009; Letai et al., 2002; Wei et al., 2001). Based on this framework, we examined the expression of core regulators of mitochondrial apoptosis in control- or Taspase1-knockdown SK-MEL-2 and U251 cells, which identified decreased MCL-1 as the common alteration (Figure 2.5 A). Therefore, Taspase1 may function to maintain the MCL-1 level and thus modulate the apoptotic threshold in GBM and melanoma (Figure 2.11 B). To examine this hypothesis, we first knocked down MCL-1 to a comparable level as observed in Taspase1-knockdown cells. When comparing the propensity of Taspase1- or MCL-1-knockdown cells to undergo anoikis or DNA damage-induced apoptosis, we observed a comparably enhanced apoptotic sensitivity in both U251 and SK-MEL-2 cells (Figure 2.5 and Figure 2.12). Notably, the Taspase1 deficiency-induced down-regulation of MCL-1 is of potential clinical significance. As ABT-737, a specific inhibitor of BCL-2/BCL-XL, is ineffective at killing MCL-1 over-expressing cancer cells (Oltersdorf et al., 2005; Opferman, 2006; van Delft et al., 2006), inactivation of Taspase1 may offer an effective strategy to sensitize these resistant cancer cells to ABT-737-induced apoptosis. Accordingly, we treated control- or Taspase1-knockdown U251 and SK-MEL-2 cells with ABT-737 and demonstrated increased apoptosis in Taspase1 deficient cancer cells (Figure 2.5 C and Figure 2.12 B). In summary, deficiency of Taspase1 confers sensitivity to apoptosis in GBM and melanoma cancer cells through down-regulation of MCL-1, suggesting a potential therapeutic benefit from combining Taspase1 inhibitors with currently-used cytotoxic agents as well as ABT-737 for cancer treatment.

2.7 Taspase1 regulates the protein half-life of MCL-1.

The MCL-1 protein level can be titrated through transcriptional, translational, and post-translational mechanisms, which explains its unusual capacity among BCL-2 family members to rapidly respond to environmental cues for cell death control (Opferman, 2006). As Taspase1 functions mainly through processing nuclear factors and thus orchestrating transcription, we determined if Taspase1 directly regulates the transcription of MCL-1. Interestingly, there was no decrease of the MCL-1 transcript level in Taspase1 deficient U251 and SK-MEL-2 cells (Figure 2.5 D and Figure 2.12 C). Rather, Taspase1 deficiency shortened the protein half-life of MCL-1 from ~1 hour to ~20 minutes in U251 cells (Figure 2.5 E). Furthermore, treatment with proteasome inhibitor MG132 prevented the degradation of MCL-1 in both control- and Taspase1-knockdown U251 cells. The resultant half-life of MCL-1 is comparable between control- and Taspase1-knockdown cells upon MG132 treatment, suggesting that Taspase1 sustains the MCL-1 protein by enhancing its protein stability.

The control of MCL-1 degradation is complex and context dependent, which at least involves the E3 ligase MULE, the GSK3 β signaling, and the inactivator BH3 NOXA (Chen et al., 2005a; Ding et al., 2007; Maurer et al., 2006; Zhong et al., 2005). To provide further mechanistic details regarding how Taspase1 controls the MCL-1 degradation, we determined the expression of MULE and did not detect an increased transcript level of MULE in Taspase1-knockdown cells (Figure 5F and Figure 2.12 C). Nor did we detect a difference in transcript of another described E3-ubiquitin ligase known to regulate MCL-1, β -TRCP, or a stabilizing chaperone for MCL-1, TCTP (Figure 2.5 F) (Ding et al., 2007; Liu et al., 2005). We investigated whether Taspase1 disrupts GSK3 β signaling thereby extending the MCL-1 half-life. Inhibition of GSK3 β by TZDZ-8 in Taspase1 deficient cells did not result in increased MCL-1 protein (Figure 2.13). We also determined the expression of NOXA and did not detect an induction of NOXA protein in Taspase1-deficient cells to account for the increased degradation of MCL-1 (Figure 2.5A). Taken together, these data indicate that Taspase1 regulates the MCL-1 protein through a distinct

proteasome-dependent mechanism that appears not to involve the suppression of MULE expression, the inactivation of the GSK3 β signaling, or the suppression of NOXA expression. Taspase1 appears to regulate MCL-1 by the recently-described de-ubiquitinase for MCL1, USP9X at the transcriptional level, resulting in decreased USP9X protein and increased MCL-1 ubiquitination (Figure 2.5 F, G, H) (Schwickart et al., 2010).

2.8 Taspase1 is over-expressed in primary human GBM and melanoma tissues and its deficiency disrupts tumor growth in a xenograft model.

Our in vitro assays indicate that Taspase1 enables a full cancer phenotype by facilitating cancer cell cycle progression and suppressing cancer cell death. To probe the in vivo requirement of Taspase1 in human cancer growth, we performed a tumor xenograft assay using immunocompromised NOD;*scid*;*IL2R γ ^{-/-}* mice. Importantly, loss of Taspase1 significantly inhibited the growth of U251 tumors in NOD;*scid*;*IL2R γ ^{-/-}* mice due to a decreased proliferative index as assessed by Ki67 staining, and increased cell death (Figure 2.6 A, B, and C). Furthermore, treatment of mice bearing U251 xenografts with ABT-737 resulted in a marked increase in cell death in Taspase1-deficient tumors (Figure 2.6 C).

Several lines of evidence suggest that Taspase1 is recruited by oncogenes to maintain cancer characteristics during tumorigenesis. First, our in vitro and in vivo studies indicate that Taspase1 functions as a critical node in the oncogenic network that sustains proliferation and suppresses cell death. Second, Taspase1 is highly expressed in most of the NCI-60 human cancer cell lines (Takeda et al., 2006b). Third, there is a positive correlation between the level of Taspase1 expression and the degree of disruption in cancer phenotypes upon its inactivation in examined human cancer cell lines. Theoretically, Taspase1 may be highly-expressed in certain human cancers, and based on our data, its over-expression would indicate a favorable therapeutic outcome upon its inhibition.

To enable assessment of Taspase1 expression in primary tissues, we established an immunohistochemistry (IHC) assay using a newly raised anti-Taspase1 monoclonal antibody. We focused on GBM and melanoma as our cell line data suggested a central role for Taspase1 in the maintenance of these cancers. Remarkably, Taspase1 is abundantly expressed in primary human GBM tissues (n = 19), whereas no or weak staining of Taspase1 is observed in adjacent or control brain sections (n = 13) that mainly consist of astroglial cells—the same cellular origin of GBM (Figure 2.6B and Figure 2.15). The specificity of Taspase1 staining was confirmed as no signal was detected when the anti-Taspase1 antibody was pre-incubated with the Taspase1 immunogen (Figure 2.16). Of note, a recent, independent gene expression profiling analysis demonstrated over-expression of Taspase1 in primary human GBM tissues (Scrideli et al., 2008).

Additionally, Taspase1 is preferentially expressed in melanoma compared to melanocytic nevus (Figure 2.17). Similar expression of Taspase1 between melanocytic nevus and adjacent keratinocytes serves as an internal reference for Taspase1 expression, since normal melanocytes cannot be histologically differentiated from malignant melanocytes in the same section. To quantify the preferential expression of Taspase1 in melanoma, we compared the relative immunofluorescence signal between melanoma and keratinocytes versus that of nevus and keratinocytes, which confirmed a statistically significant over-expression of Taspase1 in melanomas (Figure 2.17). In summary, IHC and IF assays established to assess the expression of Taspase1 in primary human tissues demonstrate the over-expression of Taspase1 in primary, human GBM and melanoma. This suggests that Taspase1 may have an important role in the pathogenesis of these human cancers and that it may serve as a new therapeutic target for these currently intractable diseases.

2.9 Discussion

Taspase1 plays an essential role in regulating embryonic cell cycle, as evidenced by the smaller body size of *Taspase1*^{-/-} mice (Takeda et al., 2006b). Molecularly, Taspase1 functions to

activate transcription of Cyclin E, A and B, and to suppress that of CDKs p16, p21 and p27 in primary MEFs for cellular proliferation. In contrast, the role of Taspase1 in adult tissue homeostasis is less clear. As Taspase1 coordinates the expression of Cyclins and—known oncogenes and tumor suppressors, respectively—inactivation of Taspase1 may offer a novel mechanism to inhibit cancer cell proliferation. In agreement with this hypothesis, deficiency of Taspase1 in human cancer cells impedes proliferation. In contrast to our prior observation that the loss of Taspase1 has no impact on the baseline cell death of primary MEFs which express low levels of Taspase1 (Takeda et al., 2006b), GBM and melanoma cancer cells that express high levels of Taspase1 exhibited increased sensitivity to death stimuli upon Taspase1 inactivation.

Mechanistically, Taspase1 deficiency in U251 and SK-MEL-2 cells resulted in an increased degradation of MCL-1 via USP9X regulation, accounting for the enhanced death phenotype. MCL-1 is unique among anti-apoptotic BCL-2 family members as it rapidly responds to external signals and can be regulated by transcriptional, translational, and post-translational mechanisms (Opferman, 2006). Regulation of MCL-1 protein turnover is itself complex and implicates multiple pathways. MULE/ARFBP-1 was the first described E3-ligase required for MCL1 degradation, though in MULE deficient cells, MCL-1 is still degraded upon initiation of apoptosis, suggesting the existence of additional mechanisms for MCL-1 degradation (Zhong et al., 2005). For example, the PI3K/AKT pathway inhibits GSK3 β -mediated phosphorylation of MCL-1 and thereby prevents β -TrCP-mediated ubiquitylation and proteasomal degradation of MCL-1 (Ding et al., 2007; Maurer et al., 2006). Additionally, MCL-1 protein stability can be regulated by direct protein-protein interactions, as its interaction with NOXA is known to modulate MCL-1 turnover, and TCTP can stabilize MCL-1 (Chen et al., 2005a; Liu et al., 2005).

How Taspase1 regulates the transcription of USP9X a matter for future study. Nevertheless, down-regulation of MCL-1 by Taspase1 knockdown in cancer cell lines has important implications in cancer therapy. The small molecule inhibitor of BCL2/BCL-XL, ABT-737, is currently

undergoing clinical trials. Although ABT-737 is quite potent in killing certain types of cancer cells, it is ineffective against MCL-1 over-expressing tumors due to its inability to inhibit MCL-1 (Konopleva et al., 2006; Oltersdorf et al., 2005; van Delft et al., 2006). Accordingly, Taspase1 inhibitors may synergize with ABT-737 to induce apoptosis in human cancers.

There has been a relatively recent shift in focus from non-specific, cytotoxic therapies to a targeted approach in cancer treatment, supported by the observation that tumor survival is dependent on the continued function of the initiating oncogene—a phenomenon known as “oncogene addiction” (Weinstein, 2002). Moreover, re-introduction of defective tumor suppressors can engage intrinsic tumor suppression mechanisms to destroy cancer cells, suggesting that the intrinsic tumor suppression network present at the inception of tumorigenesis remains largely intact yet dormant (Lowe et al., 2004). In the present study, we find that Taspase1 loss modulates proliferative and death signals through the regulation of the tumor suppressive CDKs and the pro-survival MCL-1, respectively, suggesting that Taspase1 functions as a critical node that when lost, intact tumor suppressive mechanisms can dominate, slowing cancer cell proliferation and rendering increased cancer cell susceptibility to death stimuli.

Despite its involvement in oncogenesis, when introduced with established oncogenes, Taspase1 failed to enable the survival and growth of MEFs on soft agar. Recent studies have identified cellular proteins required for tumorigenesis that are non-oncogenes, a phenomenon termed “non-oncogene addiction” (Luo et al., 2009). Hence, Taspase1 is better categorized as a non-oncogene addiction protease. Factors first described in this paradigm include the master heat shock response regulator heat shock factor 1 (HSF1) as well as interferon regulatory factor 4 (IRF4). Both are transcription factors that are positioned to regulate broad cellular processes that are required for normal cellular homeostasis, but upon which tumors have increased dependence. HSF1 not only relieves proteotoxic stress by regulating heat shock proteins, but also modulates signaling from other oncogenic pathways, including ERK, and also regulates protein translation as well as glucose metabolism (Dai et al., 2007a). IRF4 similarly executes a

broad genetic program that is involved in normal B-lymphocyte activation, but also supports the oncogenic platform by its regulation of membrane biogenesis as well as metabolic control, cell cycle progression, cell death, and differentiation (Shaffer et al., 2008). Although the concept of targeting non-oncogene addiction factors for cancer treatment is novel, this strategy has proven fruitful with the successful application of the proteasome inhibitor bortezomib in treating certain human cancers.

Taspase1 is similarly positioned to regulate a broad array of biological functions, including development, cellular proliferation, and cell death, as all of the Taspase1 substrates described to date are broad-acting transcription regulators, including TFIIA and MLL. Although Taspase1 plays a critical role in embryonic development, acute deletion of Taspase1 in mice did not incur obvious organismal distress and changes in blood counts (data not shown), supporting a potential application of Taspase1 inhibitors in treating cancers. Though the mechanisms whereby Taspase1 is co-opted to promote tumorigenesis remain to be examined, the increased requirement for Taspase1 in certain cancers represents a possibility for a therapeutic window in which Taspase1 inhibition can work in conjunction with other forms of targeted and non-targeted cancer treatments. Taspase1, as a site-specific protease, allows for rational design of substrate mimetic inhibitors as well as expedient high-throughput screening for potential small molecule therapeutic leads (Lee et al., 2009). Although targeting the non-oncogene addiction network for cancer therapeutics is in its rudimentary stage, the successful utilization of this novel strategy is likely to add effective chemotherapeutic agents to our current armamentarium for combating cancers.

2.10 Materials and Methods

Mice and MEFs

Straight and conditional knockout mice of *Taspase1* have been described. *Taspase1*^{+/-} mice were crossed with *Rosa26-cre*^{ERT} mice to generate *R26-cre*^{ERT};*T1*^{+/-} mice. *R26-cre*^{ERT};*T1*^{+/-} mice were crossed with *T1*^{f/+} mice to generate E13.5 primary MEFs. Genotyping for the *Taspase1* allele and the retroviral transduction of the oncogene pairs, MYC plus RAS^{G12V} into MEFs have been described (Takeda et al., 2006b).

Plasmids

Nucleotide 480 of the human *Taspase1* cDNA was mutated from T to A to create a silent mutation that abolished the internal EcoRI site using the QuickChange system (Stratagene). The *Taspase1* was inserted into a murine stem cell virus (MSCV) vector as a BamHI-EcoRI fragment downstream of an internal ribosomal entry site (IRES). Human c-MYC, HRAS^{G12V} and E1A from adenovirus V early region were PCR cloned upstream of the IRES site using BglIII and XhoI to generate c-MYC-IRES-T1, RAS^{G12V}-IRES-T1, and E1A-IRES-T1. Constructs for MYC-IRES-RAS^{G12V} and E1A-IRES-RAS^{G12V} were described previously (Takeda et al., 2006b). *Taspase1* RNAi oligos were generated by Oligoengine (Seattle, Washington), annealed and inserted into the vector pSuperior according to the manufacturer's protocol. h*Taspase1* was targeted using two independent target sequences (sh-T1 is 5'-GGAAAGCCAAGACTCACAT-3' and sh-T1#2 is 5'-GCAGTAGATCATGGAATAC-3'), while scrambled shRNA control was acquired from Oligoengine (5'-GCGCGCTTTGTAGGATTCG-3'). The target sequence for MCL-1 is (5'-CCCATCTCAGAGCCATAAG -3').

Cell Culture, Virus Production, and Retroviral Transduction.

All cancer cell lines were provided by the NCI Developmental Therapeutics Program (Bethesda, MD) and cultured according to the provided instructions. Amphotropic retroviruses were generated by transfection of 293T cells with a helper-free packaging system as described (19).

Infections were carried out for 48 hours with an 8 µg/mL supplement of polybrene (Sigma, St. Louis, MO) and subsequently selected for stable integrants in puromycin-containing media.

Soft Agar Assay

Cancer cell lines were plated at 10^5 cells per 6 cm dish in 0.3% agar noble layered on top of a 0.6% agar noble base. Cells were fed every 3 days with media, and after 2-3 weeks, colonies >0.1mm from 5 low power fields per plate were scored. Soft agar assays for primary MEFs were performed as previously described (Takeda et al., 2006b).

Anoikis assay

Cancer cell lines were detached from their adherent substrata by trypsinization and 10^5 cells were plated, in their normal media, per well into 6-well plates coated with 6 mg of Poly-HEMA (Sigma, St. Louis, MO) to prevent attachment to tissue culture plastic. Non-adherent and loosely adherent cells were harvested after three days, trypsinized, and stained with Annexin V-Cy3 (Biovision, Mountain View, CA) and subjected to flow cytometry analysis on a FACSCalibur cytometer (BD Biosciences, San Jose, CA) to determine viability. Primary MEFs used were under 3 passages and were cultured in IMDM, supplemented with 20% fetal bovine serum, 2 mM L-glutamine, 1 mM MEM non-essential amino acids, 1 mM sodium pyruvate, 0.1 mM β-mercaptoethanol, and 100 U/ml penicillin/streptomycin (Invitrogen). Primary MEFs were plated at 10^5 cells per well in 2 ml of normal culture media, except that the serum was reduced to 1%, on Poly-HEMA coated 6-well plates and harvested 24 hours after plating and analyzed for viability as described above.

Cell cycle analysis

Cancer cell lines with control- or Taspase1-knockdown were stained with propidium iodide and subjected cell cycle analysis as previously described (Liu et al., 2007).

Quantitative RT-PCR and Protein Degradation Assay

RNA was harvested from U251 and SK-MEL-2 cell lines using Trizol and first strand synthesis was performed using Superscript II (Invitrogen, Carlsbad, CA) according to the manufacturer's protocols. Quantitative PCR was performed using SybrGreen PCR with an ABI 7300 Real Time PCR system. Primers sequences used are as follows:

HGNC symbol	Sequence
BTRC (β-TrCP)	5' CAGGATCATCGGATTCCACGGTCAG
	3' TCTACAACATTGACAGCAGCTCGGTG
MCL1	5' GCTGCATCGAACCATTAGCAGAAAG
	3' TTGGAGTCCAACACTGCATAAACTGGT
HUWE1 (MULE)	5' CGGCATCTGTACAGTTCCATAGAGC
	3' AATGTTGTAGCCGAGTTAGCAGCG
USP9X	5' CCACCTCAAACCAAGGATCAATGAAATG
	3' CTCTCCACTCCATGTTGATTAGGAATAG
ACTB	5' CCTGGACTTCGAGCAAGAGATGG
	3' GATCTTCATTGTGCTGGGTGCCAG
TPT1 (TCTP)	5' CGAAAGCACAGTAATCACTGGTGTCG
	3' GATGTGCTTGATTTGTTCTGCAGCC
CDKN1B (p27)	5' GCTAACTCTGAGGACACGCATTTGG
	3' TTTGACGTCTTCTGAGGCCAGG

Protein degradation assays were performed as previously described (Liu et al., 2007).

Antibodies

The polyclonal antibody used to detect Taspase1 was described (Takeda et al., 2006b). Other antibodies used include BID (Kim et al., 2006), BIM (N22-40, Calbiochem), PUMA (P4743, Sigma), NOXA (ab13654, AbCam), p21 (sc-397, Santa Cruz), p27 (sc-528, Santa Cruz), p16 (G175-1239, BD Pharmingen), Cyclin E2 (4132, Cell Signaling), Cyclin A (C4170, Sigma), MCL-1 (sc-819, Santa Cruz), BCL-2 (6C8, BD Pharmingen), BCL-X_L (2762, Cell Signaling), Ubiquitin (FL-76 Santa Cruz), and USP9X (1C4, Novus Biologicals). Antibodies used specifically for murine antigens include p16 (sc-1207, Santa Cruz) and Mcl-1 (Rockland). A monoclonal antibody (10H2F6) that specifically recognizes the β 22 subunit of human Taspase1 was generated (Promab), which was utilized for the IHC and IF assays.

Immunoblot Analysis

Cellular lysates were collected in RIPA buffer (150 mM NaCl, 50 mM Tris-Cl, 0.1% SDS, 0.5% Na-deoxycholate, 1% NP-40) supplemented with Complete protease inhibitor cocktail (Roche) and separated using 10% or 12% Bis-Tris

NuPAGE gels (Invitrogen, Carlsbad, CA). Western blot images were acquired using the Fujifilm LAS-3000 system and quantified using ImageQuant software as described (Kim et al., 2006).

Immunoprecipitation of MCL-1

U251 control- and Taspase1-knockdown cell lines were lysed in EBC lysis buffer (120mM NaCl, 50mM Tris-Cl, pH 8, 0.5% NP-40) supplemented with Complete protease inhibitor cocktail (Roche) and 20mM N-ethylmaleimide. Lysates were incubated overnight at 4°C with 5µg MCL-1 antibody (SC-819, Santa Cruz) adsorbed to protein-A beads (GE Healthcare). Input and immunoprecipitated lysates were resolved on NuPAGE gels as described and blotted for MCL-1 and ubiquitin (FL-76, Santa Cruz).

Immunohistochemistry and Immunofluorescence

Paraffin-embedded primary human cancer tissue sections were obtained from the Department of Pathology and Immunology at Washington University in Saint Louis and antigen retrieval was performed using a pressure cooker (Biocare) and Target Retrieval Solution (Dako). A monoclonal antibody (10H2F6) that specifically recognizes the β 22 subunit of human Taspase1 was generated (Promab), which was utilized for the IHC and IF assays. For immunohistochemistry, glioblastoma, melanocytic nevi, and melanoma sections were stained with anti-Taspase1 monoclonal antibody (10H2F6), while melanoma and melanocytic nevi were stained with Melan A (sc20032, Santa Cruz) to detect cells of melanocytic origin. Sections were developed using the Vectastain Universal ABC Elite system (Vector Laboratories) and DAB+ chromogen (Dako) according to the manufacturer's protocol. Developed sections were counterstained with Mayer's hematoxylin (Sigma). For immunofluorescence, sections were stained with anti-Taspase1 monoclonal antibody (10H2F6) and an Alexa-488 conjugated goat-anti-mouse secondary

antibody (A11029, Invitrogen). Slides were mounted and nuclei were counterstained with Slowfade+DAPI (Invitrogen). Indirect immunofluorescence images were acquired on an Olympus (IX51) microscope with Spot Cam. Sections were quantitatively scored by capturing normal and tumor tissue in the same field of view, optimally, otherwise from the same section using identical capture settings. Pixel signal intensity was measured on acquired images using ImageJ software (NIH). For xenograft studies, freshly-isolated tumor xenografts were fixed in Bouin's fixative, and 7µm sections were subjected to antigen retrieval as stated above. Assessment of proliferative index was performed by Ki-67 staining (MIB-1 clone, Dako USA), and developed using immunoperoxidase. TUNEL staining was performed as per the manufacturer's protocol (Roche).

Tumor Xenograft Assay

U251 glioblastoma lines transduced with control- or Taspase1-shRNA retroviruses were selected for 3 days in 1.5µg/mL puromycin. Cells were then harvested and suspended in RPMI 1640 media in a 2:1 ratio with growth factor reduced Matrigel (BD Biosciences, San Jose, CA). Ten million cells were engrafted into each flank of male NOD-*scid* *IL2Rγ*^{-/-} mice (Jackson Lab) between 6-8 weeks of age. Tumor size was measured with calipers and volume determined as described previously (21). Tumor volumes were compared using a two-tailed Student's t test. For in vivo ABT-737 treatment, mice were injected with vehicle (30% propylene glycol and 5% Tween-80 in D5W, pH 4.65) when tumors reached a volume of approximately 300-500mm³.

2.11 Figures

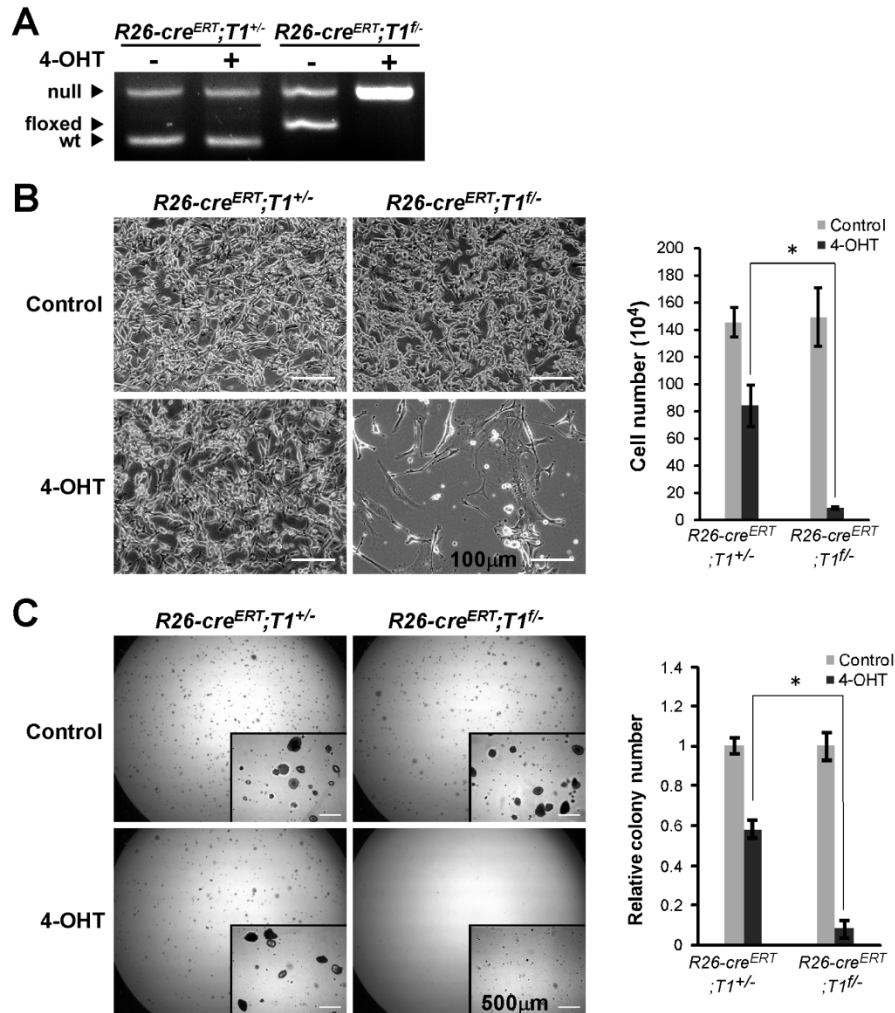


Figure 2.1. Taspase1 is required for the maintenance of MYC-RAS^{G12V} transformed mouse embryonic fibroblasts (MEFs).

A, MYC-RAS^{G12V} transduced MEFs of the indicated genotypes were treated with 500 nM 4-hydroxytamoxifen (4-OHT) for 6 hours to activate R26-creERT (a tamoxifen inducible Cre recombinase driven by the ubiquitous Rosa-26 promoter). Deletion of the conditional (*floxed*; *f*) Taspase1 allele was confirmed by PCR at day 3. **B**, 10⁵ MYC-RAS^{G12V} transduced MEFs of the indicated genotypes were mock (DMSO) or 4-OHT treated for 6 hours before plating on 6 cm dishes. Cells were photographed and counted at day 5. Data presented are mean ± SD of duplicates of three independent experiments. **C**, 5x10⁴ MYC-RAS^{G12V} transduced MEFs of the indicated genotypes were treated as in **B** and plated on soft agar. Positive clones (≥200μm) were scored 1.5-2 weeks after the initial plating. Insets are higher-magnification images. Data presented are mean ± SD of duplicates of two independent experiments. The average of colony number in mock treated plates was assigned a value of 1 for comparison. Asterisk indicates p < 0.01, determined by Fisher's exact test.

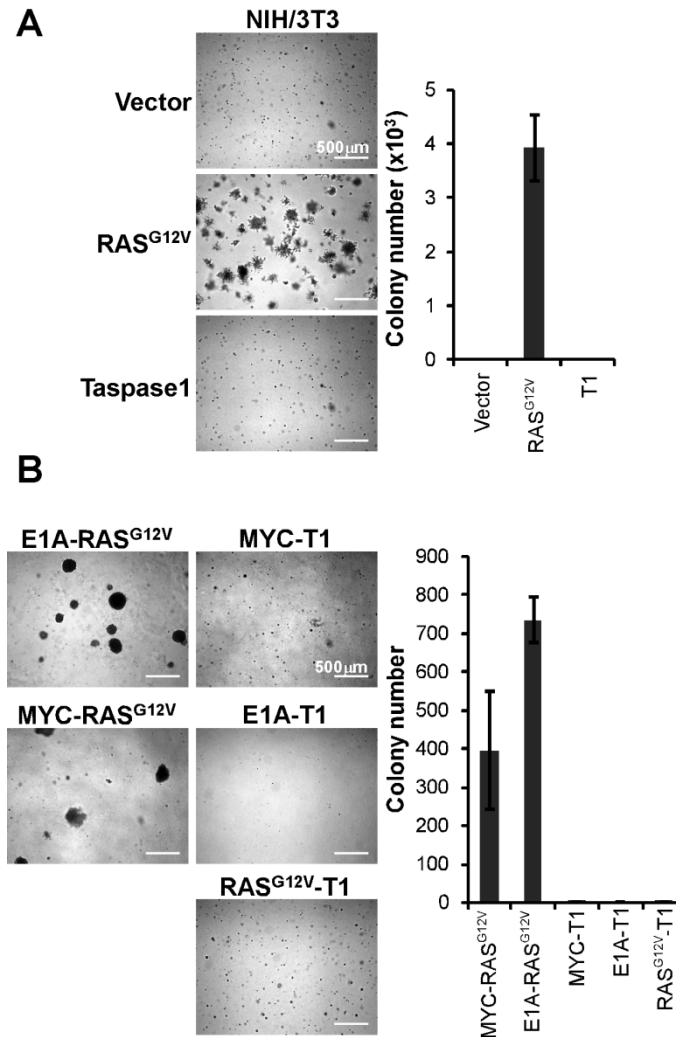


Figure 2.2. Taspase1 is not a classical oncogene.

A, NIH/3T3 cells were transduced with the indicated genes and 5×10^4 cells were plated on soft agar in each 6 cm dish. Positive clones ($\geq 200 \mu\text{m}$) were scored 10 days after the initial plating. Insets are higher-magnification images. Data presented are mean \pm SD of duplicates of two independent experiments. T1 denotes Taspase1. **B**, Wild-type primary MEFs were transduced with the indicated pairs of genes and 5×10^4 cells were plated on soft agar in each 6 cm dish. Positive clones ($\geq 200 \mu\text{m}$) were scored 2-3 weeks after the initial plating. Insets are higher-magnification images. Data presented are mean \pm SD of triplicates of two independent experiments.

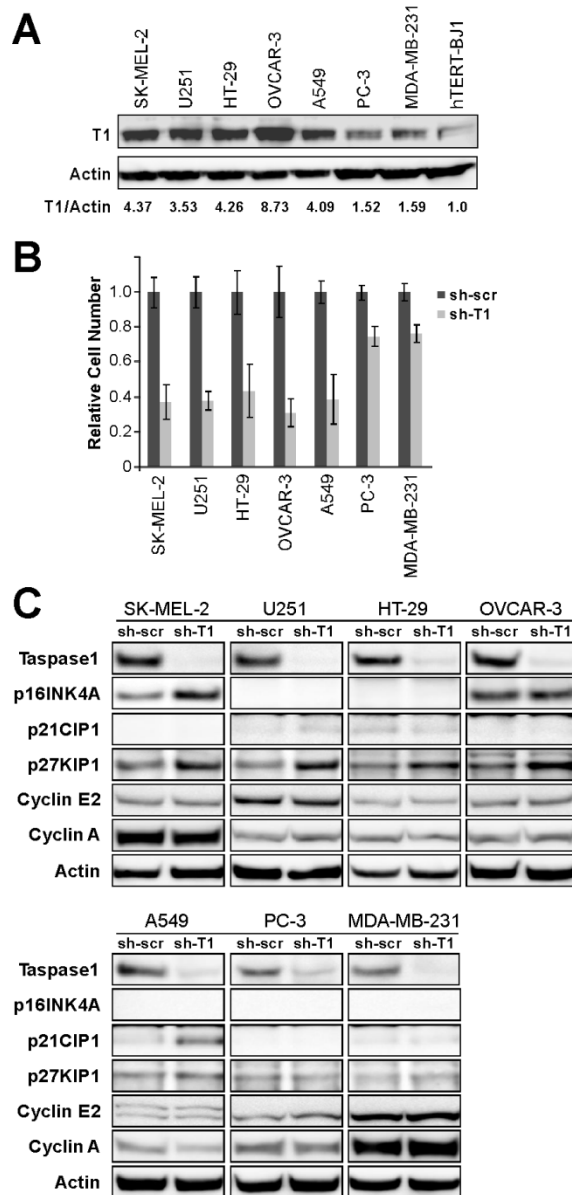


Figure 2.3. Taspase1 is required for the proliferation of human cancer cells.

A, Taspase1 protein expression of the indicated human cancer cell lines was assessed by anti-Taspase1 α 28 antibody. Western blot for β -actin indicates equal loading. The relative expression of Taspase1 versus β -actin in hTERT-BJ-1 cells was assigned a value of 1 for comparison. **B**, Human cancer cell lines with control- or Taspase1-knockdown were plated on 6-well plates and cell number was assessed four days after initial plating. The average cell number of control-shRNA cells was assigned a value of 1 for comparison. Data presented are mean \pm SD of duplicates of three independent experiments. **C**, Stable knockdown of Taspase1 in the indicated human cancer cell lines was determined by anti-Taspase1 α 28 immunoblot. The expression of p16, p21, p27, Cyclin E2, and Cyclin A was determined by respective antibodies. The β -actin immunoblots indicate equal protein loading.

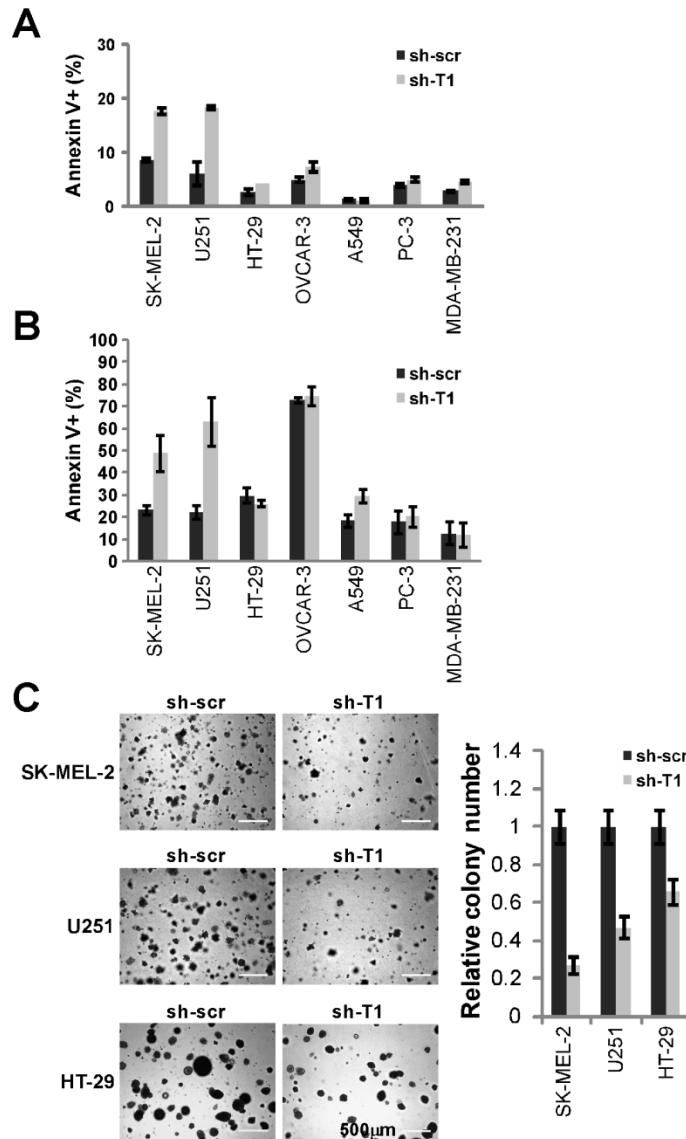


Figure 2.4. Deficiency of Taspase1 results in increased anoikis and reversion of the transformed phenotype in SK-MEL-2 melanoma and U251 glioblastoma cells.

A, Human cancer cell lines with control- or Taspase1-knockdown were stained with annexin V and analyzed by FACS to assess cell death. **B**, Human cancer cell lines with control- or Taspase1-knockdown were cultured in PolyHEMA treated 6-well plates for 3 days, stained with annexin V, and analyzed by FACS to assess cell death. **C**, SK-MEL-2 or U251 cells with control- or Taspase1-knockdown were plated on soft agar. Positive clones ($\geq 100 \mu\text{m}$) were scored 2-3 weeks after the initial plating of 10^5 cells per 6 cm dish. Annexin V stains positive for apoptotic cells. Data presented in A, B, and C are mean \pm SD duplicates of three independent experiments.

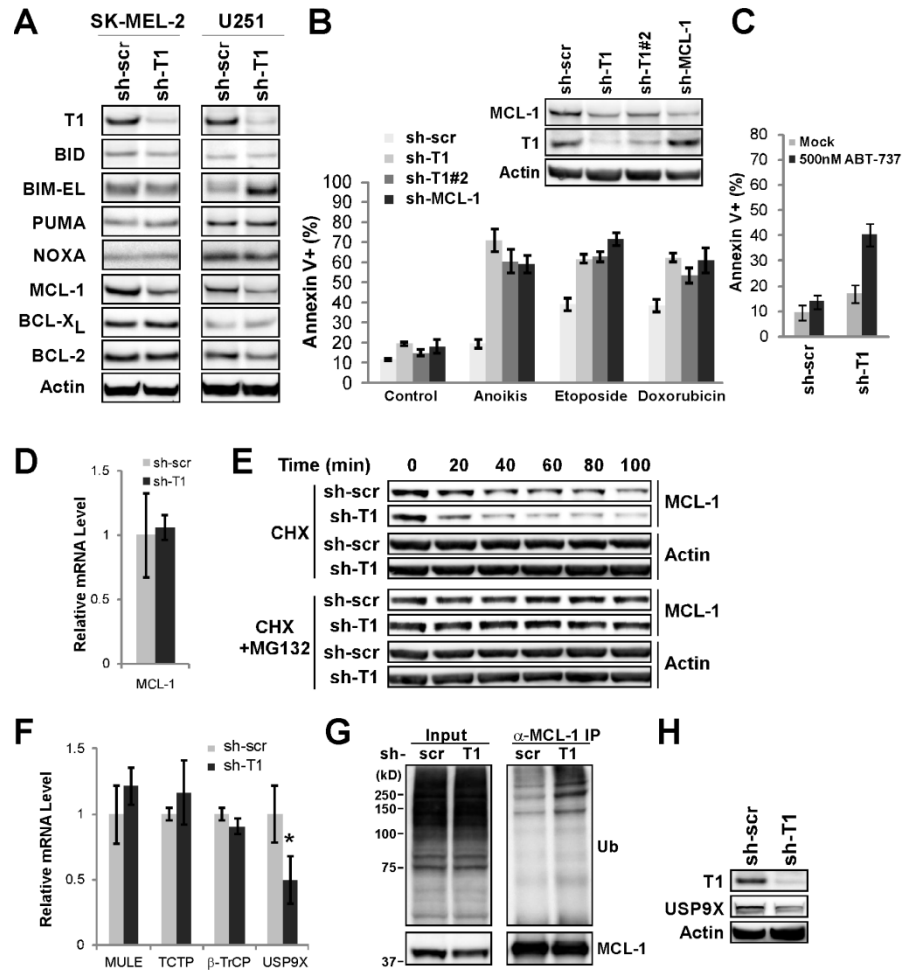


Figure 2.5. Taspase1 deficiency de-stabilizes MCL-1 protein and sensitizes U251 glioblastoma cells to cell death stimuli.

A, Cellular extracts of SK-MEL-2 or U251 cells with control- or Taspase1-knockdown were subjected to Western blot analyses using the indicated antibodies. **B**, U251 cells with the indicated knockdown were treated with various apoptotic stimuli, stained with annexin V, and analyzed by FACS. Cellular extracts of the indicated knockdown were subjected to immunoblot analyses using respective antibodies. Anoikis assay cells were plated in PolyHEMA coated plates for 3 days. For chemotherapy-induced cell death, cells were treated with 100 μ g/mL of etoposide or 10 μ M of doxorubicin for 30 hours. Data presented are mean \pm SD of duplicates of two independent experiments. **C**, U251 cells with control- or Taspase1-knockdown were mock (DMSO) or ABT-737 treated for 24 hours, and cell death assessed by FACS analysis of annexin V staining. Data presented are mean \pm SD of triplicates of two independent experiments. **D**, Transcript levels of MCL-1 in control- or Taspase1-knockdown U251 cells were determined by quantitative RT-PCR analysis where the transcript level in control-knockdown cells was assigned a value of 1 for comparison. **E**, U251 cells with control- or Taspase1-knockdown were subjected to cyclohexamide with or without MG132 treatment for the indicated periods of time, and protein levels of MCL-1 and β -actin were determined by immunoblot. **F**, Analysis of transcript levels for known regulators of MCL-1 stability, including MULE, β -TrCP, TCTP, and USP9X. **G**, U251 treated with MG132 were lysed and immunoprecipitated for endogenous MCL-1. Ubiquitin immunoblot determines MCL-1 ubiquitination state. **H**, USP9X levels were determined for U251 control- and Taspase1-knockdown by immunoblot. Thanks go to H. Liu for MCL-1 stability and ubiquitination westerns, and to S. Takeda for MCL-1 qPCR.

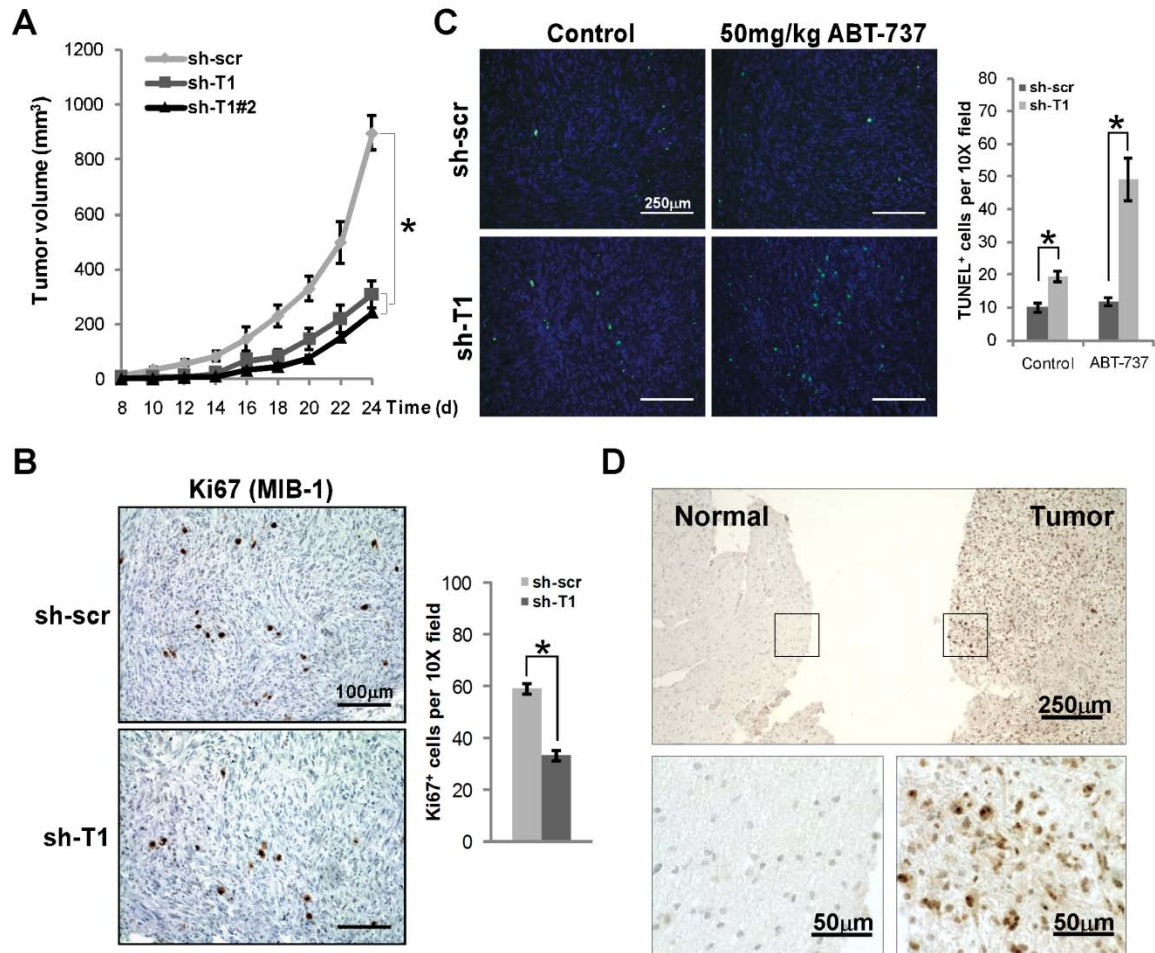


Figure 2.6. Taspase1 is over-expressed in human glioblastoma and is required for U251 glioblastoma maintenance in vivo.

A, U251 cells with control- or Taspase1-knockdown were injected into the flanks of NOD-*scid* *IL2Rγ*^{-/-} mice and tumor growth was measured every other day. * indicates $p < 0.001$. **B**, Proliferative index of U251 xenografts was determined by Ki-67 immunohistochemistry. Sections shown at 20X magnification. Bar graph represents mean \pm SEM of Ki-67+ cells per 10X field (10 fields per tumor, $n=2$ tumors each). **C**, Cell death resulting from ABT-737 treatment was assessed by TUNEL assay 12h after a single IP injection of vehicle control or ABT-737. Sections shown are 10X fields of FITC-TdT (green) and DAPI (blue). Bar graph represents mean \pm SEM of TUNEL+ cells per 10X fields (10 fields per tumor, $n=2$ tumors each). **D**, Immunohistochemical analysis of Taspase1 expression in primary human GBM and adjacent normal brain using an anti-Taspase1 monoclonal antibody (10H2F6). High magnification pictures of boxed areas are provided where the left panel is normal and the right is tumor.

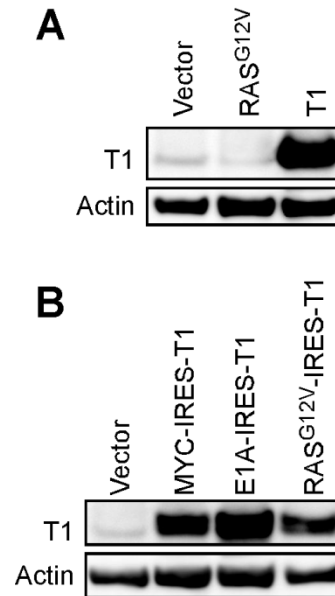


Figure 2.7. Taspase1 over-expression in NIH/3T3 and primary MEFs.

A, Western blot analysis of Taspase1 expression in NIH/3T3 cells transduced with vector control, RAS^{G12V}, and human Taspase1 (T1). **B**, Western blot analysis of Taspase1 expression in primary MEFs transduced with vector control or Taspase1 in conjunction with the indicated oncogenes.

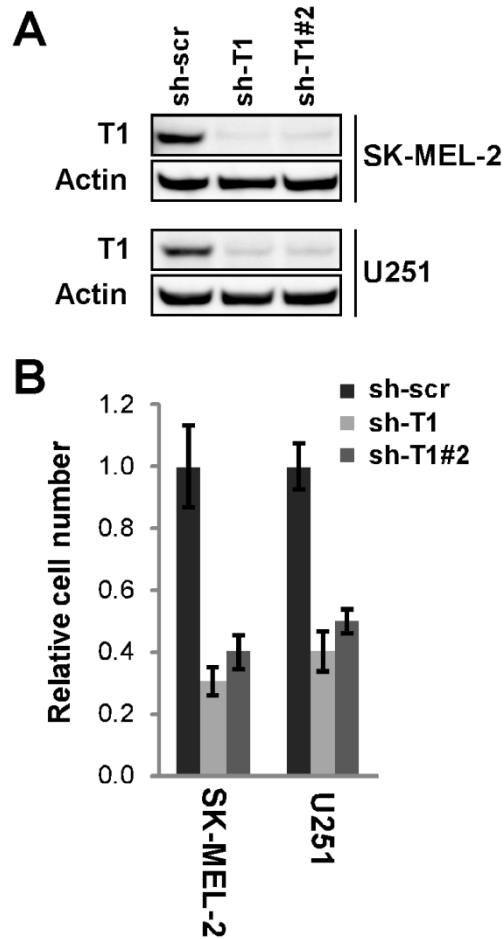


Figure 2.8. Taspase1 loss using two, independent sh-RNAs impedes proliferation in SK-MEL-2 and U251.

A, Western blot analysis of Taspase1 level in U251 and SK-MEL-2 cell lines transduced with Taspase1 shRNA constructs. **B**, Cells with the indicated knockdown were plated on 6 well plates and counted four days after the initial plating. Data represents the proportion of cells compared to control knockdown where the average cell number of control knockdown cells was assigned a value of 1. Data presented are mean \pm SD of duplicates of two independent experiments.

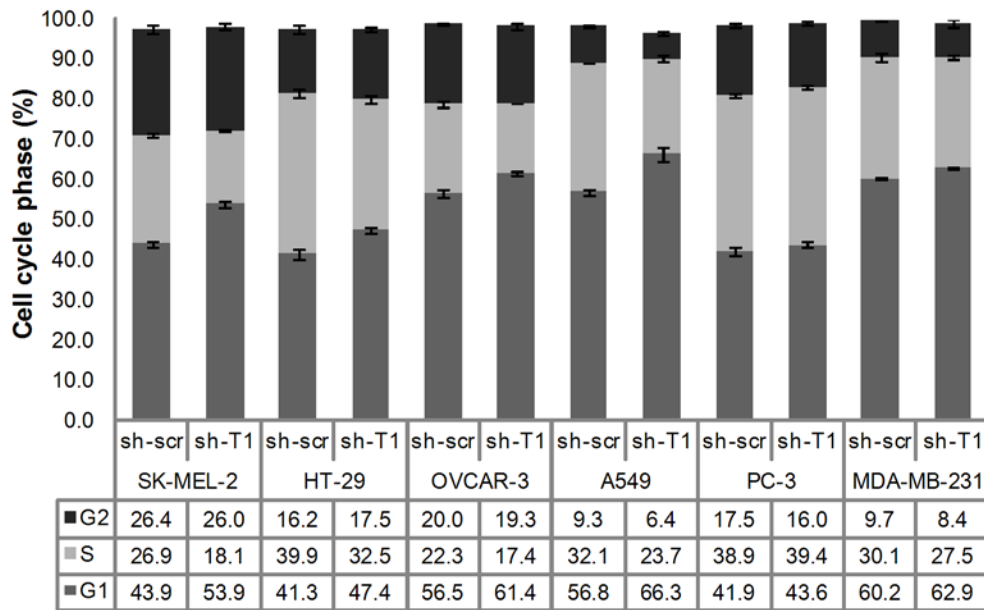


Figure 2.9. Cell cycle analysis of human cancer cell lines with Taspase1 deficiency

Cell cycle analyses of cancer cell lines with control- or Taspase1-knockdown by propidium iodide (PI) staining and FACS analysis for DNA content. U251 cells were not included due to highly variable DNA content (Pershouse et al., 1993).

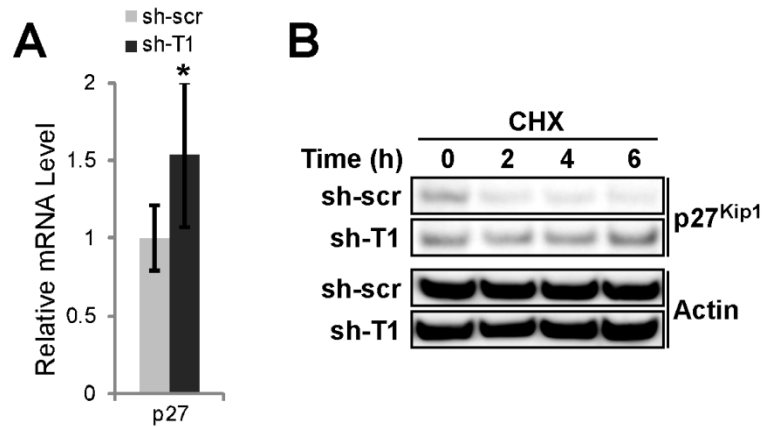


Figure 2.10. Analysis of p27^{KIP1} regulation in U251 with Taspase1 deficiency.

A, Transcript level of p27^{KIP1} was determined by qRT-PCR, where U251 control knockdown was assigned a value of 1. Asterisk indicates $p < 0.05$. **B**, U251 cells with control- or Taspase1-knockdown were treated with 10 μ g/mL cycloheximide for the indicated times and immunoblotted for p27^{KIP1}. Actin blot indicates equal loading.

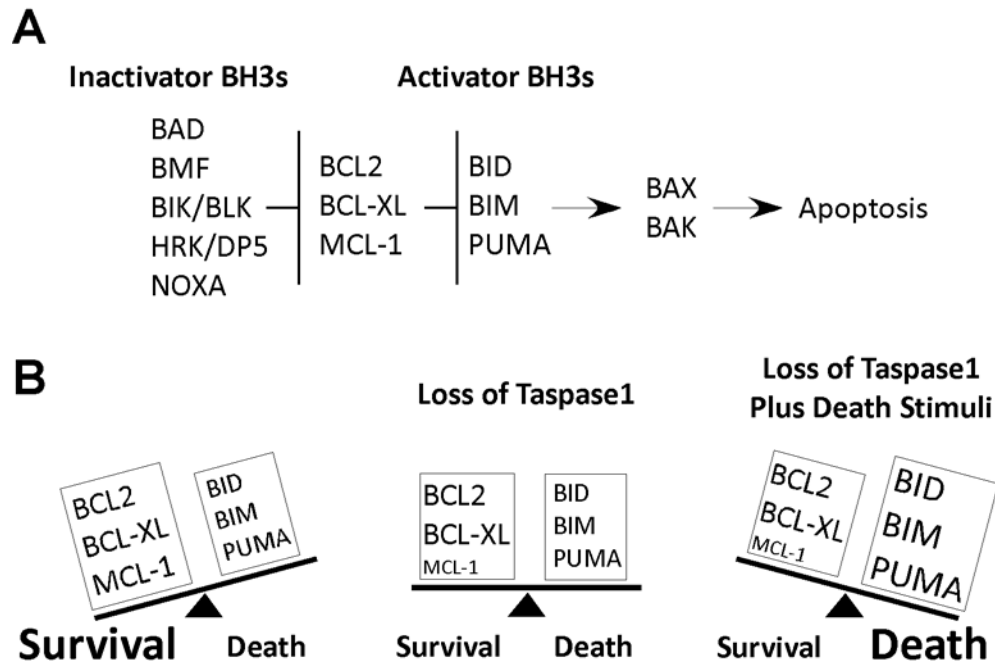


Figure 2.11. Models for the core apoptotic pathway and its interaction with Taspase1

A, Model depicts the hierarchical regulation of apoptosis. **B**, Model for the loss of Taspase1 expression in regulation of cell death in susceptible cancer cells.

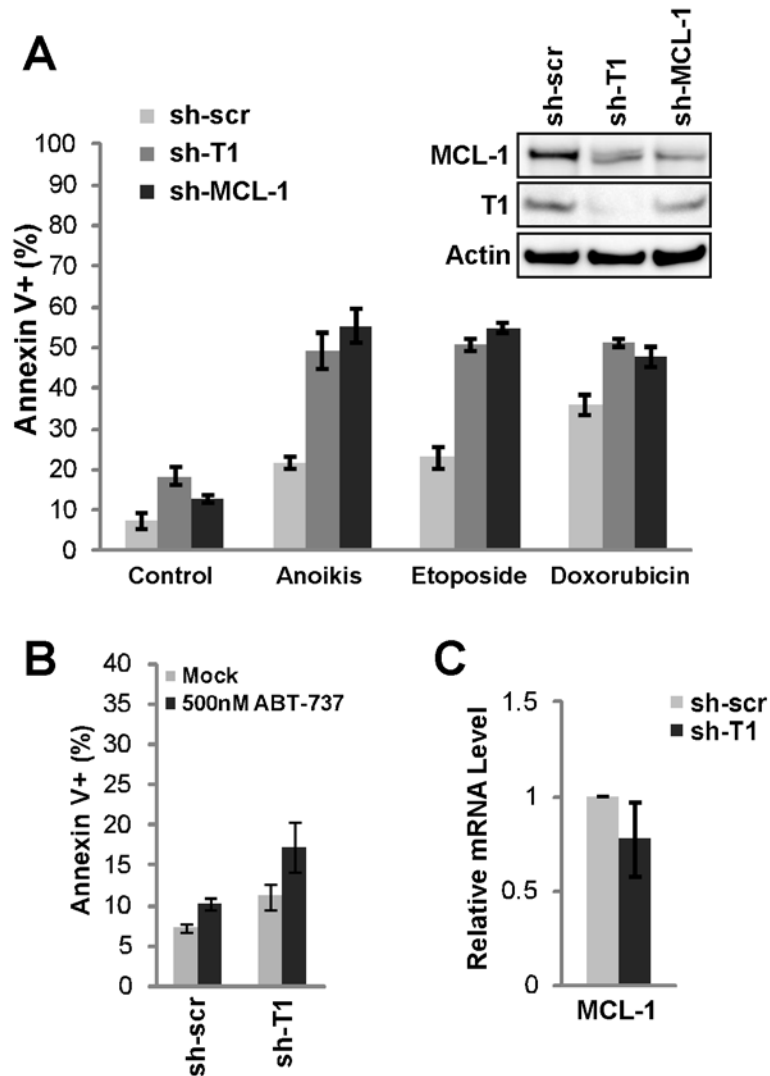


Figure 2.12. Analysis of SK-MEL-2 sensitivity to cell death with Taspase1 deficiency

A, SK-MEL-2 melanoma cells with control-, Taspase1-, and MCL1-knockdown were analyzed for cell death by annexin V staining after being subjected to polyHEMA culture for 3 days, or 200 μ g/mL etoposide or 10 μ M doxorubicin for 30 hours. Data presented are mean \pm SD of duplicates of two independent experiments. **B**, SK-MEL-2 cells with control- or Taspase1-knockdown were treated with DMSO (mock) or 500nM of ABT-737 for 24 hours and analyzed for cell death by annexin V staining. Data presented are mean \pm SD of triplicates of two independent experiments. **C**, MCL-1 transcript level in SK-MEL-2 was determined by quantitative RT-PCR analysis. Data presented are mean \pm SD of duplicates of two independent experiments.

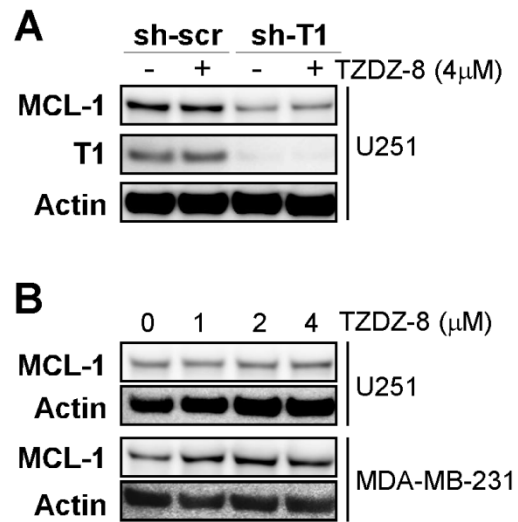


Figure 2.13. MCL-1 level is not stabilized by GSK3- β inhibition in Taspase1-deficient cells

A, U251 cells with control- or Taspase1-knockdown were subjected to treatment with 4 μ M TZDZ-8, an inhibitor of GSK3 β , for 12 hours, and protein levels were determined with the indicated antibodies. **B**, U251 and MDA-MB-231 cells were treated with the indicated doses of TZDZ-8 for 12 hours and the protein levels were determined with the indicated antibodies. MCL-1 was stabilized in MDA-MB-231 but not U251 cells upon the inhibition of GSK3- β .

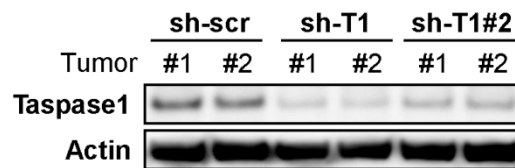
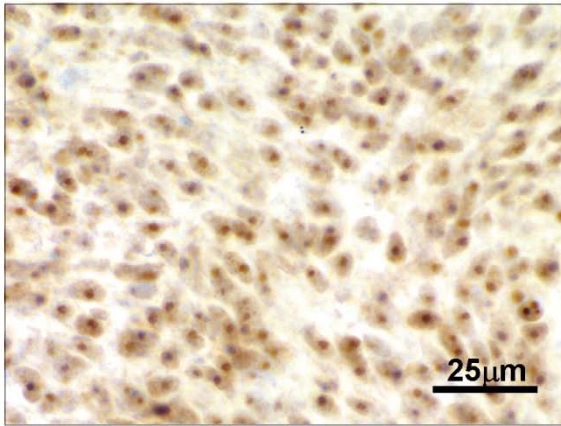


Figure 2.14. Taspase1 levels in U251 glioblastoma xenografts.

Individual tumors expressing the indicated knockdown construct were harvested from xenografted NOD-*scid*;*IL2R γ* ^{-/-} mice at day 24 post-injection. Tumor lysates were prepared and subjected to immunoblot analyses with the indicated antibodies.

Control Blocking



Immunogen Blocking

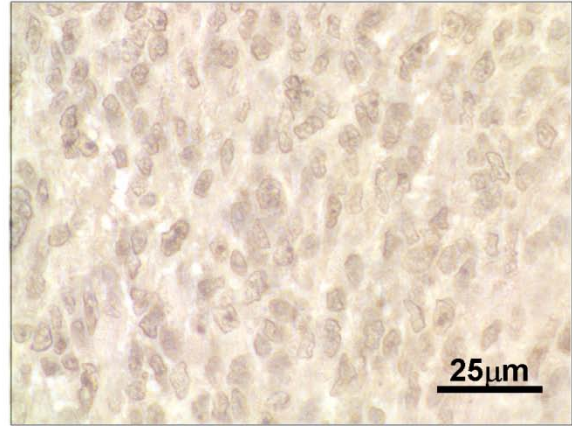


Figure 2.16. Demonstration of the specificity of Taspase1 immunohistochemistry.

The specificity of immunohistochemical staining for Taspase1 expression in primary glioblastoma tissues by the anti-Taspase1 primary antibody (10H2F6) was demonstrated by the loss of staining when 50 µg/mL of the recombinant Taspase1 immunogen but not 50 µg/mL BSA (non-specific control) was pre-incubated with the antibody before staining.

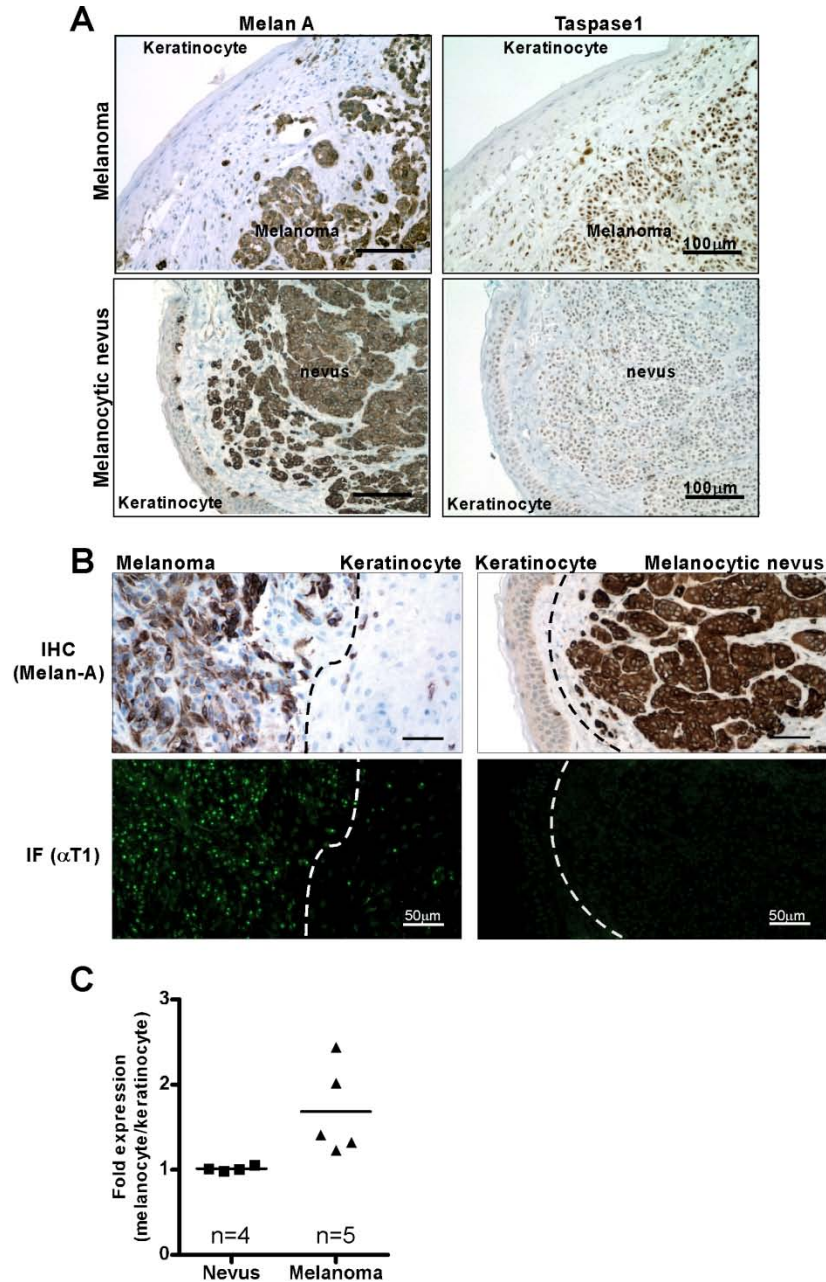


Figure 2.17. Examination of Taspase1 expression in melanoma.

A, Immunohistochemical analysis of Taspase1 expression in melanoma and melanocytic nevus was performed with an anti-Taspase1 monoclonal antibody (10H2F6) (right). Immunohistochemical stain of consecutive sections using an anti-Melan A antibody identify both benign and malignant melanocytes as a reference (left). **B**, Immunofluorescence analysis of Taspase1 expression on melanoma (left bottom panel) and melanocytic nevus (right bottom panel) was performed with an anti-Taspase1 monoclonal antibody (10H2F6), where dotted lines demarcate regions that are predominantly melanocytes from keratinocytes. Immunohistochemical stain of consecutive sections using an anti-Melan A antibody identify both benign and malignant melanocytes as a reference (top two panels).

Cell line	Type	p53	CDKN2A	Ras	STK11	PIK3CA	BRAF	SMAD4	APC	NF2	PTEN
SK-MEL-2	malignant melanoma	G245S		N-Ras Q61R							
U251	glioblastoma	R273H	M1*157del								E242fs*15
HT-29	large bowel carcinoma	R273H				P449T	V600E	Q311*	T1446FS*3, E853*		
OVCA-R-3	ovarian adenocarcinoma	R248Q									
A549	lung adenocarcinoma		M1*157del	K-Ras G12S	Q37*						
PC-3	prostate adenocarcinoma	K139fs*31									R55fs*1
MDA-MB-231	breast pleural effusion	R280K	M1*157del	K-Ras G13D			G464V			E231*	

Table 2.1. Mutation status of sequenced genes in the NCI60 cancer cell lines used in this study.

Known mutations in the cancer cell lines used in this study were retrieved from the Cancer Genome Project (<http://www.sanger.ac.uk/genetics/CGP>).

Chapter 3

Taspase1 inhibitors: rational design and small molecule high throughput screening

- 3.1 Taspase1 is an evolutionarily conserved threonine protease important in tumorigenesis and tumor maintenance
- 3.2 Rational design of peptidomimetic inhibitors for Taspase1
- 3.3 A cell based dual-fluorescence reporter screen identifies NSC48300/TASPIN-1 as a potent inhibitor of Taspase1 in vitro and in vivo
- 3.4 FRET-based screening reveals further leads for Taspase1 inhibitors
- 3.5 Methods and Materials
- 3.6 Figures

3.1 Taspase1 is an evolutionarily conserved threonine protease important in tumorigenesis and maintenance

Taspase1 is an evolutionarily conserved N-terminal nucleophile protease

Taspase1 is a threonine endopeptidase that is highly conserved from plants to fish, flies, and man. Taspase1 is translated as a 50kDa proenzyme that is comprised almost entirely of an Asparaginase_2 domain (Pfam PF01112), which is part of a larger superfamily of proteins known as the N-terminal nucleophile (Ntn) hydrolases. As the name suggests, reactive nucleophiles of this family reside on the N-terminus of mature Ntn hydrolases, which are typically translated as proenzymes that require autoproteolytic activation. At the core of the Ntn hydrolase structure resides an $\alpha\beta\alpha$ folding motif with α helices flanking anti-parallel β sheets, which is true of Taspase1 as well (Figure 3.1), though the crystal structure reveals significant conformational divergence from other Asparaginase_2 proteins (Khan et al., 2005).

Other members of the Asparaginase_2 family include L-asparaginase, which catalyzes the deamidation of asparagine to aspartic acid and aspartyl-glucosaminidase (AGA), which is involved in the breakdown of N-linked glycoproteins, thus making Taspase1 the only protease in this family. Despite divergence in structural conformation and substrate specificity, autocatalytic activation is a common feature of Ntn hydrolases, where the active nucleophile in the mature enzyme is also thought to be the autocatalytic nucleophile (Saarela et al., 2004). The maturation from Ntn pro-enzymes involves an initial N \rightarrow O acyl rearrangement, which reveals the catalytic α -amino group on the threonine nucleophile. In lysosomal AGA, like Taspase1, aspartic acid precedes the threonine nucleophile, and it is thought to provide conformational strain, promoting activation.

Autoproteolysis of the Taspase1 pro-enzyme forms a mature $\alpha 28/\beta 22$ heterodimeric enzyme which further assembles into the active heterotetrameric enzyme (Hsieh et al., 2003a; Khan et al., 2005). Taspase1-mediated cleavage follows distinct aspartate residues of conserved

Q Ψ D/GXXD motifs (Figure 3.1). Taspase1 was cloned as the protease responsible for the proteolytic maturation of the human homolog of *Drosophila trithorax*, Mixed Lineage Leukemia (MLL). Since its discovery, additional Taspase1 substrates were identified, including MLL2, TFIIA α - β (GTF2A1), ALF (TFIIA τ), and *Drosophila* HCF (dHCF), which are all nuclear factors, suggesting that Taspase1 potentially modulates a broad array of biological processes (Capotosti et al., 2007; Takeda et al., 2006b; Zhou et al., 2006). Indeed Taspase1-mediated maturation of HCF and MLL is critical for orchestrating cell cycle progression (Julien and Herr, 2003; Takeda et al., 2006b).

Taspase1 is required for tumor maintenance

Our prior studies demonstrated that Taspase1 is required for efficient oncogenic transformation and is critical for maintenance of the transformed phenotype in genetically defined murine tumor cells. Deficiency of Taspase1 decreased the proliferative capacity of a variety of human cancer cell lines, including melanoma, glioblastoma and adenocarcinoma of the colon, ovary, lung, prostate, and breast. In certain cell lines, Taspase1 maintains the expression of the anti-apoptotic BCL-2 family member MCL-1. Loss of Taspase1 in the glioblastoma cell line U251 increased its sensitivity to chemotherapies like doxorubin and etoposide, in vitro. Mechanistically, we expected the decrease in MCL-1 level to increase the sensitivity to the selective BCL-2/BCL-X_L antagonist ABT-737. Indeed, Taspase1 deficiency caused U251 glioblastoma to have a lower proliferative index, increased basal cell death, and increased sensitivity to ABT-737 treatment in vivo. The anti-cancer effect of Taspase1 loss in cancer cell lines in vitro and in vivo, and that Taspase1 is over-expressed in human cancers, spurred the search for Taspase1 inhibitors to validate Taspase1 as a pharmacological target for cancer therapy (Niehof and Borlak, 2008; Scrideli et al., 2008; Takeda et al., 2006b).

3.2 Rational Design of peptidomimetic inhibitors of Taspase1

Structural properties of Taspase1 guide rational design of peptide inhibitors

Taspase1 has an exquisite specificity for its substrate cleavage site. MLL harbors two Taspase1 cleavage sites—cleavage site 1 and 2 (CS1 and CS2), which are separated by 53 amino acids, where CS2 is thought to be more efficiently processed than CS1 (Hsieh et al., 2003a). Alanine scanning mutagenesis of the MLL CS2 (KISQLD/GVDD) reveals a low tolerance for substitutions in the cleavage site consensus. Mutations revealed that the P1 aspartate and P1' glycine are essential, while P2 leucine, P3 glutamine, and P5 isoleucine are important but non-essential for Taspase1-mediated proteolysis, whereas aspartates at position P3' and P4' are dispensable (Chen, et al. in preparation). With such specificity, rational design of a Taspase1 inhibitor might be possible, based on a short peptide specific to Taspase1 substrate MLL CS2.

Methods for assessment of Taspase1 inhibition

To assess potential inhibitors, we generated three assays and adapted them for validation of Taspase1 inhibition, screening for further inhibitors of Taspase1, or both. The first was established while isolating Taspase1, employing an activity-based purification scheme which utilized an in vitro cleavage system to chase MLL-cleavage ability in cellular fractions (Hsieh et al., 2003a). An in vitro transcribed and translated (IVTT), ³⁵S methionine-labeled fragment of human MLL1 (aa2,500-2,800) with a mutation engineered at the CS1, was employed as a CS2-specific cleavage reporter (p45^{MLL/CS2}). The cleavage of p45^{MLL/CS2} by recombinant Taspase1 (rTaspase1) was resolved by SDS-PAGE and examined by autoradiography. Inhibition of Taspase1 cleavage results in the disappearance of cleaved product p33 and an increase in the non-cleaved p45^{MLL/CS2} (Figure 3.2). Though this method benefits from high specificity, it is not practical for use as a high-throughput screening method.

The second assay is a cell-based assay developed as a method to assess the ability of potential Taspase1 inhibitors to penetrate the plasma membrane and inhibit Taspase1 mediated cleavage of a dual-fluorescent reporter substrate. A 293T human embryonic kidney cell line was

engineered to stably express a dual fluorescent Taspase1 proteolytic reporter (DFPR). The DFPR is constructed from a peptide similar to the in vitro cleavage assay described previously. The DFPR reporter consists of the MLL polypeptide (aa2,400-2,900, p75^{MLL}), which contains the CS1 and CS2 Taspase1 cleavage sites and is flanked on the N-terminal by EGFP/NES (nuclear export signal) fusion and on the C-terminal by a NLS (nuclear localization signal)/dsRED2 fusion. Upon Taspase1-mediated cleavage, DFPR displays cytosolic green (eGFP/NES-p47) and nuclear red fluorescence (p28-NLS/dsRED2) that can be detected by fluorescence microscopy. Inhibition of Taspase1 results in non-cleavage of newly synthesized DFPR, exhibiting increased yellow fluorescence upon the merge of green and red fluorescence (Figure 3.3). This method is suitable for microscopy based high throughput screening, and though the sensitivity and specificity of Taspase1 cleavage inhibition is less than that of the in vitro cleavage assay, this assay readily identifies compounds which are already bioactive.

The final assay developed to assess Taspase1 inhibition is a FRET (Fluorescence Resonance Energy Transfer)-based in vitro cleavage assay. The FRET-based Taspase1 proteolytic reporter (FRPR, MCA-KISQLDGVDD-DNP) consists of a 10 amino acid MLL CS2 consensus sequence conjugated with a fluorogenic coumarin (MCA) group and a 2,4-dinitrophenyl (DNP) quenching group at its N- and C-terminus, respectively (Figure 3.4). Cleavage of the FRPR substrate can be monitored over time using a spectrofluorometer, and the kinetics of inhibition can be determined by varying the inhibitor concentration and performing non-linear regression on the aggregated reaction progress curves. In this regard, this FRET-based assay was validated by establishing that HTI-9 (ISQLAGVDD) which is an alanine mutant of the cleavage reporter acts as a competitive inhibitor of the FRPR cleavage reaction (Figure 3.5). This assay has been adapted for both for determination of inhibition kinetics as well as a high throughput screen, where a dose-responsive decrease in endpoint fluorescence is scored as positive for Taspase1 inhibitory activity.

Rational design of peptide-based Taspase1 inhibitors

The only other characterized threonine nucleophile protease in the human genome is the proteasome, which, like Taspase1, is a member of the Ntn hydrolase superfamily. The original proteasome inhibitors consisted of peptidyl aldehydes which inhibited the proteasome by forming a hemi-acetal adduct with the threonine nucleophile. Based on subsequent studies revealing that leucine is the preferred P1 position for proteasomeal cleavage, a Phe-Leu dipeptidyl boronic acid was developed with specific sub-nanomolar inhibitory activity against the proteasome. The boronic acid was postulated to form stable tetrahedral intermediates with the threonine nucleophile, while remaining much less reactive to cysteine proteases because of the weak bonding efficiency between sulfur and boron (Adams et al., 1998). The dipeptidyl boronic acid, known now as Velcade (bortezomib), has single agent efficacy in treatment of multiple myeloma (MM) and non-Hodgkin's lymphoma (NHL).

Second generation peptide-based proteasome inhibitors have been generated with epoxyketone pharmacophores, which was a development based on the observation that a microbial anti-tumor natural product epoxomicin had inhibitory activity at the proteasome (Sin et al., 1999). The potent and specific inhibition of the proteasome was structurally defined by its selective binding of the peptide sequence to the substrate binding site of the proteasome as well as the stereospecific and irreversible interaction of the epoxyketone with the reactive threonine nucleophile (Groll et al., 2000). Subsequent modification of a Phe-Leu-Phe-Leu tetrapeptide epoxyketone generated the proteasome inhibitor carfilzomib, which is currently under clinical trial for MM (Demo et al., 2007; Eloffson et al., 1999).

Based on the proteasome as a precedent for rational design of effective threonine protease inhibitors, we collaborated with M. Bogoy and colleagues at Stanford University to design, generate, and test short peptide inhibitors for Taspase1. Additionally, the evolutionary history of Taspase1 informs the placement of reactive pharmacophores. As a descendant of an

asparaginase, which cleaves the isopeptide bond on asparagines to generate aspartate, Taspase1 may have specificity for either main chain substrates, or isopeptide substitutions.

Based on the MLL CS2, the ISQLD peptide was modified on the P1 aspartic acid residue to bear vinyl sulfone, vinyl ketone, epoxyketone, and boronic acid pharmacophores, which are known to be effective at inhibiting the proteasome threonine nucleophile (Figure 3.6) (Lee et al., 2009). Using the FRET-based kinetics assay, the vinyl sulfone substitution (yzm18) on the main backbone of the peptide inhibitor exhibited the most potent activity with an IC_{50} of $29\mu\text{M}$, while the vinyl ketone (yzm19) was less potent with an IC_{50} of $63\mu\text{M}$. Interestingly, the vinyl sulfone placed on the P1 aspartate side chain was minimally active with an $IC_{50} > 100\mu\text{M}$, suggesting pharmacophores, at least the vinyl sulfone, placed on the main chain are likely to be more potent inhibitors of Taspase1 (Figure 3.6). Continued incubation with yzm18 did not increase the potency of substrate cleavage inhibition, suggesting that yzm18 is not acting as a covalent, irreversible inhibitor of Taspase1 (Figure 3.7).

Treatment of SV40-transformed murine embryonic fibroblasts (MEFs) with the ISQLD-vinyl sulfone had minimal ability to inhibit cellular proliferation, which is a phenotype expected from Taspase1 loss, based on our previous studies (Figure 3.8) (Takeda et al., 2006b). Whether this is due to poor cell permeability, relatively weak ability to inhibit Taspase1, or both is a matter for further investigation. Although the in vivo application of ISQLD-vinyl sulfone was limited, these inhibitors represent a proof of principal of rationally designed, peptide-based Taspase1 inhibitors and offers valuable mechanistic insights to aid the future development of more potent inhibitors.

3.3 A cell based dual-fluorescence reporter screen identifies TASPIN-1 as a potent inhibitor of Taspase1 in vitro and in vivo

A cell-based screen to identify small molecule inhibitors of Taspase1

To identify bioactive Taspase1 inhibitors, we employed a cell-based screen using a 293T cell line expressing a dual fluorescence Taspase1 substrate cleavage reporter where inhibition of Taspase1 results in the non-cleavage of the reporter and subsequent co-localization of red and green signals, as described in section 3.2. We screened the National Cancer institute's Developmental Therapeutics Program (NCI-DTP) diversity set library of 1,900 compounds and identified 50 candidate inhibitors. A secondary screen using the in vitro cleavage assay was performed, which confirmed five compounds as highly active Taspase1 inhibitors (Figure 3.9). To further characterize these inhibitors, a tertiary screen was undertaken in which we employed the well-characterized Caspase-8-mediated cleavage of the BH3-only molecule BID as a reporter system to assess the target promiscuity of identified inhibitors. Caspases, like Taspase1, proteolyze substrates after the P1 aspartate of their target cleavage sequence (Zha et al., 2000) and thus can serve as a stringent control for the specificity of any observed inhibitory activity. Among the top five compounds exhibiting Taspase1 inhibitory activity, four have no specificity for Taspase1 over Caspase 8 inhibition, while one compound—NSC48300—only targets Taspase1 (Figure 3.9). This establishes NSC48300, [4-[(4-arsenophenyl)methyl]phenyl] arsonic acid, as a very specific small-molecule Taspase1 inhibitor and was thus designated as TASPIN-1.

TASPIN-1 is a non-competitive and reversible inhibitor of Taspase1

To characterize NSC48300/TASPIN-1 further, we employed the in vitro cleavage assay to determine whether TASPIN-1 is a more potent inhibitor than our previously described peptide vinyl sulfone (yzm18). The IC_{50} for TASPIN-1 is less than $10\mu\text{M}$ (Figure 3.10 A), which is less than the IC_{50} of yzm18. Like yzm18, it appears that TASPIN-1 is a reversible inhibitor of Taspase1 as increased time of incubation with Taspase1 does not increase the inhibition of substrate cleavage (Figure 3.10 B). Interestingly, the overall structure of TASPIN-1, including its

hydrophobic, symmetric core specifies its inhibitory capability as free arsenic acid itself does not inhibit Taspase1, even at high concentrations (Figure 3.10 A). In silico pharmacophore modeling based on TASPIN-1 predicted several possible inhibitors already in the NCI chemical repository by docking TASPIN-1 in the crystal structure for Taspase1 and assuming a tetrahedral Asp-Gly adduct as a model. These structural probes, when tested, suggest that the arsenic acid moiety is still important for inhibitory activity, and that substitutions on the hydrophobic core of NSC48300/TASPIN-1 decrease the potency of inhibition (Figure 3.10).

To characterize the mechanism by which NSC48300/TASPIN-1 inhibits Taspase1, we performed kinetic analyses using a FRET-based kinetics assay. Taspase1 incubation with the quenched pair fluorescence probe MCA-KISQLDGVDD-DNP results in its cleavage and release of the DNP quencher and subsequent linear accumulation in fluorescent signal over time (Figure 3.5 and 3.11). This analysis determined an apparent K_M of the FRPR as $9.20 \pm 2.43 \mu\text{M}$ (Figure 3.11). Reaction progress was monitored with varying concentrations of TASPIN-1 and steady state rates were plotted against varying reporter substrate concentrations. Non-linear regression was performed and fitting the model from equation 1 (see Methods and Materials) revealed that TASPIN-1 is a non-competitive inhibitor of Taspase1 with a K_i of $4.22 \pm 0.46 \mu\text{M}$ and α value of 1.01 (Figure 3.11, equation 2 in Methods and Materials).

TASPIN-1 treatment recapitulates the biology of the genetic loss of Taspase1

As the initial screen employed to identify TASPIN-1 specifically identifies bioactive molecules, we assessed the molecular effects on cells treated with TASPIN-1 to determine whether TASPIN-1 could recapitulate the effects resulting from the acute, genetic deficiency of Taspase1. MYC and RAS^{G12V} transformed murine embryonic fibroblasts (MEFs) generated from *Rosa26-cre^{ERT};Taspase1^f* mice can be induced to excise the remaining allele of Taspase1 by induction of Cre-recombinase activity by treatment with the estrogen analog 4-hydroxytamoxifen. After the excision of and subsequent loss of Taspase1 expression, MYC-RAS^{G12V} transformed MEFs exhibit a proliferative block characterized by down-regulation of G1/S Cyclins, including Cyclin A

and Cyclin E2, with minimal increase in the upstream cyclin dependent kinase inhibitors (CDKIs) in contrast to that observed in the human cancer cell lines that lose Taspase1 expression by sh-RNA. Transformed fibroblasts that do not bear a conditional allele of Taspase1 (*Rosa26-cre^{ERT};Taspase1^{+/-}*) serve as a control for Cre-recombinase induction (Figure 3.12).

Concordantly, treatment of primary MEFs with TASPIN-1 caused a dose-dependent inhibition of substrate cleavage, as assessed by disappearance of the MLL^{C180} cleavage product as well as the increase in non-cleaved TFIIA $\alpha\beta$ and loss of the TFIIA α cleavage product (Figure 3.13). Loss of Taspase1 substrate cleavage results in a corresponding loss of Cyclin A expression to the level seen in Taspase1-null MEFs (Figure 3.13). Taken together, treatment with TASPIN-1 recapitulates the Taspase1 null phenotype, suggesting that it can effectively inhibit Taspase1 function in cells. Furthermore, TASPIN-1 treatment of SV40-transformed MEFs preferentially prohibits proliferation of Taspase1-expressing cells rather than Taspase1-null cells. As genetic loss of Taspase1 in MEFs causes decreased proliferation, the biological effects of TASPIN-1 likely due, at least in part, to on-target Taspase1 inhibition. This is demonstrated by the restored sensitivity of Taspase1-null MEFs to TASPIN-1 treatment when reconstituted with Taspase1 expression (Figure 3.13).

TASPIN-1 is a Taspase1-specific anti-cancer drug

Publicly available data from the NCI Developmental Therapeutics Program NCI60 cancer cell line panel anticancer drug screen yielded a distinct pattern of growth inhibition by NSC48300/TASPIN-1 (Shoemaker, 2006). Remarkably, the sensitivity of individual cancer cell lines to TASPIN-1 correlates well with the expression of Taspase1 within certain subtypes of human cancer, namely breast and glioblastoma (Figure 3.14 and 3.15). Our prior analysis of the NCI60 panel of cell lines reveals that many cancer cell lines highly express Taspase1 when compared to the non-transformed, immortalized fibroblast cell line hTERT-BJ1 (Takeda et al., 2006b). In agreement with our prior study, which suggests that cell lines which express higher levels of Taspase1 are more dependent on Taspase1 for continued proliferation and survival, the

ability of TASPIN-1 to cause growth inhibition (GI_{50}) correlates well with the relative expression of Taspase1 in breast cancer and glioblastoma cell lines (Figure 3.14 and 3.15).

Comparison of MCF7 and MDA-MB-231, high and low Taspase1-expressing breast cancer cell lines, respectively, with acute loss of Taspase1 expression mediated by Taspase1 shRNA reveals that MCF7 is more sensitive to Taspase1 loss than MDA-MB-231. Taspase1 down-regulation results in a more severe proliferative defect in MCF7, as exhibited by decreased cell count compared to control cells. Moreover the proportion of actively proliferating cells is decreased specifically in MCF7 with Taspase1 deficiency as determined by propidium iodide staining (Figure 3.16). Accordingly, MDA-MB-231 is less sensitive to TASPIN-1. Similarly, U251 glioblastoma is much more sensitive to TASPIN-1 than the Taspase1-low line SF295 (Figure 3.15). Other cancer cell lines in the NCI60 have varying degrees of correlation between Taspase1 expression and TASPIN-1 mediated growth inhibition (data not shown).

The striking correlation between Taspase1 expression and TASPIN-1 sensitivity, taken with our studies demonstrating that Taspase1 function is critical to tumor maintenance, suggests that Taspase1 is the major target of TASPIN-1 in blocking cancer cell growth. Even so, due to its chemically simple composition, TASPIN-1 likely targets more than one cellular protein or pathway. Indeed, NSC48300 was recently shown to inhibit autotaxin, which is an extracellular protein involved in cellular migration (Saunders et al., 2008a). Autotaxin catalyzes the conversion of lysophosphatidylcholine (LPC) to lysophosphatidic acid (LPA), which is a potent phospholipid mediator of tumor and non-tumor cell motility, cellular proliferation, and tumor cell survival (Contos et al., 2000; Hoeglund et al., 2010). Treatment with LPA, which is downstream of autotoxin, at levels shown to promote migration in both breast and glioblastoma cell lines (Samadi et al., 2009; Saunders et al., 2008b) does not rescue the inhibition of growth resulting from TASPIN-1/NSC48300 treatment (Figures 3.14 and 3.15). Therefore, the generalized anti-tumor activity of TASPIN-1/NSC48300 is likely not to be due to the inhibition of autotaxin, rather it is more likely due to inhibition of Taspase1.

In vivo studies and other future directions

The general strategy for in vivo assessment of NSC48300/TASPIN-1 utilizes both xenografted established human cancer cell lines as well as mice genetically engineered to spontaneously develop tumors. Though the benefits of using spontaneous tumor models are clear—that they are genetically defined tumors (with a discreet initiating event), are anatomically correct, have no host-tumor mismatch, and have an intact immune system/tumor interface—there are multiple benefits to using an orthotopic engraftment model. Most notably, the use of human, rather than murine cancers, more accurately represents human tumors and consequent tumor response to experimental therapy. Xenograft models, in general, are well-suited for pre-clinical drug studies because of their high penetrance, synchrony, and ease of assessment, though they suffer from the lack of stepwise genetic changes that occur in development of the tumor in the animal. This combined with the accrual of genetic and epigenetic alterations due extended in vitro culture often results in the cancer cell line not being able to accurately recapitulate the histology of the original tumor (Fomchenko and Holland, 2006). Nevertheless, the degree of control offered by xenograft models makes it a tenable system to do the initial in vivo assessment of NSC48300/TASPIN-1.

Because breast cancer cell lines respond to TASPIN-1 in a Taspase1-dependent manner, an MMTV-Neu transgenic mouse model system was employed to gauge the efficacy of TASPIN-1 in treating Her2/Neu driven breast tumors in vivo. In vitro, the Her2 over-expressing line BT-474 was the most sensitive of all tested breast lines to Taspase1 knockdown (Figure 3.16 B and C). The MMTV-Neu transgene drives mammary gland specific expression of the Her2/Neu oncogene, which results in the formation of breast tumors in female mice beginning at around 30 weeks of age. Breast cancer cell lines with *ERBB2* amplifications tend to have higher expression of Taspase1 (Figure 3.16 A). Furthermore, Taspase1 deficient MMTV-Neu mice (MMTV-Neu;MMTV-Cre;T1^{ff}) are resistant to tumor formation, suggesting that Taspase1 is a critical permissive factor for Neu-mediated breast tumorigenesis but not in MMTV-Wnt-driven tumors in a similar system (B. A. Van Tine, unpublished data). Female mice with established tumors

measuring 1cm in the long dimension were initiated on a regimen of TASPIN-1 at 1, 2.5, and 5mg/kg intravenously through the lateral tail vein. There was no overt toxicity in mice, other than an apparent injection site necrosis. Tumors initially decreased in volume, as determined by caliper measurement, and then remained stable. Injections were discontinued when the tail vein became hard to inject into after around four doses. At current doses and formulation, there is an in vivo regression and cytostasis for Neu breast tumors and no change in MMTV-Wnt-driven tumors (data not shown). Though these results are preliminary, they hold promise for TASPIN-1 as a tenable lead compound for treatment of *ERBB2* over-expressing tumors, while lacking non-specific toxicity as shown by the lack of response in MMTV-Wnt tumors. Mechanistically, it is interesting that though Her2/Neu over-expressing breast cell lines generally have high Taspase1 expression, MCF7 appears to express Taspase1 at higher levels, suggesting that the Her2/Taspase1 axis is particularly important in Her2/Neu dependent tumors, while in non-Her2/Neu amplified tumors have a different mechanism for Taspase1 dependence.

Glioblastoma cell lines, like the breast cancer cell lines, respond to TASPIN-1 with sensitivity that correlates with Taspase1 expression. Since there are very few drugs available for glioblastoma treatment, identification of new therapeutic targets and compounds to treat glioblastoma is of great importance. To test the effect of TASPIN-1 on glioblastoma, U251 transduced with a firefly luciferase and green fluorescent protein fusion protein (fLuc-GFP plasmid a generous gift from D. Piwnicka-Worms) retrovirus was subcutaneously engrafted into the flanks of NOD-scid/IL2R $\gamma^{-/-}$ mice. Following engraftment, mice were initiated on a 2.5mg/kg intravenous regimen of NSC48300/TASPIN-1, administered every other day, resulting in decreased tumor growth compared to vehicle-treated control (Figure 3.17).

To assess the ability of TASPIN-1 to kill glioblastoma in its native site, U251-Fluc/GFP was orthotopically engrafted into the white matter of immunodeficient NOD/SCID/IL2Rg null mice under stereotaxic guidance. Mice were initiated on either 2.5mg/kg or 5mg/kg intravenous

TASPIN-1 regimen, administered every other day. Tumor growth was monitored by bioluminescence. Whether this will result in tumor regression is still being investigated.

Gaining access to the CNS is a significant challenge for targeting therapies to disorders across the blood-brain barrier (BBB). Roughly all large-molecule and over 98% of small molecule drugs are excluded by the BBB. Though it is difficult to predict which specific small molecule will cross the BBB, there are a few characteristics associated with drugs known to cross the BBB, including a molecular mass (less than 400-500 Da) and formation of 10 or fewer hydrogen bonds with water. Increases in mass (and hence, surface area) are strongly correlated with exclusion from the BBB, and increased lipid solubility has little effect on permeation of the BBB when the surface area is higher (Pardridge, 2005).

Arsenic-containing molecules have been described to cross the blood brain barrier. Arsenic trioxide (As_2O_3), used to treat relapsed acute promyelocytic leukemia (APL), has been shown to cross the blood brain barrier in the treatment of CNS relapse of APL (Au et al., 2006). Although this is the case, there are significant differences between arsenic trioxide and TASPIN-1. The physical properties of NSC48300/TASPIN-1, with a molecular weight of 416 g/mol, hydrophobic core, and 10 total hydrogen bond donor/acceptors, place it near the limits of compounds that are known to permeate the BBB. Common solvents like dimethylsulfoxide (DMSO) and non-ionic surfactants like Tween 80 can facilitate passage through the BBB (Azmin et al., 1985; Broadwell et al., 1982). Though TASPIN-1 delivery in this vehicle may increase the likelihood of a therapeutic dose in the CNS, increased or repeated dose of intravenous TASPIN-1 did not inhibit tumor growth in initial studies. Whether TASPIN-1 gains access to the CNS in meaningful quantities remains to be addressed through further testing, which involves repeated sampling the CSF and either mass spectroscopy, HPLC, or other method to monitor the accumulation and clearance of TASPIN-1.

It is important to note that aside from the injection site necrosis, there was no overt toxicity observed in mice treated with repeated doses of TASPIN-1—they maintained normal activity, body weight, and blood count. Studies are underway to determine the pharmacokinetics of TASPIN-1 as well as changes in serum values in the basic metabolic panel (BMP). Acute deletion of Taspase1 in *Mx1-cre;Taspase1^{f/-}* in adult mice is well tolerated in both male and female mice over the long term (>16 weeks after cre recombinase induction, A. Searleman, unpublished data). Though Taspase1 is critical for murine embryonic development, it appears to be largely dispensable to normal health in adult mice. Concordant with the classification of Taspase1 as a non-oncogene addiction protease, it seems that certain biological circumstances, like cancer, exhibit increased reliance on Taspase1 function and hence are exquisitely sensitive to Taspase1 loss. This idea harkens back to the original description of HSF1 as a non-oncogene addiction factor in which HSF1 deficient mice were overtly normal and only exhibited pathology in situations of increased reliance on normal HSF1 function, like in situations of proteotoxic stress, yet were resistant to tumor formation (Dai et al., 2007a; Solimini et al., 2007). The defining feature—the relative of insensitivity of normal tissues compared to the sensitivity of tumors—of non-oncogene addiction factors results in a therapeutic window which makes inhibition of the non-oncogene addiction protease Taspase1 a promising new development in cancer therapy.

The identification of NSC48300/TASPIN-1 as a specific inhibitor of Taspase1 is of potential clinical significance. We previously described the critical importance of Taspase1 in maintenance of tumor proliferation and survival, and we further demonstrate that TASPIN-1 treatment can inhibit cancer cell proliferation in vitro and in vivo. Although presence of arsenic acid may limit the clinical application of this particular compound because of potential non-specific toxicity, structural determination of the Taspase1-TASPIN-1 complex would assist the future development of Taspase1 inhibitors for cancer therapy.

3.4 FRET-based screening reveals further leads for Taspase1 inhibitors

The tyrphostin family of tyrosine kinase inhibitors inhibit Taspase1

In collaboration with the NCI DTP, we screened the Library of Pharmacologically Active Compounds (LOPAC 1280), which consists of 1,280 compounds that have described pharmacological actions, including kinase inhibitors, inducers of cellular stress, and antibiotics among others. Adaptation of the FRET-based kinetics assay as an endpoint assay converts the detailed kinetics assay into a useful method for high throughput screening method to identify inhibitors of in vitro Taspase1 proteolysis of the FRPR substrate. Dose-dependent decrease in fluorescence endpoint reading is scored as a positive hit for Taspase1 inhibition, which we subsequently validate using the radiographic in vitro cleavage assay. Interestingly, the tyrphostin family of tyrosine phosphorylation inhibitors had multiple members that were able to inhibit Taspase1 to different degrees (Figure 3.18). The tyrphostin family of inhibitors appears to irreversibly inhibit Taspase1 as inhibition of Taspase1-mediated proteolysis of the radiographic MLL reporter increased with longer pretreatment times of Taspase1 with the tyrphostin (Y. Lee unpublished data). Though Tyrphostin AG538 appears to be a more potent inhibitor of Taspase1 than TASPIN-1, it may suffer from off-target effects, as it is known to be a potent inhibitor of IGFR (Blum et al., 2000). As such, the application of tyrphostins as clinical inhibitors of Taspase1 requires further investigation.

3.5 Methods and materials

Radiographic in vitro cleavage assay

To assess Taspase1 cleavage in vitro, an MLL cleavage reporter with a cleavage site 1 (CS1) mutation was generated, representing aa 2500-2800 of MLL1. Mutation of CS1 by substitution of Asp-Gly with Ala-Ala at aa 2666 results in non-cleavage at CS1 but retention of CS2, generating two fragments p33 and p12 from the p45 non-cleaved substrate. The MLL cleavage reporter was transcribed and translated in vitro in the presence of ³⁵S-methionine using the TNT rabbit reticulocyte lysate system according to the manufacturer's protocol (Promega, Madison, WI). Cleavage assays were performed in a total volume of 25 microliters with cleavage buffer (20mM HEPES, pH 7.9, 5mM MgCl₂, 20mM KCl, 10% sucrose, and 2mM DTT) with 15ng recombinant Taspase1 pre-incubated with DMSO or appropriate amount of yzm peptide derivative (10, 100, 500μM) for 30 minutes at 30°C before addition of 0.1 microliters of MLL reporter substrate for an additional 30 minutes at 30°C. Reactions were resolved on 10% Bis-Tris NuPage gels in MES buffer (Invitrogen, Carlsbad, CA). Gels were fixed in 25% isopropanol/10% acetic acid for 30 minutes followed by signal amplification for 30 minutes using Amplify solution (G.E. Healthcare Life Sciences, Piscataway, NJ). Gels were dried at 80°C for 1h and exposed to BioMax MR film (Kodak).

FRET-based kinetics assay

A quenched fluorescent probe for Taspase1 activity (FRPR) was generated by conjugating the N-terminus with a 7-methoxycoumarin-4-acetyl (MCA) fluorophore and a dinitrophenyl (DNP) quencher at the C-terminus of the sequence Lys-Ile-Ser-Gln-Leu-Asp-Gly-Val-Asp-Asp, which represents the cleavage site 2 (CS2) sequence of MLL1 (Tufts University Core Facility, Boston, MA). Reactions were conducted in reaction buffer (100mM HEPES, pH 7.9, 10% sucrose, 1mM DTT) in the presence of TASPIN-1 or vehicle control (DMSO). For inhibition studies, recombinant Taspase1 was pre-incubated with TASPIN-1 for 30 minutes at room temperature before initiation of the reaction by addition of FRPR to a final concentration 15μM FRPR and 100nM Taspase1,

respectively. Taspase1 activity was monitored by recording the accumulation of emitted fluorescence signal ($\lambda_{\text{excitation}} = 328\text{nm}$, slit = 10nm and $\lambda_{\text{emission}} = 393\text{nm}$, slit = 10nm) over time using an LS55 fluorescence spectrometer with a 96-well plate adapter (Perkin Elmer, Inc., Waltham, MA). Steady state rates were determined for each reaction and K_M , K_I , and IC_{50} values were determined using Prism software (GraphPad Software, Inc., La Jolla, CA), assuming Michaelis-Menten kinetics (Khan, et al. Structure 2005). The following equations model the mechanism of inhibition, where $\alpha \ll 1$ fits un-competitive inhibition, $\alpha = 1$ fits non-competitive inhibition, and $\alpha \gg 1$ fits competitive inhibition (Saunders et al., 2008b).

$$\frac{v}{[E]_{tot}} = \frac{k_{cat}[S]}{K_M + [S]}$$

Equation 1: Briggs Haldane equation

$$\frac{v}{[E]_{tot}} = \frac{k_{cat}[S]}{K_S \left(1 + \frac{[I]}{K_I}\right) + [S] \left(1 + \frac{[I]}{\alpha K_I}\right)}$$

Equation 2: General Equation for inhibition

Cell viability assay

Wild type and Taspase1-null SV40-transformed MEFs were cultured in IMDM supplemented with 10% FBS, 100U/mL penicillin/streptomycin, 2mM L-glutamine, 1mM sodium pyruvate, and 1mM non-essential amino acids (Invitrogen, Carlsbad, CA). Five thousand cells per well were plated 16h before drug treatment in 96-well plates. After 48h of drug treatment, an MTT cell viability assay was performed as recommended by the manufacturer (Roche, Indianapolis, IN). Cell viability was expressed as a fraction of control (DMSO) treated cells.

Xenograft assay

A reporter cell line was generated from the glioblastoma cell line U251 by transduction with an amphotropic retrovirus encoding both GFP and firefly luciferase. Cells were harvested and resuspended in 1:2 suspension of growth factor-depleted matrigel and RPMI and one million cells

were engrafted subcutaneously in each flank of male NOD-*scid* *IL2R γ* ^{-/-} mice between 6-8 weeks of age. Tumors were engrafted on day 0 and treated with an IV preparation of NSC48300 at 2.5mg/kg every other day starting at day 1. Tumor growth was monitored by bioluminescence imaging using an IVIS 100 system.

3.6 Figures

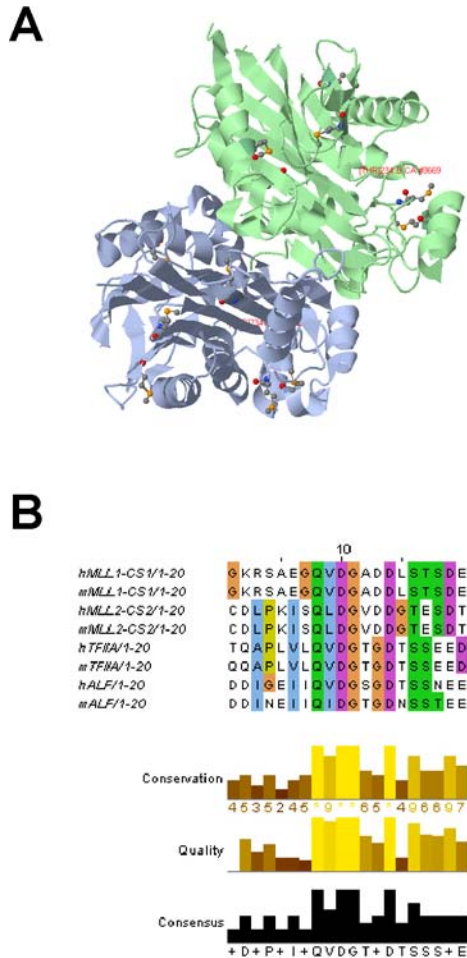


Figure 3.1. Structural characteristics of Taspase1 and its substrates.

A, Ribbon diagram of the Taspase1 active heterotetramer crystal structure (PDB 2A8I) in an orientation where the major features are visible. The N-terminal catalytic threonine (T234) is *en face* on the green protomer, while the $\alpha/\beta/\alpha$ structure is clearly visible in the blue protomer, though its threonine nucleophile is facing into the page. **B**, Cleavage site consensus alignment of known mammalian Taspase1 substrates reveals significant conservation of the cleavage site residues (ClustalW2, <http://www.ebi.ac.uk/Tools/clustalw2>). Cleavage occurs after the aspartate in QVDG.

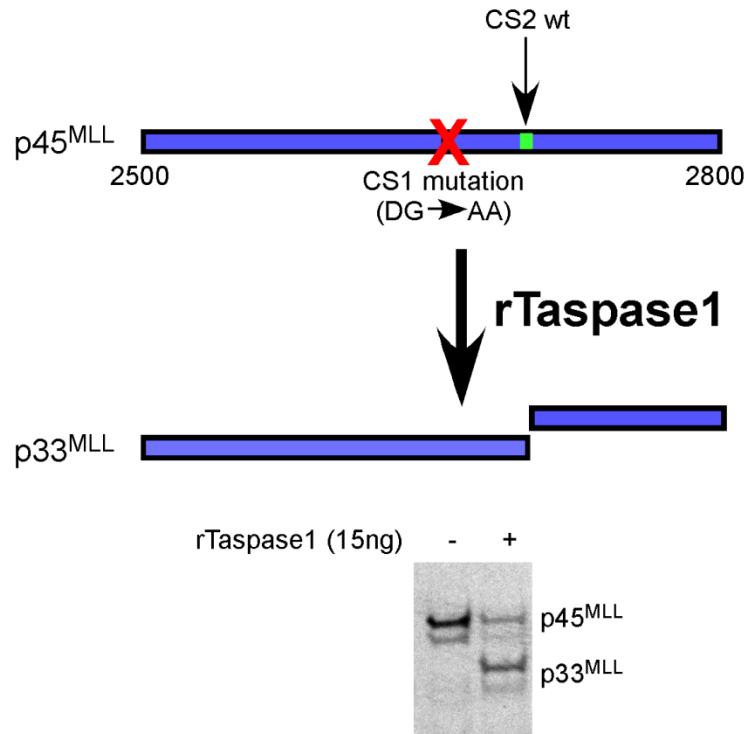


Figure 3.2. Assessing Taspase1 inhibition I—the in vitro cleavage assay.

An in vitro transcribed and translated (IVTT) fragment of MLL was synthesized using a rabbit reticulocyte lysate system, in the presence of ^{35}S -methionine so that newly synthesized proteins could be detected by autoradiography. This fragment of MLL, from aa 2500 to 2800, encompasses the endogenous cleavage sequences CS1 and CS2, where CS1 is mutated by site-directed mutagenesis, leaving only CS2. Upon introduction of recombinant Taspase1 (rTaspase1), p45^{MLL} reporter is cleaved at CS2, which is detected by autoradiography. Inhibition of cleavage results in the accumulation of the p45^{MLL} non-cleaved band, and decrease in the cleaved p33^{MLL} product.

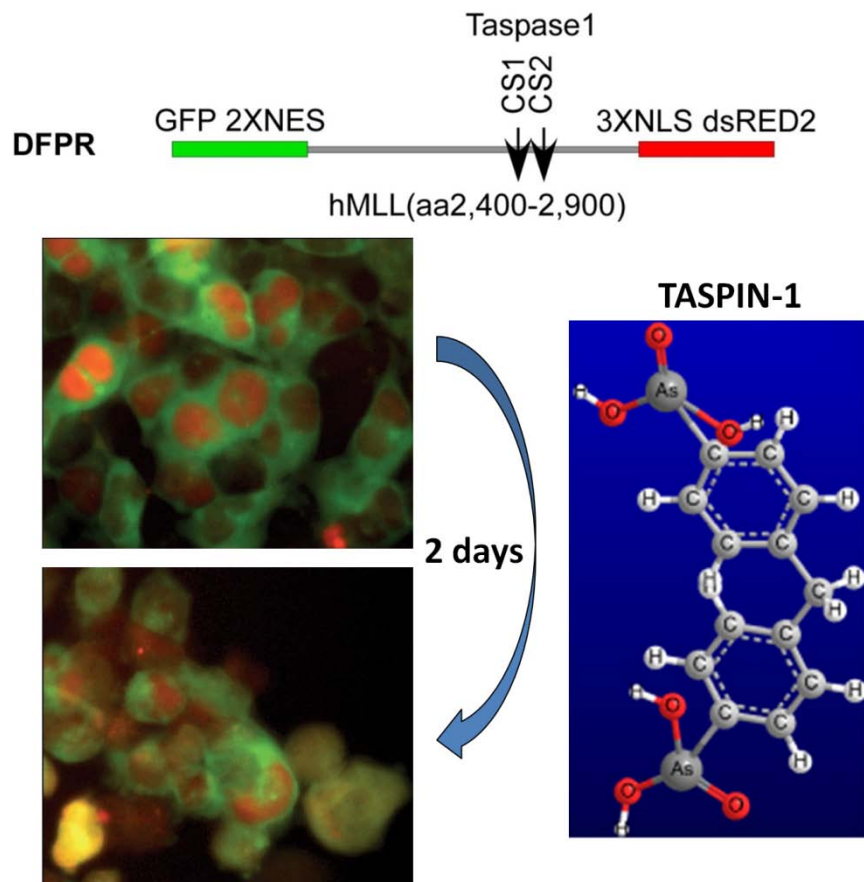


Figure 3.3. Assessing Taspase1 inhibition II—the cell-based screening assay.

The dual fluorescence proteolysis reporter (DFPR) consists of a fragment of MLL1 between aa2400 – 2900, which includes both endogenous Taspase1 cleavage sites (CS1 and CS2). The N-terminus is fused to GFP and a nuclear export signal (NES), while the C-terminus is fused to dsRED2 and a nuclear localization signal. When stably expressed in healthy 293T cells, the C-terminal/red fragment can be clearly discerned from the N-terminal/green reporter fragment by their color and localization. Inhibition of Taspase1 to levels that substantially prevent proteolysis of the reporter causes mislocalization of both GFP- and dsRED2-tagged fragments,

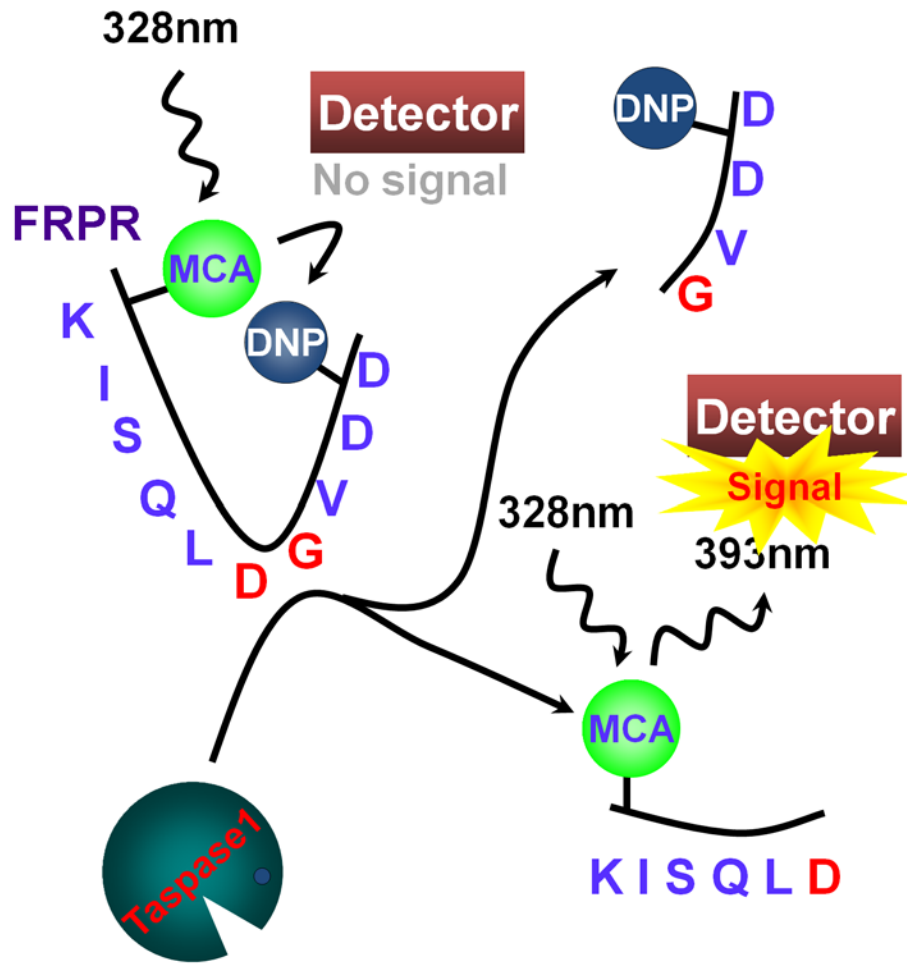


Figure 3.4. Assessing Taspase1 inhibition III—the FRET based kinetics assay.

The reporter FRPR is a short peptide representing the MLL1 CS2. The N-terminus is conjugated to a methoxycoumaryl fluorophore (MCA), while the C-terminus is conjugated to a dinitrophenyl quenching group (DNP). In its native state, incident excitatory light at $\lambda_{ex}=328\text{nm}$ does not produce an emission signal at $\lambda_{em}=393\text{nm}$. When stably expressed in healthy 293T cells, the C-terminal/red fragment can be clearly discerned from the N-terminal/green reporter fragment by

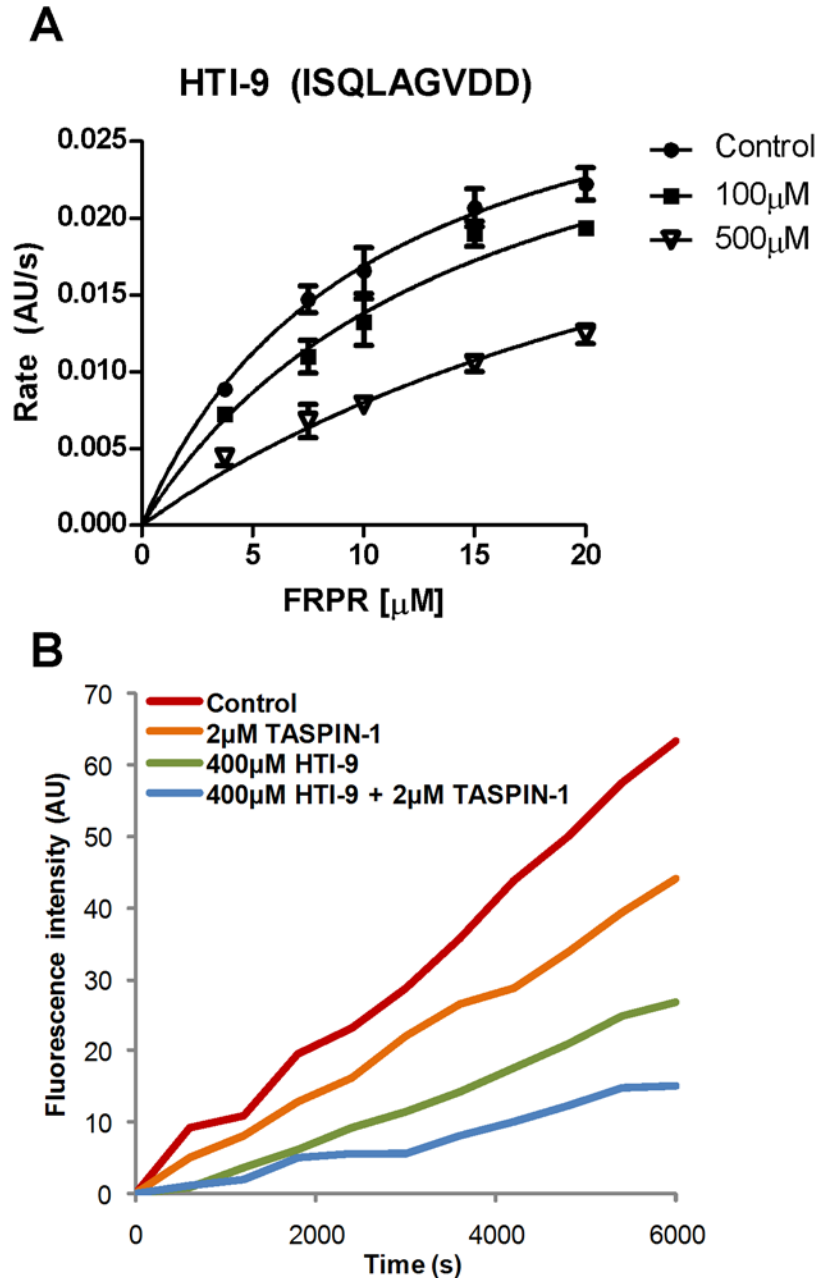


Figure 3.5. HTI-9 is a competitive inhibitor of Taspase1 and cooperates with non-competitive inhibitor NSC48300/TASPIN-1.

A, HTI-9 peptide inhibitor was determined to be a competitive inhibitor of Taspase1 using the modified version of the Briggs-Haldane equation (equation 3.2, methods and materials), where competitive inhibition has an $\alpha > 1$. HTI-9 is a relatively weak inhibitor of Taspase1, with a $K_i = 228 \pm 31 \mu\text{M}$. **B**, Non-competitive inhibitor NSC48300/TASPIN-1 cooperates with HTI-9 to inhibit Taspase1 cleavage of the FRPR reporter. Shown here is the reaction progress plot.

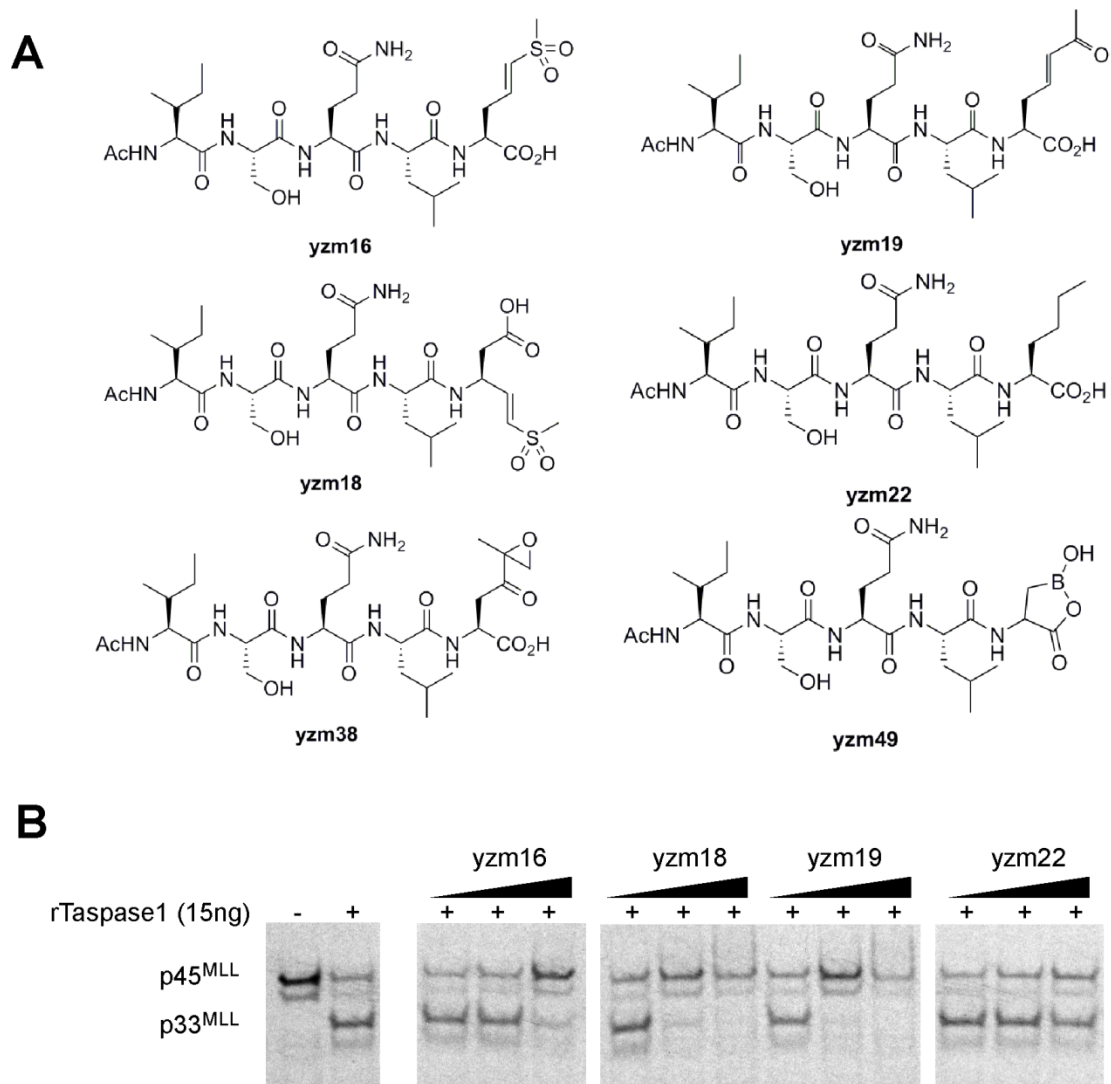


Figure 3.6. Proof of principle in rational design of peptide inhibitors of Taspase1.

A, Short peptide Taspase1 inhibitors are based on the cleavage site (CS2) sequence of MLL1 to engender specificity, for engagement of Taspase1 with various pharmacophores, including vinyl sulfones (yzm16, yzm18), vinyl ketone (yzm19), boronic acid (yzm49), and epoxyketone (yzm38). Norleucine (yzm22) is a control peptide. These inhibitors were generated in collaboration with M. Bogoy and colleagues at Stanford University. **B**, In vitro cleavage assay demonstrates inhibition of Taspase1 cleavage of the p45^{MLL} reporter substrate with increasing doses of peptide inhibitor (10, 100, and 500 μ M).

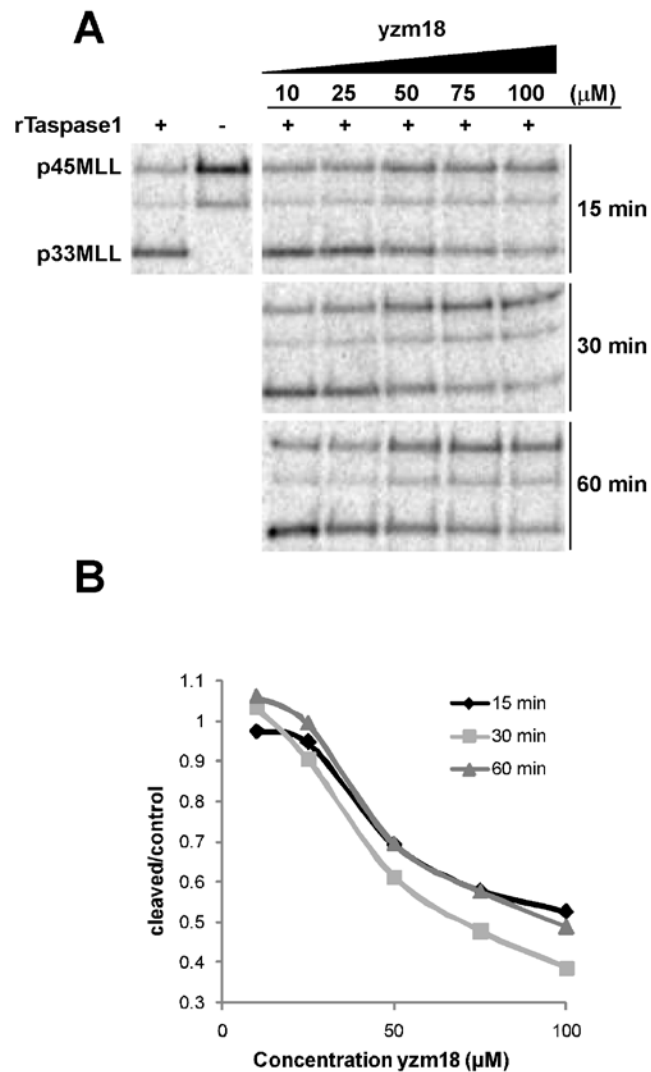


Figure 3.7. The vinyl sulfone yzm18 is a reversible inhibitor of Taspase1.

A, Reversibility was determined by pre-incubation with yzm18 and Taspase1 with increasing time (15, 30, and 60 minutes) before introducing the p45^{MLL} substrate. Irreversible inhibition is marked by decreased ability to process substrate with longer pre-incubation times. **B**, Band intensities for the radiographic cleavage assay were quantified using the STORM phosphorimaging system.

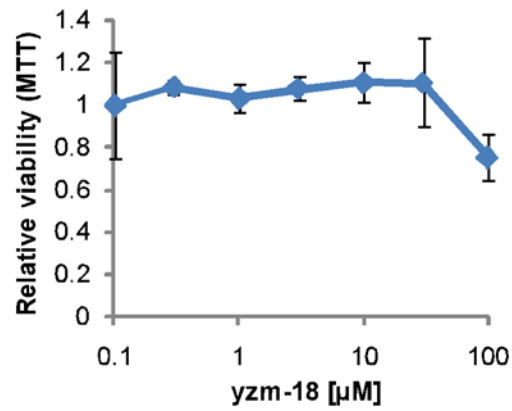


Figure 3.8. The vinyl sulfone yzm18 is not a potent inhibitor of Taspase1 in vivo.

The effect of yzm18 in vivo was assessed by incubation of with SV40-transformed wild type Taspase1 MEFs over 3 days before performing an MTT assay to assess viable cell mass. Low concentration (0.1 μM) yzm18 treated cells were assigned a value of 1.

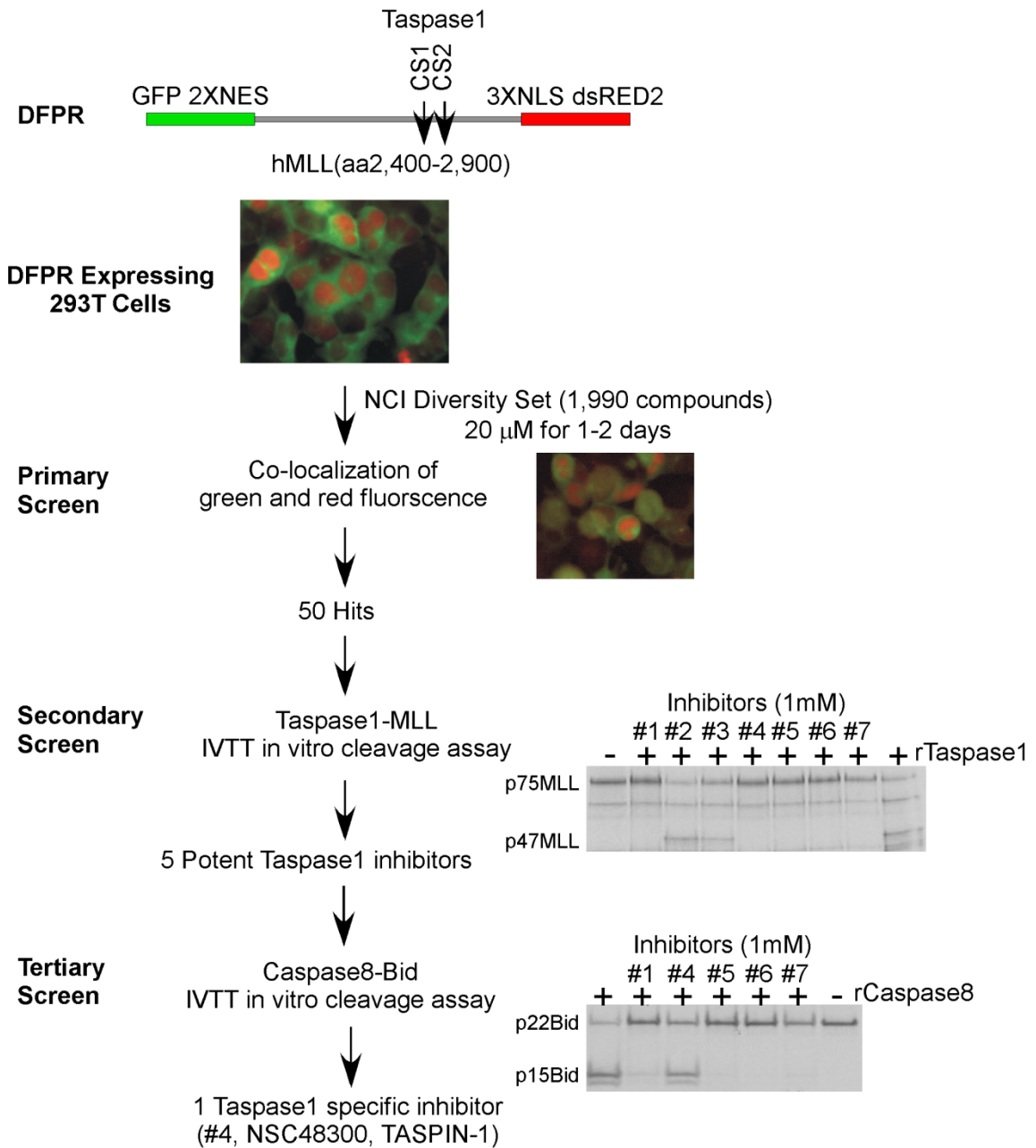


Figure 3.9. An in vitro screen identifies NSC48300/TASPIN-1 as a potent bioactive inhibitor of Taspase1.

293T cells expressing DFPR were plated in 96-well plates the day before treatment with the NCI Diversity Set of 1900 compounds. Hits were validated by the in vitro cleavage assay and subsequently evaluated for Taspase1 inhibition specificity using rCaspase8 (cysteine aspartase) and its proteolytic target Bid. Of 1900 compounds, only NSC48300/TASPIN-1 was a bioactive and specific inhibitor of Taspase1. Thanks goes to S. Takeda for contributing work to this screen.

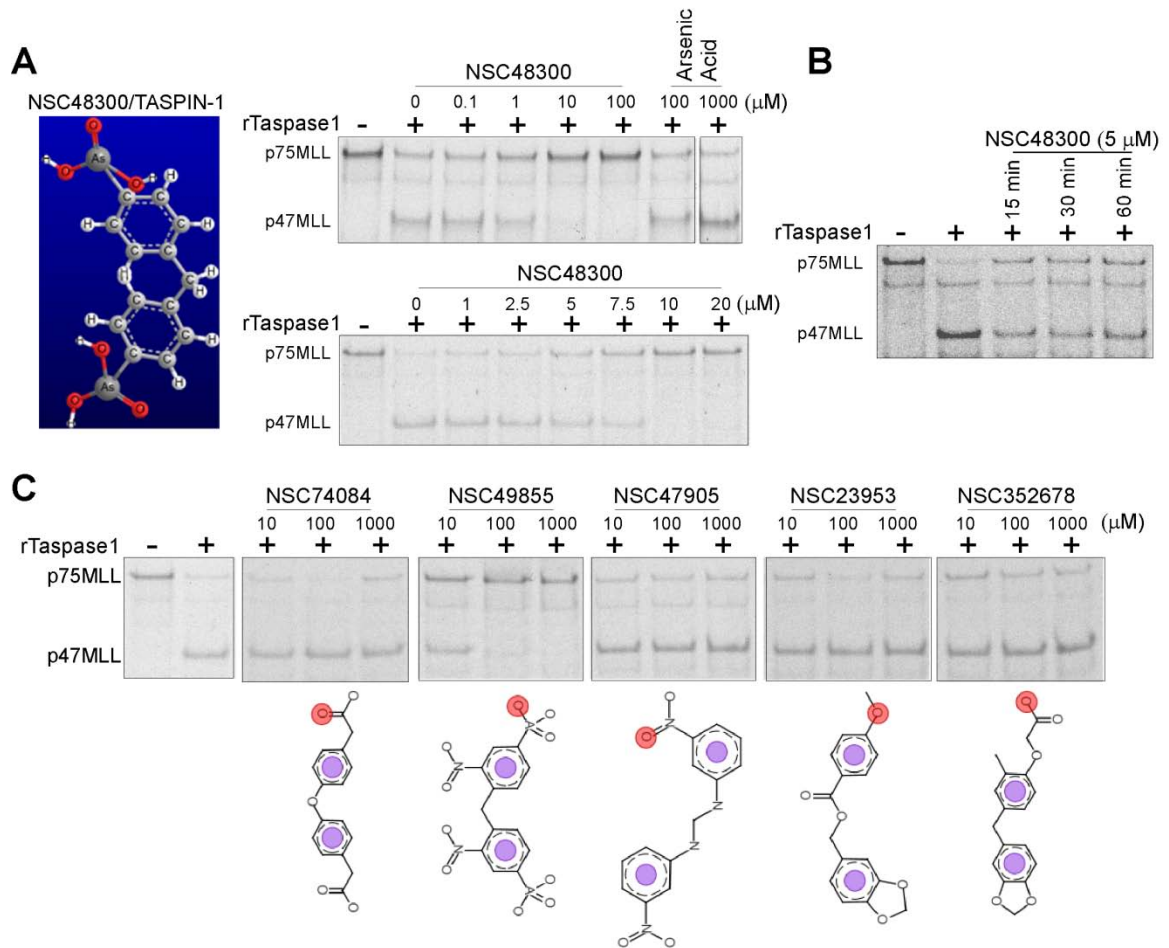


Figure 3.10. Structural features of TASPIN-1 define its Taspase1 inhibitory activity.

A, TASPIN-1 is a potent inhibitor of in vitro Taspase1 reporter cleavage, with an $IC_{50} \sim 5\mu M$. **B**, To determine if TASPIN-1 is a reversible or irreversible inhibitor of Taspase1, TASPIN-1 was pre-incubated with Taspase1 for the indicated times before addition of radiolabeled $p45^{MLL}$. **C**, Pharmacophore modeling identifies putative Taspase1 inhibitors based on the TASPIN-1 pharmacophore. In vitro cleavage of $p45^{MLL}$ was used to test the efficacy of inhibition. Thanks goes to Y. Lee for contributing this figure.

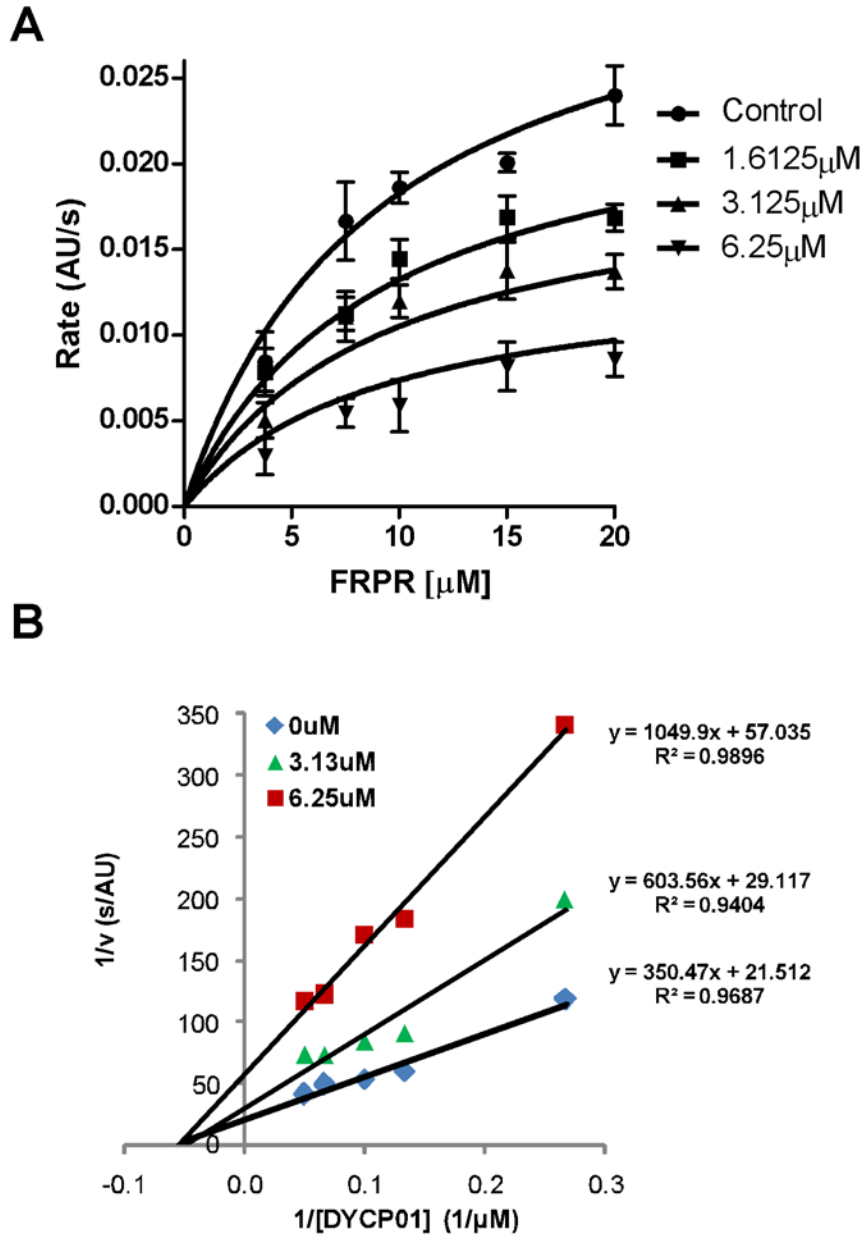


Figure 3.11. NSC48300/TASPIN-1 is a non-competitive inhibitor of Taspase1.

A, Non-linear regression of reaction progress curves of the FRET-based kinetics assay with TASPIN-1 treatment revealed that Taspase1 is non-competitive inhibitor of Taspase1 ($\alpha=1.01$, equation 2 in the Methods and materials section) with a K_i of $4.24 \pm 0.46 \mu\text{M}$. **B**, Lineweaver-Burk plot indicates that unlike V_{max} , K_M does not vary with Taspin-1 concentration, consistent with non-competitive inhibition.

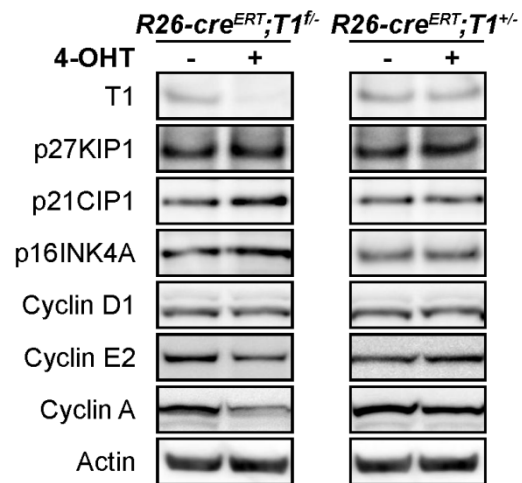


Figure 3.12. Molecular consequences of genetic loss of Taspase1.

MYC/RAS^{G12V} transformed primary MEFs bearing a conditional allele of Taspase1 (*R26-cre^{ERT};T1^{f/-}*) or control (*R26-cre^{ERT};T1^{+/+}*) were subjected to a 6h pulse of 500nM of 4-OH tamoxifen to induce Cre-recombinase activity. Lysates were generated 48h after treatment and immunoblotted with the indicated antibodies.

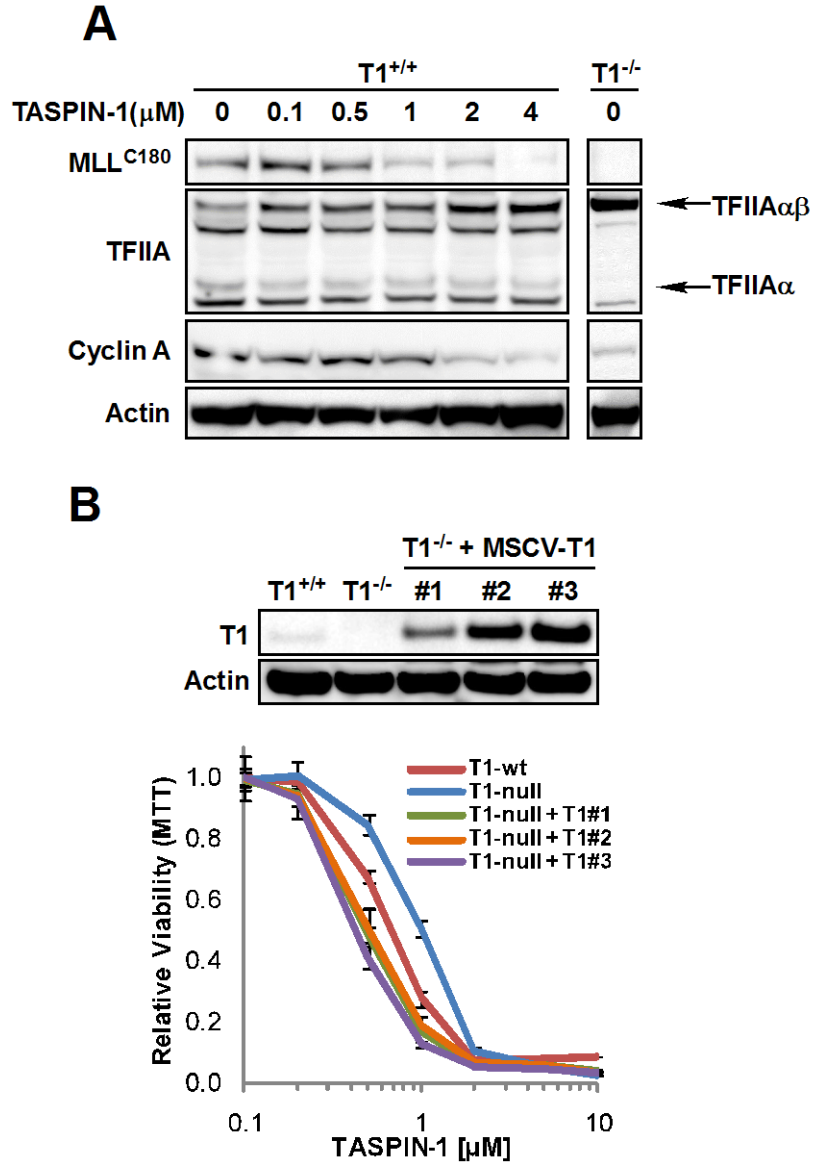


Figure 3.13. TASPIN-1 treatment recapitulates the Taspase1-null phenotype.

A, Primary Taspase1 wild type or null MEFs were subjected to treatment with the indicated concentration of TASPIN-1. Lysates were generated 24h after treatment and immunoblotted with the indicated antibodies. **B**, Taspase1 null SV40-transformed fibroblasts were reconstituted with various amounts of hTaspase1 by retroviral transduction and subjected to treatment with TASPIN-1. Viable cell mass was determined by MTT assay. Lysates were generated from wild-type, Taspase1-null, and Taspase1 reconstituted SV40-transformed MEFs and subjected to Taspase1 immunoblot and actin immunoblot to demonstrate equal loading

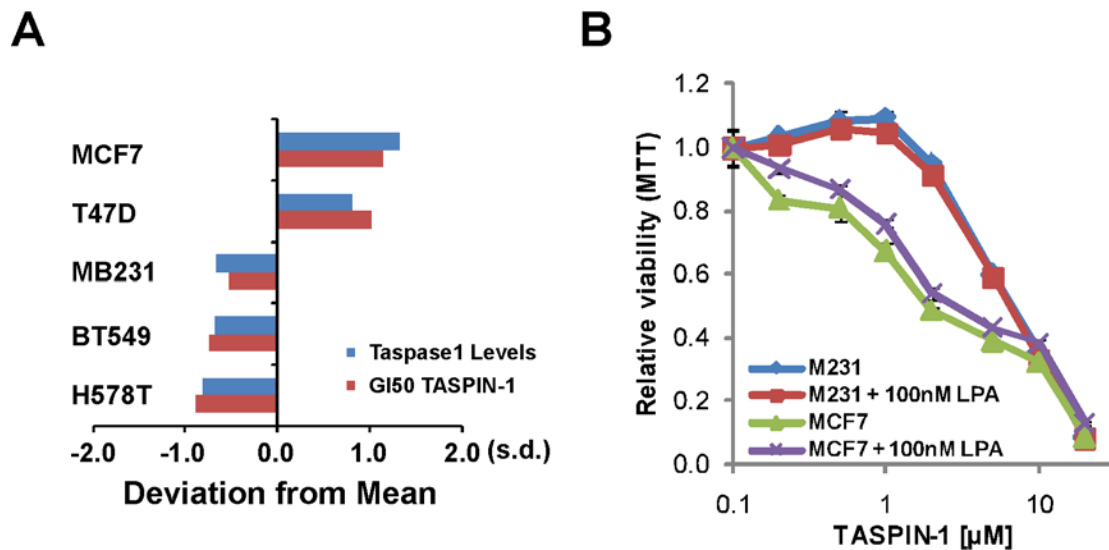


Figure 3.14. TASPIN-1 sensitivity is correlated with relative Taspase1 expression level in breast cancer cell lines.

A, Comparison of normalized Taspase1 protein expression with the GI_{50} concentration of TASPIN-1 demonstrated that the sensitivity of growth inhibition to TASPIN-1 correlates well with the protein expression of Taspase1 breast cancer cell lines. Protein expression data of Taspase1 in NCI60 cell lines has been described (Takeda et al., 2006b), while GI_{50} data is obtained from the NCI DTP website (<http://dtp.nci.nih.gov>). The protein expression and the GI_{50} is compared to the mean of all five breast cancer cell lines and presented as a fraction of the standard deviation. GI_{50} denotes growth inhibition 50%. **B**, To exclude effects of autotoxin inhibition, breast cancer cell lines were treated with 100nM LPA or mock treated in addition to TASPIN-1 treatment. MTT assay was performed after two days of treatment to determine viable cell mass.

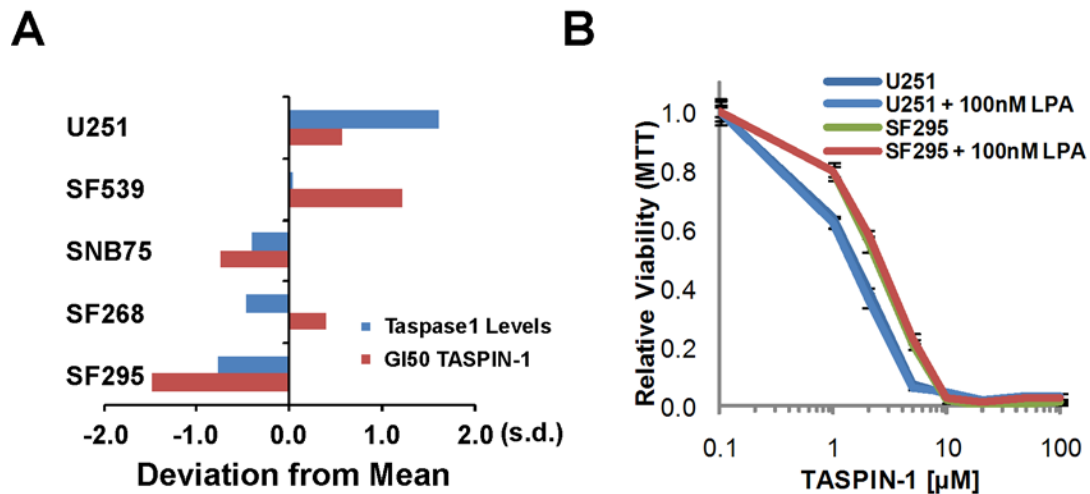


Figure 3.15. TASPIN-1 sensitivity is correlated with relative Taspase1 expression level in brain cancer cell lines.

A, Comparison of normalized Taspase1 protein expression with the GI_{50} concentration of TASPIN-1 demonstrated that the sensitivity of growth inhibition to TASPIN-1 correlates well with the protein expression of Taspase1 central nervous system (CNS) cancer cell lines. Protein expression data of Taspase1 in NCI60 cell lines has been described (Takeda et al., 2006b), while GI_{50} data is obtained from the NCI DTP website (<http://dtp.nci.nih.gov>). The protein expression and the GI_{50} is compared to the mean of all five brain cancer cell lines and presented as a fraction of the standard deviation. GI_{50} denotes growth inhibition 50%. **B**, To exclude effects of autotoxin inhibition, brain cancer cell lines were treated with 100nM LPA or mock treated in addition to TASPIN-1 treatment. MTT assay was performed after two days of treatment to determine viable cell mass.

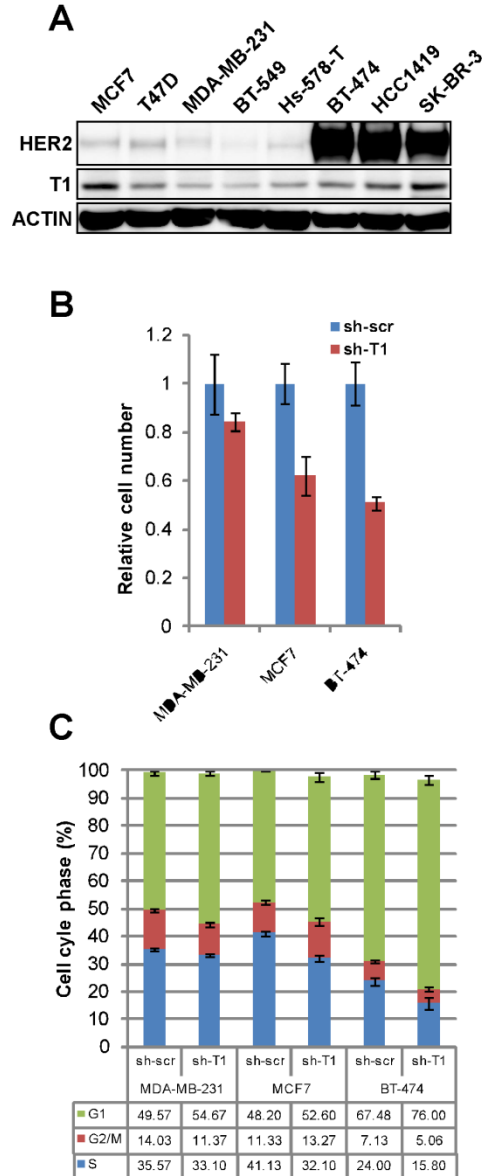


Figure 3.16. Breast cancer cell lines expressing higher Taspase1 are more sensitive to Taspase1 loss.

A, Comparison of HER2 positive cell lines with HER2 negative lines by Western blot. Lysates were subjected to immunoblot for HER2, Taspase1, and actin blot for comparison. **B**, Taspase1-shRNA transduced cells were plated at 10^5 cells per well in 6-well plates and counted 4 days after plating. Control-shRNA cell count average was assigned the value 1 for comparison. **C**, Proliferative status for cell lines expressing Taspase1- or control-shRNA was determined by PI staining for DNA content and subsequent FACS analysis.

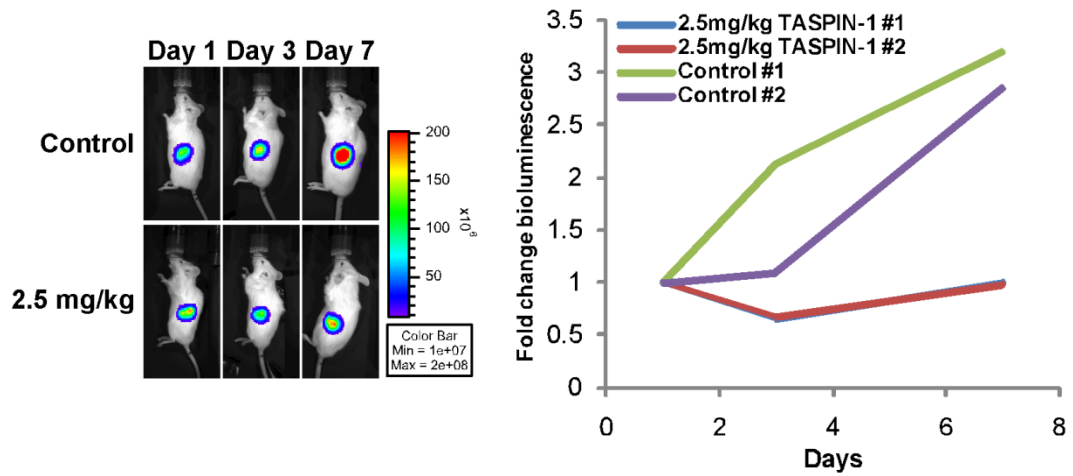
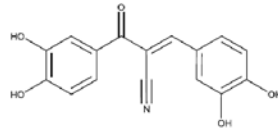
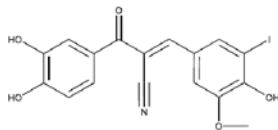


Figure 3.17. Glioblastoma xenografts respond to TASPIN-1 treatment in vivo.

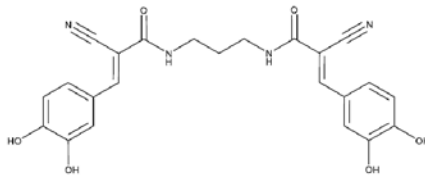
To gauge the effect of Taspase1 inhibition in vivo, a U251 glioblastoma cell line expressing a firefly luciferase and GFP fusion protein was injected subcutaneously into the flanks of NOD-*scid* *IL2R γ* ^{-/-} mice (day 0) and treated with an IV preparation of NSC48300/TASPIN-1 at 2.5mg/kg every other day starting at day 1. Tumor growth was monitored by bioluminescence imaging.



Tyrphostin AG538



Tyrphostin I-OMe-AG538



Tyrphostin AG537

Compound	IC ₅₀ (μM)	
	average	stdev
NSC48300/TASPIN-1	6.44E-06	2.0E-06
AG538	1.70E-06	3.6E-07
IOMe AG538	5.95E-06	3.1E-06
AG537	8.27E-06	2.6E-06

Figure 3.18. Tyrphostins are potent inhibitors of Taspase1 in vitro.

Library of pharmacologically active compounds (LOPAC 1280) screening from the FRET-based assay identified a family of receptor tyrosine kinase inhibitors that potently inhibit Taspase1. The table is a comparison of Taspase1 inhibition in a FRET-based determination of IC₅₀.

Chapter 4

Therapeutic implications of Taspase1 non-oncogene addiction and proposed future studies

- 4.1 Future directions: in vitro studies
- 4.2 Future directions: in vivo studies
- 4.3 Therapeutic implications of non-oncogene addiction and Taspase1 inhibition
- 4.4 Figures

4.1 Future directions: in vitro studies

Balancing proliferation and apoptosis

This body of work represents the first establishment of a role for Taspase1, a non-oncogene protease, in tumor maintenance. Because the nature of non-oncogene addiction factors is, by definition, insufficient to drive tumorigenesis by itself, it is particularly challenging to define what functions are critical to the ability of such factors to mediate efficient tumorigenesis. It is clear, though, that Taspase1 is required for oncogenic transformation and maintenance of tumor phenotypes. Taspase1 deficiency in non-transformed, primary murine fibroblasts first established the role of Taspase1-mediated proteolysis of MLL in the orchestration of cell cycle progression through its obligate role in driving the expression of key Cyclins E, A, and B (Takeda et al., 2006b). In certain tumor types like glioblastoma, in contrast with non-transformed MEFs, Taspase1 also regulates cellular survival. We establish that Taspase1 regulates the deubiquitinase (DUB) protein USP9X, which was recently described as a critical regulator of the protein stability of the anti-apoptotic BCL-2 family member MCL-1 (Schwickart et al., 2010). Taspase1 deficiency decreased proliferation in cancer cell lines in which Taspase1 is normally highly expressed, though unlike in MEFs, Cyclin E and A expression remain unchanged. Rather, the CDKI p27^{KIP1} was up-regulated with acute Taspase1 deficiency, which is consistent with the G1/S phase cell cycle block observed with Taspase1 loss in cancer cell lines.

Pleiotropic regulation of proliferation and death is commonly observed in oncogenic signaling, as well-established by the role of the transcription factor MYC in regulating both. Interestingly, all of the described substrates for Taspase1 are nuclear factors involved broadly in regulating transcriptional programs, giving us some insight into how a single protease might sufficiently regulate both proliferative and apoptotic programs, and, as will likely be demonstrated later, many other important biological programs.

Taspase1 and the regulation of Cyclin-dependent kinase inhibitors p16^{INK4A}, p21^{CIP1}, and p27^{KIP1}

Though Taspase1 regulates both Cyclins and the upstream Cyclin-dependent kinase inhibitors (CKDIs), it is unclear whether the cleavage of MLL has a role in modulating CDKI expression. Direct binding of MLL, through E2F transcription factors, at Cyclin promoters has been demonstrated, resulting in increased histone H3 lysine 4 (H3K4) trimethylation, which is an epigenetic mark associated with positive transcriptional activity. Taspase1 loss results in hypomorphic H3K4 methyltransferase activity and decreased H3K4 methylation at the Cyclin E promoter. Yet, MLL targeting to the p16^{INK4A} locus is increased in Taspase1 deficiency and the H3K4 methylation remains unchanged (Takeda et al., 2006b).

It seems counterintuitive that though MLL non-cleavage is associated with hypomorphic transactivation capabilities, loss of Taspase1 causes an increase in p16^{INK4A} transcript. Regulation of p16^{INK4A} is primarily through transcriptional control, and many possibilities exist for why we observe p16 transcript and protein up-regulation with Taspase1 deficiency. First, it is possible that increased targeting of non-cleaved MLL to the p16^{INK4A} promoter simply displaces its functional antagonist BMI-1, which is an oncogene known to repress p16^{INK4A} transcription (Jacobs et al., 1999). The MLL N-terminal repression domain has been shown to interact with BMI-1 (Xia et al., 2003), which brings up the interesting possibilities that non-cleaved MLL may displace BMI-1, lose interaction with BMI-1 (and hence MLL may become hypo-functional in its gene-repressive activity rather than gaining a trans-activating property), or cause an allosteric inactivation of BMI-1. A simple approach to addressing the role of BMI-1 in regulating the *INK4A* locus in the absence of Taspase1 would be to assess whether the occupancy of the p16^{INK4A} promoter by BMI-1 is changed. Alternatively, non-cleaved MLL could bind a different set of co-factors than cleaved MLL, rendering either enhanced trans-activation capability or loss of transcriptional repression in a BMI-1 independent manner. For instance, MLL has been shown to interact with the DDB1/CUL4A ubiquitin ligase machinery, which is required for RAS-induced p16^{INK4A} induction, though the biochemical mechanism explaining this induction remains unknown

(Kotake et al., 2009). Finally, it is also possible that substrates other than MLL, like TFIIA or ALF regulate the expression of p16^{INK4A}.

Transcript levels of another CDKI, p21^{CIP1} are elevated in Taspase1-null MEFs, which is likely dependent on the activation of a canonical p53-dependent pathway. *TP53* is frequently mutated in cancer cell lines, and shRNA-induced Taspase1 loss increases p21 expression an appreciable amount only in the lung adenocarcinoma line, A549, which is the singular cell line in the tested panel that harbors wild type *TP53*. Whether Taspase1 regulates the p53 pathway is a matter for further study.

Perhaps the most important Taspase1-regulated CDKI is p27^{KIP1}. Sharing significant homology to p21^{CIP1}, the cyclin dependent kinase inhibitor p27^{KIP1} potently inhibits Cyclin D1-cdk4 and Cyclin E-cdk2 complexes at the G1/S cell cycle phase boundary. A distinguishing feature of p27^{KIP1}, however, is that its expression responds to mitogenic stimuli, as its levels are kept high in quiescent cells, but drop rapidly upon mitogen stimulation. Translational and post-translational mechanisms are implicated in p27 regulation, including negative feedback by Cyclin E/cdk2 phosphorylation and subsequent inactivation by proteasomal degradation (Sherr, 1996). Protein expression of p27^{KIP1} is regulated post-translationally by the ubiquitin-proteasome pathway and depends on the action of the E3-ubiquitin ligase SKP2, which recognizes the phosphorylated state of p27^{KIP1} conferred by Cyclin E/cdk-2 (Carrano et al., 1999; Pagano et al., 1995). The transcription factors of the forkhead family, including AFX (MLLT7/FOXO4), FKHR (FOXO1), and FKHR-L1 (FOXO3A) regulate p27^{KIP1} transcript through RAS/PI3K (Dijkers et al., 2000; Medema et al., 2000). Further integration with growth factor pathways occurs through the direct phosphorylation at T157 of p27 by AKT, which causes the retention of p27 in the cytoplasm and titrating it away from its target Cyclins, thereby preventing G1 arrest (Liang et al., 2002; Shin et al., 2002; Viglietto et al., 2002). Recently, other oncogenic kinases such as Src, Lyn, and BCR-ABL, have been implicated in the direct phosphorylation of p27 tyrosine residues to regulate its stability as well as impairing its ability to effectively inhibit the Cyclin E-cdk2 kinase (Chu et al.,

2007; Grimmier et al., 2007), which suggests that p27 inactivation is an important task that oncogenes must accomplish in the process of transformation.

Taspase1 down-regulation in cancer cell lines that express high basal levels of Taspase1 uniformly up-regulate p27^{KIP1}. Transcript levels in U251 glioblastoma cells are up-regulated by roughly 1.5 fold, while protein is concomitantly stabilized. These two features are reminiscent of AFX over-expression in MEFs (Medema et al., 2000). It is therefore possible that Taspase1 regulates p27^{KIP1} expression indirectly through forkhead transcription factors. Forkhead transcription factors, like FOXO3A, are regulated in part by growth factor signaling through the PI3K/AKT pathway by phosphorylation and cytoplasmic retention (Brunet et al., 1999). Preliminary evidence suggests that Taspase1 may regulate p27 in a PI3K dependent manner. Glioblastoma cell line U251 treated with U0126 (MEK/ERK inhibitor) or LY294002 (PI3K inhibitor) up-regulate p27^{KIP1}. In Taspase1 deficiency, which causes an up-regulation of p27 level compared to the control, further increase in p27^{KIP1} is seen only with MEK inhibition and not PI3K inhibition, suggesting that Taspase1 is not downstream of MEK in p27 regulation, but may be downstream of PI3K (data not shown). Alternatively, because Taspase1 is involved in the processing of multiple transcription factors, it is possible that Taspase1 may involve other factors important in p27 degradation, including E3 ligases SKP2 and KPC (Carrano et al., 1999; Hara et al., 2005; Kotoshiba et al., 2005).

Taspase1 and the regulation of the anti-apoptotic BCL-2 family member MCL-1

In primary cells, Taspase1 does not appear to regulate cell death, even upon application of death stimuli, and Western blotting reveals that MCL-1 does not depend on Taspase1 expression (Figure 4.3). It is only in cancer cell lines in which we see MCL-1 regulation, and even then this phenomenon was only observed in a specific subset of cell lines. In U251 and SK-MEL-2 glioblastoma and melanoma cell lines, respectively, Taspase1 deficiency causes a significant destabilization of MCL-1 protein. However, among the other cell lines tested, only the A549 lung adenocarcinoma line exhibits appreciable MCL-1 down-regulation, and even then, the down-

regulation is modest (data not shown). Though Taspase1 is down-regulated with high efficiency with sh-RNA targeting, there is still residual Taspase1 protein as assessed by Western blot, and transcript levels persist at roughly 20% of control (data not shown). Taspase1 is a highly efficient enzyme, though it seems to more efficiently process certain substrates over others, as Taspase1 sh-RNA can deplete Taspase1 expression enough to fully inhibit TFIIA $\alpha\beta$ cleavage, but only partially inhibit MLL cleavage. Since genetic studies in mice demonstrate that Taspase1 is the obligate protease for MLL and TFIIA $\alpha\beta$ cleavage, it is likely that some Taspase1-deficiency phenotypes like MCL-1 regulation may be masked by insufficient inhibition of Taspase1 function by this particular strategy.

We identified USP9X, a deubiquitinase that is known to stabilize MCL-1, as a Taspase1-regulated gene. There are approximately 100 enzymes in the DUB family which play diverse roles in cancer progression, from stabilizing receptor tyrosine kinases like EGFR and MET, to regulation of the MDM2/p53 pathway, and the regulation of NF- κ B signaling (Lopez-Otin and Hunter, 2010). USP9X is located on the X-chromosome and is known to deubiquitinate Survivin, regulating its association with centromeres, and hence chromosome alignment and segregation, without affecting its protein degradation (Vong et al., 2005). Recently, USP9X was described to remove ubiquitin from MCL-1, stabilizing the protein. Suppression of USP9X by sh-RNA knockdown resulted in the destabilization of MCL-1 protein in multiple myeloma cells, in which over-expression of MCL-1 is a poor prognostic factor (Schwickart et al., 2010). Decreased levels of MCL-1 resulting from USP9X deficiency increased cancer cell susceptibility to ABT-737, which inactivates BCL-2 and BCL-X_L, but not MCL-1. We demonstrated that Taspase1-deficient glioblastomas have impaired transcription of *USP9X*, enriched levels of ubiquitinated MCL-1, and consequent increase in sensitivity to ABT-737 in vitro and in vivo. Importantly, Dixit and colleagues noted that increased *USP9X* transcript correlated with increased protein in diffuse large B-cell lymphoma (DLBCL) cell lines, suggesting that USP9X protein expression is controlled at the transcriptional level (Schwickart et al., 2010), just as we demonstrated in the context of Taspase1 deficiency.

It is interesting to note that U251 and SK-MEL-2 lose MCL-1 expression to a much higher degree than A549 with Taspase1-loss, while in other cancer cell lines MCL-1 levels remain rather unperturbed. To gain clues about the mechanistic details of Taspase1-mediated MCL-1 regulation, multiple questions must be addressed. The first piece of information to be acquired, however, is the USP9X expression level of each cell line upon Taspase1 knockdown. One possibility is that the Taspase1/USP9X axis is disrupted in resistant cell lines. Additionally, we have ruled out many of the other known mechanisms by which MCL-1 stability is regulated, since Taspase1 knockdown in U251 did not respond to GSK-3 β inhibition, did not down-regulate described E3-ubiquitin ligases MULE or β -TRCP, nor did it down-regulate the stabilizing chaperone TCTP. A remaining possibility is that ERK-mediated phosphorylation of the MCL-1 PEST domain may dictate Taspase1-mediated control of MCL-1 stability (Domina et al., 2004). Because Taspase1 regulates transcription factors, USP9X expression may be modulated by one of the described Taspase1 substrates, including MLL1, MLL2, TFIIA, or ALF.

The U251 and SK-MEL-2 cell lines also differ from the other cell lines in the panel by their embryonic origin. Glioblastoma multiforme is thought to be of astrocytic origin and melanomas from benign melanocytes. Both of these cell lineages are derived from the neuroectoderm, while in contrast, the epithelium of colon, breast, lung, and prostate arise from the endoderm. MEFs, on the other hand, are derived from the mesoderm. Historical cancer classification has relied on this inherent and readily observable phenomenon, which provides the basis for categorization on particular differentiation states (classification of leukemias), tissue lineage (cancers of different tissue origins), embryonic germ layer (ectoderm-, mesoderm-, and endoderm-derived), and histological lineage (squamous carcinoma compared to adenocarcinoma) (Garraway and Sellers, 2006). Thus, the implication is that the developmental history of a cell determines the particular molecular constitution, whether by genetic or epigenetic means, from which tumors are formed and by which tumors can be dismantled. In point of fact, there are no mutations in common that distinguish SKMEL2 and U251 from the other cancer cell lines examined (Table 2.1); however,

deregulated cellular programs arising from mutations, whether characterized or awaiting characterization in these cell lines, perhaps interact in a unique fashion with the distinct developmental makeup of the cell. This, in turn, may dictate the observed difference in response to Taspase1 inhibition. Consistent with this notion of “lineage addiction” mediated by broad epigenetic changes occurring in development (Garraway and Sellers, 2006), Taspase1 regulates broad-acting transcriptional regulators such as TFIIA and MLL. MLL, in particular, is implicated in multiple developmental processes and is a key actor in the interplay between the *Trithorax* and *Polycomb* groups of developmental regulators. MLL deregulation causes global epigenetic changes and gene expression changes in pathological conditions like cancer (Krivtsov and Armstrong, 2007). To control for cellular context, and to better understand Taspase1-mediated regulation of MCL-1, additional glioblastoma and melanoma cell lines should be analyzed for their sensitivity to Taspase1 loss-induced MCL-1 destabilization.

The role of Taspase1 in the natural history of a tumor

Though we previously established that Taspase1 is required for tumorigenesis in vitro, it is unclear what function a protease like Taspase1 could play in tumorigenesis. As a protease with no known signaling role, it is difficult to imagine that simple over-expression of a protease would confer tumorigenic capabilities, and indeed, over-expression of Taspase1 in conjunction with established oncogenes in primary MEFs, or supraphysiological expression of Taspase1 in immortalized NIH/3T3 fibroblasts does not confer a tumor phenotype (Figure 2.2). However, soft agar colonies from MEFs transformed by co-expression of complementary oncogenes MYC/RAS^{G12V}, E1A/RAS^{G12V}, and DNP53/RAS^{G12V}, which represent tumorigenic clones, uniformly express Taspase1 to a much higher level than the non-selected pool of transformed cells, which include non-tumorigenic clones (Figure 4.3). Furthermore, Taspase1-deficient MEFs are resistant to transformation by the same complementary oncogenes. Taken together, this implies that oncogenic signaling programs, in order to fulfill the requirements of tumorigenesis, co-opt Taspase1 function to efficiently transform primary cells. However, the

mechanism by which Taspase1 is co-opted as well as the effector functions of Taspase1 required to facilitate tumorigenesis and maintenance await description.

The signals upstream of Taspase1 are still unknown. However, in silico analysis of the Taspase1 promoter indicates that multiple transcription factors bind in a conserved fashion between humans, mice, and other species. The promoter analysis pipeline (PAP) (Chang et al., 2006) identified conserved MYC, HIF1- β /ARNT, and forkhead transcription factor sites, among others in the Taspase1 promoter region (Table 4.1). Additionally, the intracellular domain of NOTCH1, was found to bind directly to the MYC promoter, resulting in the transactivation of MYC. This opens up the possibility that NOTCH1 may indirectly regulate Taspase1 through MYC activity, though MYC binding to the Taspase1 promoter remains to be demonstrated. In the same study, intracellular Notch was found to directly bind to the Taspase1 promoter by ChIP-on-chip assay. Treatment of T-ALL cell lines harboring activating *NOTCH1* mutations with a γ -secretase inhibitor prevented NOTCH1 cleavage, resulting in markedly decreased promoter occupancy by NOTCH1, and decreased expression of, known targets *HES1* and *DELTEX1*, as well as *MYC* and *TASP1* (Palomero et al., 2006). Indeed, Taspase1 is highly expressed in T-cell lymphomas compared to other types of blood tumors (Figure 4.5). Further investigation into the putative NOTCH1/Taspase1 pathway may reveal mechanistic insight to how Taspase1 is regulated and further delineate its role in development and cancer.

4.2 Future directions: in vivo studies

Taspase1 is over-expressed in multiple human cancers

In vitro tumorigenesis, using the soft agar assay, revealed that Taspase1 expression is selectively up-regulated in tumorigenic clones of oncogene pair-transduced MEFs compared to the non-selected pools of cells. Evidence suggests that this phenomenon holds true in human tumorigenesis as well. In a murine model of hepatocellular carcinoma (HCC) *TASP1* was found to be a target of the HNF4 α transcription factor, which elevated *TASP1* transcript in tumors

compared to transgenic but pre-tumorigenic livers, while primary human HCC exhibited elevated Taspase1 protein (Niehof and Borlak, 2008). Furthermore, in an analysis of candidate disease genes for glioblastoma, *TASP1* transcript was enriched in glioblastoma but not in normal white matter (Scrideli et al., 2008). This is consistent with our histological examination of glioblastoma tumor sections, which exhibited up-regulation of Taspase1 protein in tumor compared to histologically normal astrocytes from the same patient (Figure 2.6 and 2.15).

Other tumor types were examined by immunofluorescence show similar increase in Taspase1 protein, including in breast (Figure 4.5) and colon adenocarcinomas (Figure 4.6) as well as in melanomas (Figure 4.7). Melanoma sections were compared to benign melanocytic nevi to gauge the difference in Taspase1 expression between benign and malignant melanocytes, using adjacent keratinocytes to normalize fluorescent signal. In all of the tumors examined, Taspase1 was localized primarily to a sub-nuclear compartment that co-localizes with the C23 marker for the nucleolus (Figure 4.5, 4.6, and 4.7). This is surprising finding since Taspase1 was initially isolated from the light membrane and S100 fractions of 293T cells (Hsieh et al., 2003a). In GFP-Taspase1 over-expressing SV40-transformed MEFs, Taspase1 is localized diffusely in the nucleus as well as concentrated in the nucleolus (data not shown). While in tumor sections, diffuse nuclear staining was in most cases low, and the presence of nucleoli nearly always accurately predicted the presence of Taspase1. What function Taspase1 plays in the nucleolus is a matter of active investigation, but possibilities include the processing of nucleolus-restricted proteolytic targets, cryptic enzymatic activity (for example, activity more akin to its evolutionary heritage as an asparaginase), or that it may serve as a scaffold for important factors or co-factors for nucleolar function. Whether Taspase1 activity is regulated is also an open matter, especially since Taspase1 seems to remain in the nucleolus in most situations, though preliminary evidence suggests that Taspase1 may re-localize given cellular stresses like DNA damage. Other work from our laboratory indicates that Taspase1 shares an interaction with DDB1 and DNAPK, further implicating a role for Taspase1 responsiveness to DNA damage.

Murine models of tumorigenesis will elucidate mechanisms of Taspase1 addiction in cancer

Examination of publicly available data from primary human samples provides some insight regarding which tumor types might depend on Taspase1 for continued propagation. As our studies demonstrate, high basal Taspase1 expression in tumors correlates with the degree of their dependence on continued Taspase1 expression. Though squamous carcinomas of the cervix and of the head and neck have markedly up-regulated Taspase1 expression, tractable murine models of tumorigenesis exist for blood tumors in which we have evidence that Taspase1 is up-regulated. This evidence was gathered from a study done by Radich and colleagues (Radich et al., 2006), which examined gene expression changes based on progression of CML from its indolent chronic phase, through the accelerated, and terminal blast crisis phases. When examining Taspase1 expression in CML progression, a pattern emerges—that Taspase1 is expressed highly specifically in blast crisis cells (Figure 4.8).

Because blast crisis is largely refractory to treatment, and because Taspase1 up-regulation suggests a developed dependence on its continued expression, we chose to examine its dependence on Taspase1 because it could potentially be an important tumor maintenance factor amenable to pharmacological inhibition. Progression to blast crisis typically involves genetic alterations that complement the BCR/ABL oncogenic tyrosine kinase translocation, which drives proliferation through multiple effectors, including RAS and PI3K/AKT. Most secondary mutations either directly or indirectly inactivate p53 or Rb, which have positive effects on survival and proliferation. Yet, it is unclear what causes the loss of differentiation observed in blast crisis—whether it is a proliferative expansion of undifferentiated blasts, or whether there is an active program causing de-differentiation (Calabretta and Perrotti, 2004). However, there is evidence that a translocation associated, albeit at low frequency, with blast crisis—NUP98/HOXA9—can cause both proliferation and differentiation block of primary human CD34+ cells (Takeda et al., 2006a). When co-expressed with BCR/ABL in primary murine bone marrow, NUP98/HOXA9 causes a short latency, de-differentiated, and transplantable leukemia reminiscent of human blast crisis (Dash et al., 2002; Neering et al., 2007).

We adopted this co-transduction model for our mice, which bear a conditional allele of *Taspase1*^{f/f} as well as Cre-recombinase under the control of an interferon-responsive Mx1 promoter (Mx1-*Cre+*; *Taspase1*^{f/f}). Bone marrow from conditional *Taspase1* mice as well as control (Mx1-*Cre+*; *Taspase1*^{+/+}) mice were subjected to retroviral transduction with a virus encoding MSCV-p210^{BCR/ABL} and MSCV-NUP98/HOXA9-IRES EGFP (vectors courtesy of M. Tomasson, Washington University in Saint Louis) and transplanted into lethally irradiated recipient mice. Tumor latency for these primary recipients was around 17-21 days. Spleens from primary recipient mice were analyzed for CD34⁺/c-Kit⁺ positive cells as well as absence of differentiated granulocytic or lymphoid markers (Mac1/Gr1 and B220/CD4/CD8, respectively), and comparable number of cells sorted for hematopoietic stem cell enriched immunophenotype (HSC, Lin⁻/Sca1⁺/Kit⁺) were injected into sub-lethally irradiated mice to synchronize the onset of disease. One week after injection, poly-I-C injections were initiated to induce *Taspase1* deletion, which was largely successful, as assessed by PCR genotyping.

We were not able to resolve a survival difference between mice bearing *Taspase1* deficient tumors and control. However, in vitro culture of leukemic blasts from the spleens of the primary transplant (the same as used for secondary transplant, Figure 4.8) exhibited a decreased ability for *Taspase1* deficient cells to survive in the long term. Murine recombinant interferon β (mIFN- β) treatment was able to induce *Taspase1* deletion in a fraction of cultured blasts, resulting in a decreased proliferation, increased cell death, and eventual loss of the *Taspase1*-deficient population (Figure 4.8). Why there was a significant portion of cells that was not responsive to in vitro mIFN- β is unclear; however, that it took roughly 35 days for *Taspase1*-wild type blasts to fully out-compete *Taspase1*-null blasts suggests that *Taspase1* deficiency causes leukemic blasts to be disadvantaged but is, alone, not sufficient to cause rapid death or severe proliferative block.

Though in vitro data shows some anti-cancer effect in leukemic blasts in vitro, the failure to observe an extension in survival could be due to a variety of reasons. Since *Taspase1* deficiency

does not kill tumor cells rapidly, leukemic blasts may still proliferate sufficiently to overwhelm the host before a therapeutic effect can take place. Alternatively, the secondary transplant may reflect a different kind of leukemia between the wild type control and the floxed conditional Taspase1 leukemia because pools of bone marrow are transduced, with transfection efficiencies that are roughly 5% for the GFP-tagged NUP98/HOXA9 and less than 0.1% likely transduced with both BCR/ABL and NUP98/HOXA9. Thus, it is unclear which cell of origin gives rise to the observed leukemia.

To address the first problem, serial transplant from secondary recipients to tertiary recipients may help resolve a difference between Taspase1-null leukemias and Taspase1-wild type. As was observed in cancer cell lines, Taspase1 loss requires additional death stimuli to achieve an appreciable gain in cell death, and this may be the case in blast crisis leukemias as well. Further characterization of BCL-2 family members, such as MCL-1 and BIM may provide insight into the possible molecular regulation of cell death in these cells, since changes in these proteins might dictate response to therapies like ABT-737 and imatinib. Decreased proliferation may be evident by staining Taspase1-deficient cells to assess actively cycling cells, while probing for expression levels of known Taspase1 regulated genes Cyclins D, E, A, and CDKs p16^{INK4A}, p21^{CIP1}, and p27^{KIP1}. BCR/ABL is known to repress p27^{KIP1} and p18^{INK4C} through activation of the PI3K pathway (Gesbert et al., 2000), while our prior work demonstrates an inverse relationship between Taspase1 function and p27 expression.

More recent studies using the BCR/ABL and NUP98/HOXA9 model of blast crisis have taken measures to ensure the generation of more homogeneous tumors. Using a *MSCV-BCR/ABL-IRES-GFP* co-transduced with *MSCV-NUP98/HOXA9-YFP* to isolated LSK cells allowed Jordan and colleagues to track and immunophenotype the leukemia initiating cells in this model as Lineage⁻/Kit⁺/Flt3⁺/Sca⁺/ CD34⁺/CD150⁻ that are simultaneously GFP and YFP double positive (Neering et al., 2007). Transduction of the LSK compartment of bone marrow limits the subtypes of cells that can give rise to leukemia, decreasing variability in the resultant phenotype.

4.3 Implications of non-oncogene addiction in cancer therapy

Non-oncogene addiction

Cancer cells exhibit deregulated signaling pathways with adaptations that overcome cellular safeguards that prevent oncogenic transformation. This “intrinsic tumor suppression” represents a pleiotropic balancing act seen in much of biology, in this case with aberrant signaling eliciting biological countermeasures to maintain homeostasis (Lowe et al., 2004). The product of tumorigenesis, then, is the phenotypic manifestation of accrued genetic and epigenetic changes that drive proliferative and survival signals, or that disarm the intrinsic anti-tumor responses. The phenomenon of oncogene addiction suggests that perturbation of this balance can be catastrophic for the tumor cell, as the signaling pathways have re-wired themselves through the natural history of the genesis of the tumor to require persistent signaling to maintain unrestricted, malignant growth (Weinstein, 2000). Though this is the concept underlying most of the current, successful targeted therapies, these therapies do not cure cancer, suggesting that just as cancers can evolve their signaling to accommodate increased proliferative drive against the balance of growth suppression and cell death, their addictions evolve away from particular apical oncogenes to other oncogenes that employ shared, or perhaps distinct, subordinate processes.

Lindquist and colleagues described a rate-limiting factor in tumorigenesis—the heat shock factor 1 (HSF1) transcription factor, which is required for efficient tumorigenesis and tumor maintenance. Deficiency in HSF1 impaired chemical skin carcinogenesis as well as a p53-mutant carcinogenesis in mice and prevented transformation of MEFs by the well-established oncogene PDGF-B. Human cancer cell lines also depend on HSF1 for continued proliferation and survival, while normal fibroblasts did not, suggesting an increased reliance on HSF1 in cancer. Concordantly, HSF1 knockout mice were also overtly normal. Lindquist and colleagues also demonstrated the involvement of HSF1 in a broad array of biological pathways, including glucose metabolism, PKA signaling, and protein translation. Importantly, HSF1 over-expression did not

drive tumorigenesis, which, like Taspase1, excludes it as a classical oncogene (Dai et al., 2007a). Increased dependence on the normal functions of cellular non-oncogenes like HSF1 was termed “non-oncogene addiction” (Solimini et al., 2007). Since tumors strongly enforce signaling to many biological processes, and thus can be thought of as cells in “overdrive,” this potentially implicates a large number of non-oncogenes which may be rate-limiting in the formation and maintenance of cancer.

Two classes of non-oncogene addiction, and likely more

The functions of HSF1 serve as a general paradigm for the action of non-oncogene addiction factors. As a transcription factor responsive to proteotoxic stress, HSF1 contributes to heat tolerance through resolution of non-native protein stress. Examination of other putative non-oncogene addiction factors formed the basis for postulating two general classes of non-oncogene addiction—one which, as a result of deficiency in the non-oncogene, lowers the general threshold of stress resistance in a cell and one that increase cellular stresses to overwhelm the supportive networks in place to permit the inherently stressful cancer state. Cancers are subjected, by their nature, to increased genotoxic, proteotoxic, oxidative, and metabolic stresses (Luo et al., 2009). Causing an imbalance in the stress state, as evidenced by HSF1 loss, can severely impede tumor growth. Even dietary restriction alone, causing metabolic stress, can hamper growth in tumors that do not constitutively activate the PI3K pathway (Kalaany and Sabatini, 2009)

Other non-oncogene addiction factors are readily discernable from the increased or altered normal cellular physiology adopted by the tumor. A recent study demonstrated that ribosomal haploinsufficiency severely impaired MYC-mediated tumorigenesis. Many cancers, to accommodate for increased proliferation and other cellular functions, have increased overall protein production as well as ribosome biosynthesis. MYC has been described to be a master regulator of multiple aspects of ribosome biogenesis and translational control (Ruggero and Pandolfi, 2003). Haploinsufficiency of ribosome subunit L24 caused total protein production to fall from its elevated state, when driven by MYC, to basal levels, which significantly prolonged the

latency to development of MYC-driven lymphomas (Barna et al., 2008). An earlier study demonstrated, conversely, that increased expression of ribosomal subunit L11 provided a negative feedback signal that down-regulated MYC activity (Dai et al., 2007b), suggesting that in abnormally driven states, perturbation of up-regulated normal cellular functions (ribosomal biogenesis in this case) can have anti-tumor effects.

Perhaps what substantiates the notion that non-oncogene addiction is relevant to cancer therapy is the clinical success of targeted inhibitors of the proteasome. The proteasome performs the crucial function of protein turnover to alleviate any potential stress caused by accumulation of expired proteins, as well as allowing proper execution of biological cascades that depend on the periodic loss of signaling molecules. Bortezomib, as discussed in Chapter 3, is a dipeptidyl boronic acid that inhibits the threonine protease function of the proteasome, which elevates the inhibitor of NF- κ B, I κ B, to prevent NF- κ B-mediated activation of pro-cancer targets, including IL-6, Cyclin D1, and MYC (Hideshima et al., 2001). Bortezomib has been used with clinical success to treat multiple myeloma (Shah and Orlowski, 2009) and a newer, cyclic peptide proteasome inhibitor Argyrin A has been demonstrated to inhibit cancer growth in a p27^{KIP1} dependent manner (Nickeleit et al., 2008).

It is interesting to note that though multiple myelomas exhibit addiction to proteasomal function, the targets of proteasome inhibition, through stabilizing the majority of cellular proteins, include both oncogenes as well as tumor suppressors. On the balance, however, proteasome inhibition exerts an anti-cancer effect. It seems, then, that a third category of non-oncogene addiction exists—one which depends on the re-activation of latent tumor suppressive mechanisms or inactivation of oncogenes. Argyrin A, as mentioned, has anti-cancer effects due to its stabilization of the cell cycle inhibitor p27, activating a latent tumor suppressor function. IRF4 is an example of a non-oncogene addiction factor causing the down-regulation of oncogenic function in multiple myeloma. IRF4 is a transcription factor involved in the maturation of antigen-stimulated B-cells to plasma cells. In multiple myeloma, IRF4 was demonstrated to participate in

a positive feedback cycle with MYC, though the repertoire of its function is broad—ranging from cell cycle regulation, metabolic control, membrane biogenesis, cell death, and differentiation. IRF4 depletion breaks this feedback and was lethal to multiple myeloma cells. Consistent with its role as a non-oncogene addiction factor, its loss had little effect on normal blood cells (Shaffer et al., 2008; Shaughnessy, 2008).

Taspase1 as a non-oncogene mediator of tumorigenesis and maintenance

Taspase1, much like IRF4, is a non-oncogene addiction factor that regulates tumor suppressor and oncogene functions. Taspase1 also orchestrates multiple developmental processes through its proteolytic regulation of MLL, which in turn maintains proper *HOX* gene expression. Taspase1 targets TFIIA and ALF also are general transcription factors likely involved in other important developmental processes (S. Sasagawa, unpublished data). This and the possibility that there are other substrates awaiting description intimates a substantial and complex repertoire of Taspase1 function. This is in keeping with current non-oncogene factors described, which are generally transcription factors (IRF4, HSF1) or members of normal cellular machinery with very general functions (the ribosome and proteasome). It is possible that this is coincidence, or that too few non-oncogene addiction factors have been validated. Alternatively, there may be some underlying reason that cells become addicted to these discreet molecular nodes that integrate broad-ranging inputs and effectors.

It is possible that the plasticity of the inputs and effectors for non-oncogene addiction factors obviates the need for tumors to select genetic mutants, because these factors are so pliable that their tumorigenic outputs are but extensions of their normal day jobs. Though they are subordinate to oncogene signaling, the transformed state still depends on the continued function of these pieces of normal cellular machinery and will depend on them to a higher degree than non-transformed cells. Yet, it may also be an eventuality that cancer, since it is a dynamic and evolving organism, will find a way to circumvent reliance on non-oncogene addiction factors in a similar way it divorces itself from apical oncogenes (Merlo et al., 2006). It has been suggested

then, as demonstrated in the case of Taspase1 inhibition (Figure 2.11), that additional “orthogonal” treatments will bolster therapeutic effects of non-oncogene addiction targeting (Luo et al., 2009). To this end, we have demonstrated that DNA damaging agents as well as the BCL-2/BCL-X_L-targeted chemotherapeutic ABT-737 cooperate strongly with Taspase1-deficiency to kill the glioblastoma cell line U251 in vitro and in vivo.

Our studies demonstrate that Taspase1 coordinates both proliferation and apoptosis in cancer cell lines via its regulation of p27^{KIP1} and MCL-1, respectively. We have also found that human tumors over-express Taspase1 likely reflecting an increased reliance on its function. Further, we show that the bioactive small molecule TASPIN-1 demonstrates specific Taspase1 inhibition and anti-tumor effects in vitro in breast adenocarcinoma and glioblastoma cell lines, and in vivo in murine tumor models. Together, this body of work places Taspase1 firmly as a promising drug target for cancer therapy, warranting further study of Taspase1 regulation and other Taspase1 effector functions, as well as the characterization and modification of new and current Taspase1 inhibitors for therapy in cancer patients.

4.4 Figures

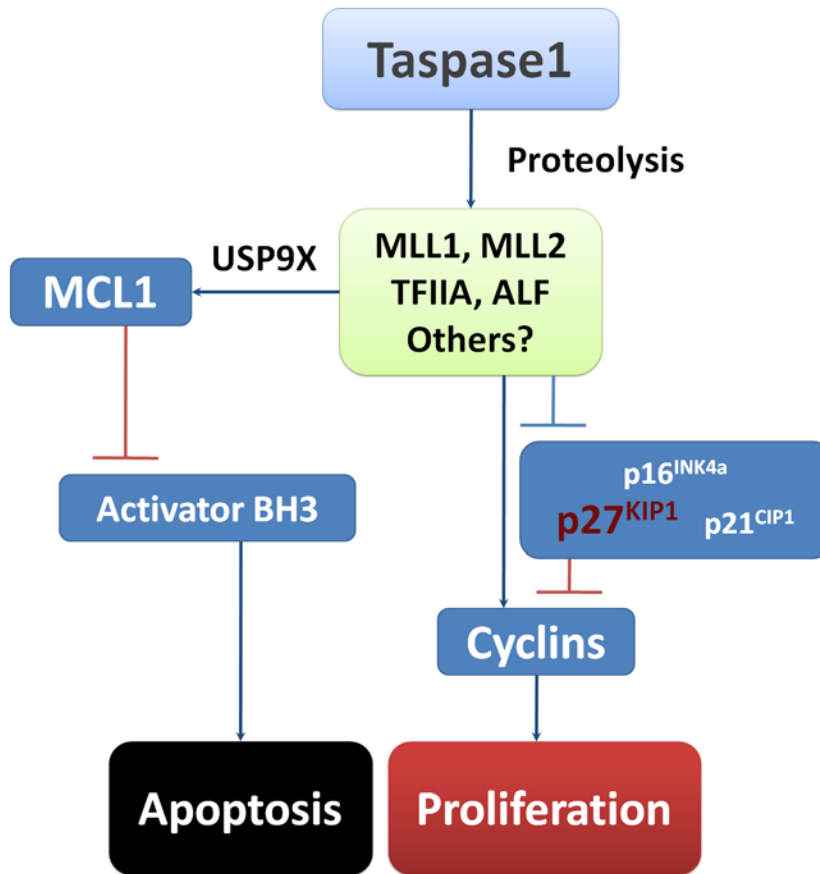


Figure 4.1. Taspase1 coordinates proliferation and apoptosis through its regulation of Cyclin-dependent kinase inhibitors (CDKIs), Cyclins, and MCL-1.

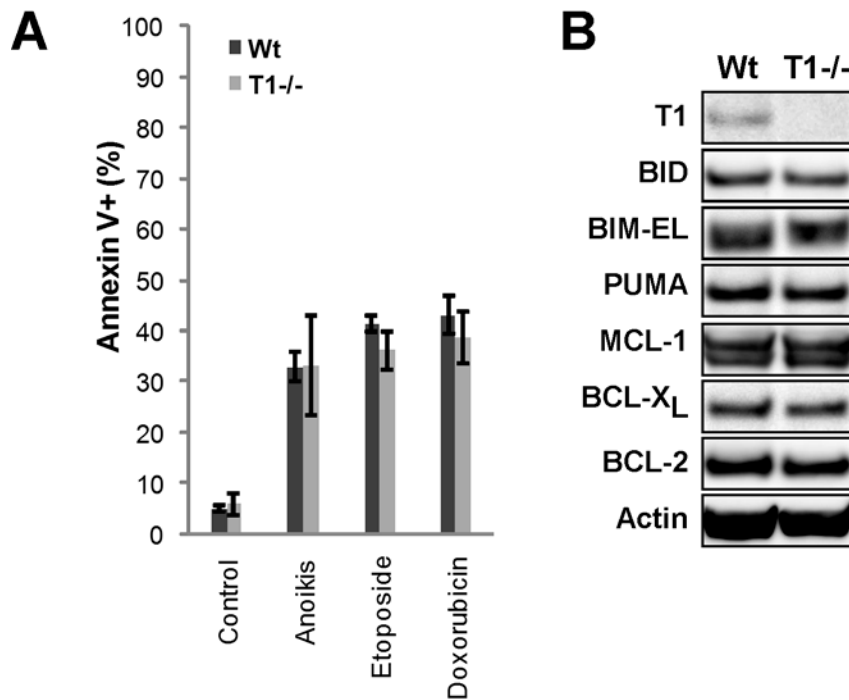


Figure 4.2. Primary MEFs are not sensitized to cell with Taspase1 deficiency.

A, Cell death was determined by Annexin V-Cy3 staining of primary MEFs subjected to various the following death stimuli – 24h detachment in 1% serum (anoikis), 24h in 100µg/mL etoposide, and 24h in 2µM doxorubicin. Control cells were adherent cells analyzed 24h after plating. **B**, Western blot analysis of pro-apoptotic BH3-only proteins Bid, Bim, and PUMA and anti-apoptotic MCL-1, BCL-X_L, and BCL-2. Equal protein loading was determined by β-Actin immunoblot.

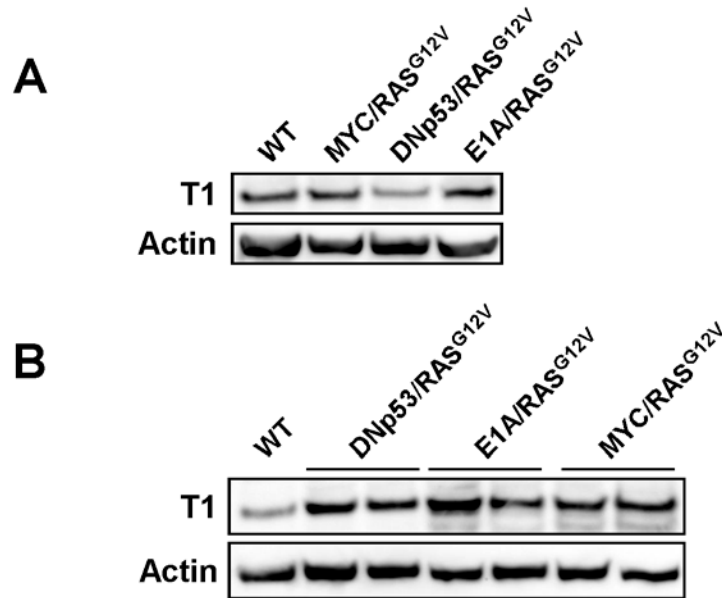


Figure 4.3. Transformed clones up-regulate Taspase1 expression

A, Primary MEFs were transduced with retroviruses encoding the oncogene pairs indicated. Immunoblot compares expression of Taspase1 in primary MEFs to oncogene transduced MEFs prior to soft agar selection. **B**, Western blot analysis of Taspase1 expression in primary MEFs compared to clones selected for their survival in soft agar culture.

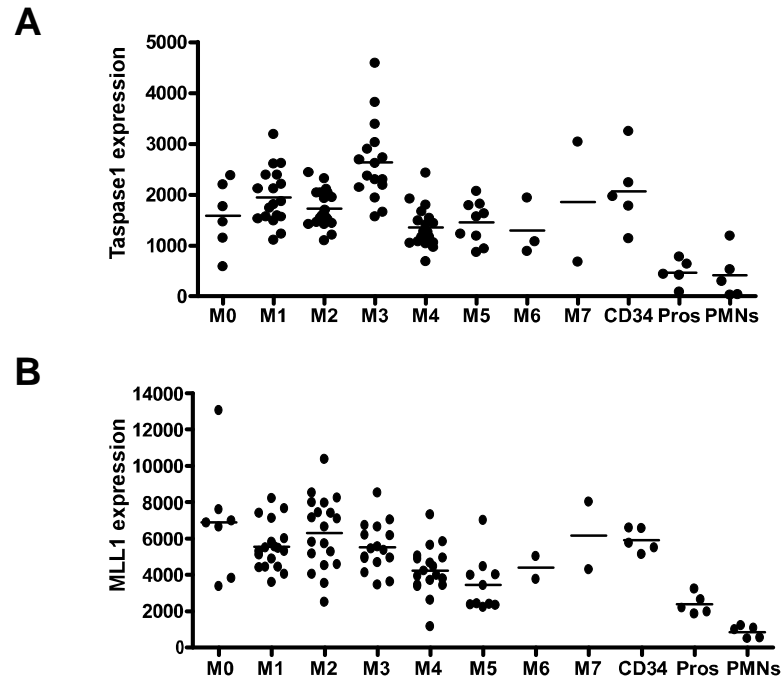


Figure 4.4. Taspase1 expression is up-regulated in subsets of blood tumors.

A, Taspase1 transcript from human leukemias designated by their FAB subtype. **B**, MLL1 transcript from human leukemias designated by their FAB subtype. Data courtesy of T. Ley and N. Grieselhuber.

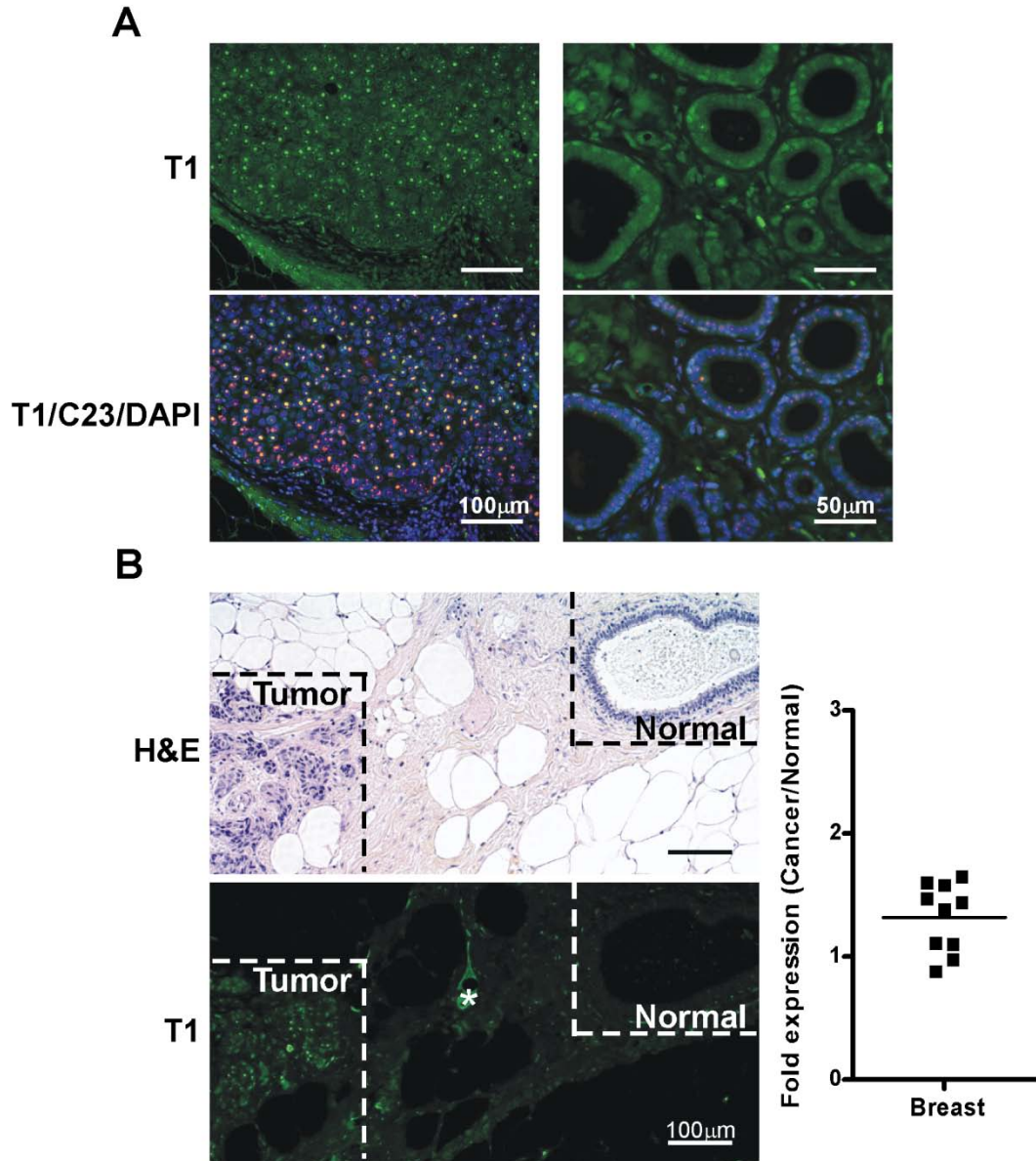


Figure 4.5. Taspase1 is over-expressed in human breast cancer.

A, Immunofluorescence analysis of Taspase1 in breast cancer (left panels) and histologically normal ducts (right panels). Taspase1 was detected using a polyclonal antibody raised against Taspase1 (DF380, Alexa-488, green), as well as nucleolar antigen C23 (Alexa-568, red), and DAPI (blue) for nuclei. The top two panels are Taspase1 staining alone, and the bottom two are merged red, green, and blue images. **B**, Breast cancer stained with a monoclonal antibody raised against Taspase1 (9G1D1, Alexa-488, green). Fluorescence intensity was quantified and compared between histologically normal and tumor tissue within the same section. The mean intensity is 1.31 (1.19-1.518, 95% CI), where intensity of normal tissue = 1.

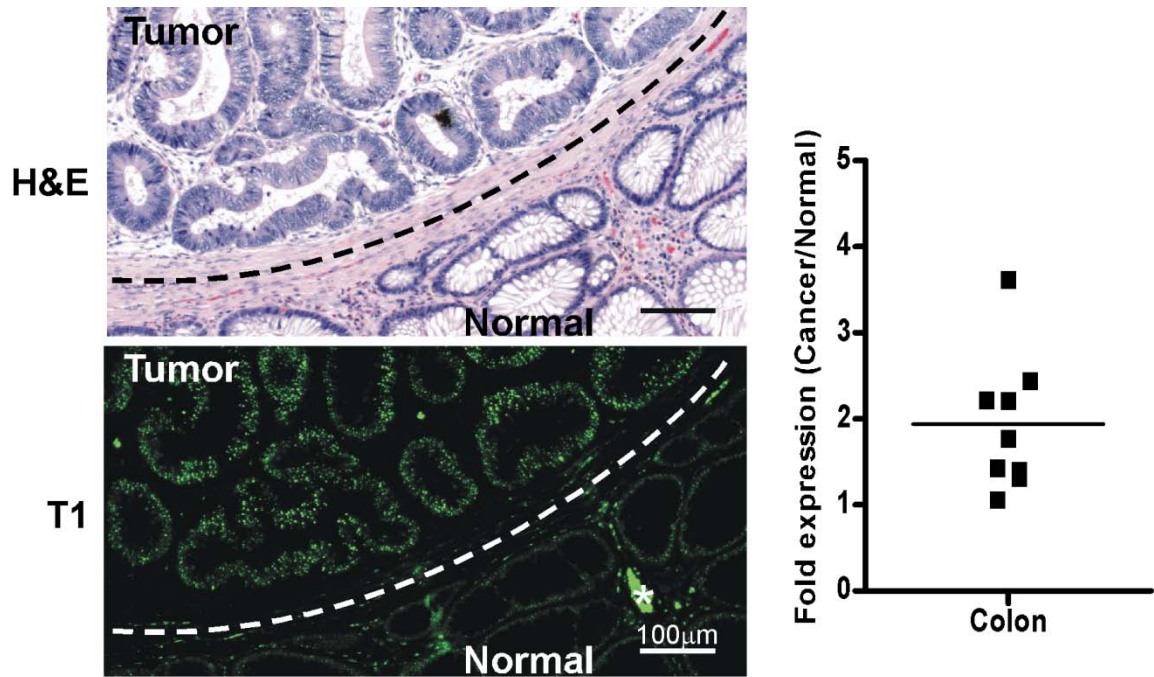


Figure 4.6. Taspase1 is over-expressed in human colon cancer.

Immunofluorescence analysis of Taspase1 in colon cancer was performed using a monoclonal antibody raised against Taspase1 (10H2F6, Alexa-488, green). Fluorescence intensity was quantified and compared between histologically normal and tumor tissue within the same section. The mean intensity is 1.94 (1.34-2.55, 95% CI), where intensity of normal tissue = 1.

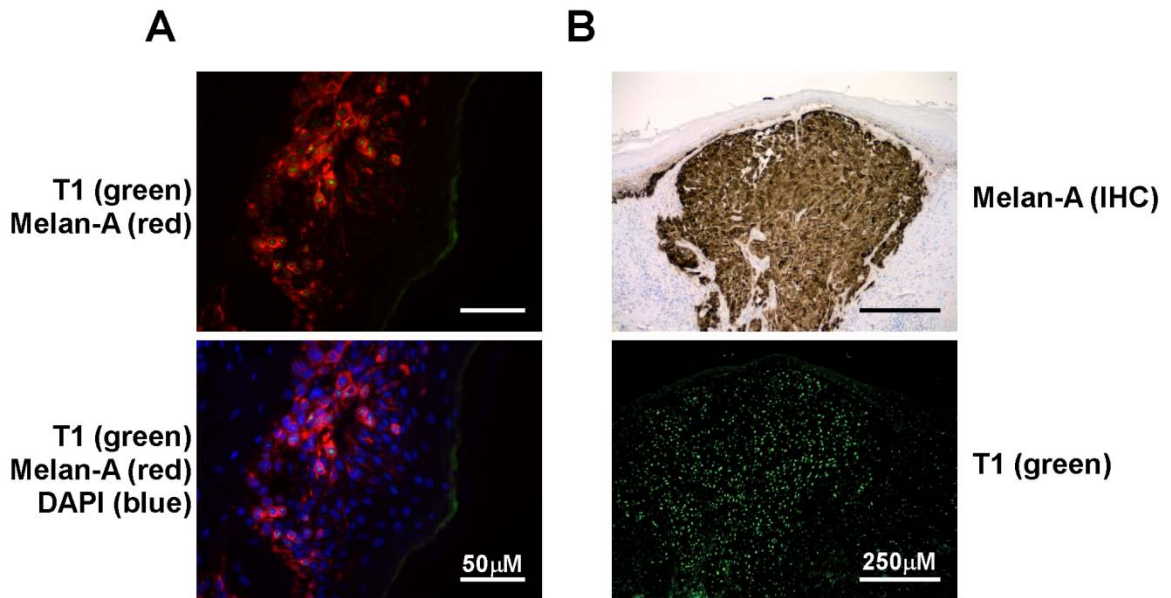


Figure 4.7. Taspase1 is highly expressed in human melanoma.

A, Immunofluorescence analysis of Taspase1 in melanoma was performed using a polyclonal antibody raised against Taspase1 (DF380, Alexa-488, green). Melan-A was detected using a monoclonal antibody (Alexa-568, red), and nuclei were visualized by DAPI stain (blue). **B**, Melan A staining of malignant melanocytes was performed by immunoperoxidase development of DAB (brown). Taspase1 was visualized by staining with a monoclonal antibody against Taspase1 (10H2F6, Alexa-488, green).

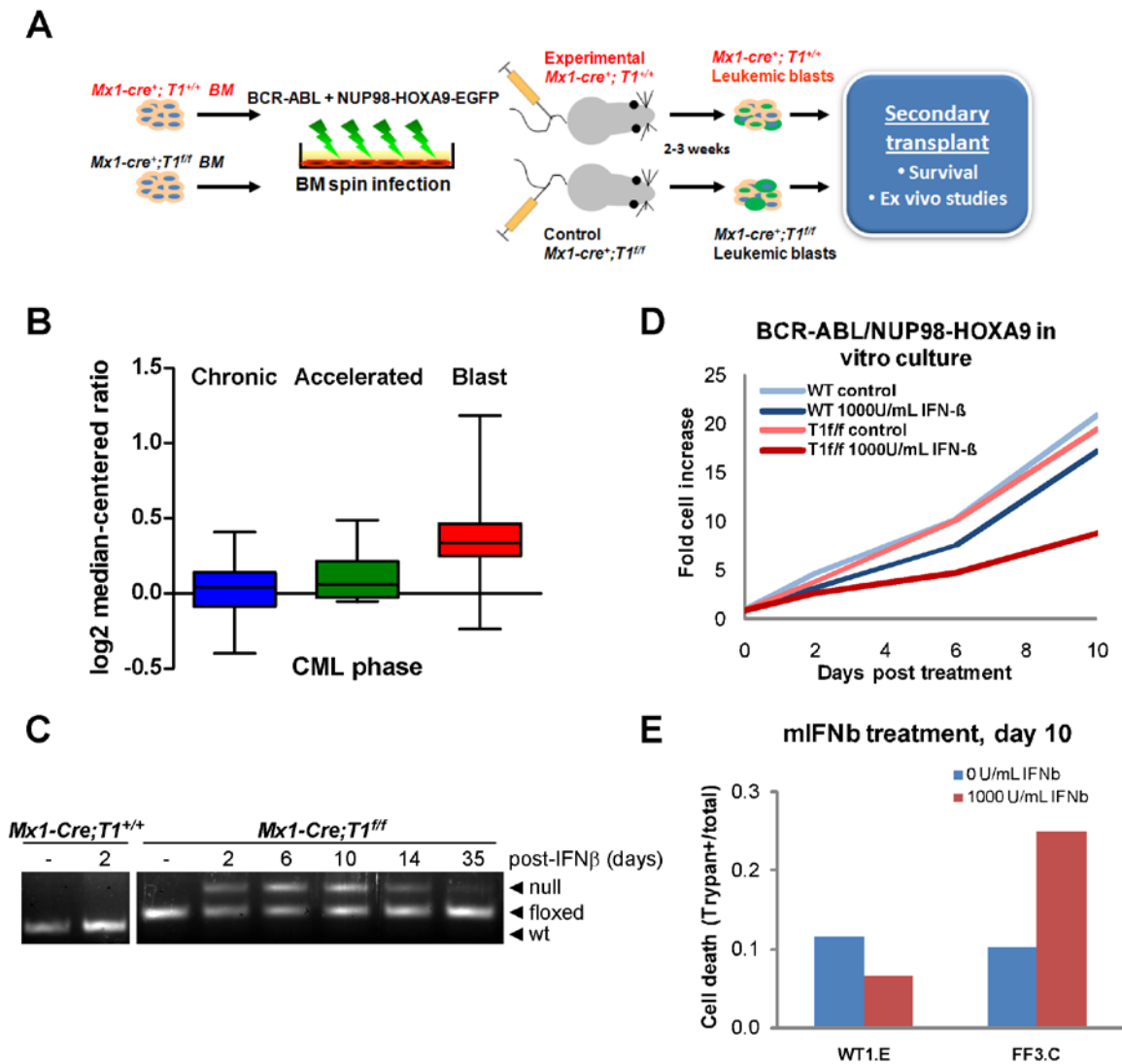


Figure 4.8. A murine model for Taspase1-dependence in CML blast crisis.

A, A schematic representation of the blast crisis model, comparing tumors derived from donor bone marrow from *Mx1-Cre* wild type and *Taspase1*^{-/-} mice. **B**, *Taspase1* transcript level from a study of 57 cases of chronic phase CML, 17 cases of accelerated phase, and 37 cases of blast crisis CML done by Radich, et al. *Taspase1* is overexpressed in blast crisis ($p=3.45 \times 10^{-9}$, statistics from www.oncomine.org). **C**, Primary transplant cells were cultured with a 2 day puls of 1000U/mL murine IFN- β in IMDM/15% FBS/50nM β -mercaptoethanol supplemented with 10ng/mL IL-3, 10ng/mL IL-6, and 100ng/mL SCF. Cre-mediated *Taspase1* deletion was assessed by PCR. **D**, Continued culture of blast crisis cells of indicated treatment and genotype were counted by Hemavet 950 (Drew Scientific, Dallas, TX). **E**, Cell death in continuous culture was determined by trypan blue exclusion.

Accession	TF name	TF gene ID	Symbol	P-value
MA0058	Max			0.0003
M00118	c-Myc:Max	4149	MAX	0.0005
M00118	c-Myc:Max	4609	MYC	0.0005
M00960	PR, GR	5241	PGR	0.0007
M00960	PR, GR	2908	NR3C1	0.0007
M00799	Myc	4149	MAX	0.0009
M00799	Myc	4609	MYC	0.0009
M00473	FOXO1	2308	FOXO1A	0.002
MA0093	USF	7391	USF1	0.0021
MA0059	Myc-Max	4609	MYC	0.0035
M00472	FOXO4	4303	MLLT7	0.0036
M00236	Arnt	405	ARNT	0.0066

Table 4.1. Promoter analysis pipeline analysis of the Taspase1 promoter.

Promoter analysis pipeline (PAP, [http://bioinformatics.wustl.edu/webTools/Home Action.do](http://bioinformatics.wustl.edu/webTools/Home_Action.do)) analysis of conserved transcription factor binding sites between mouse and human Taspase1 promoters.

REFERENCES

- Adams, J. (2004). The proteasome: a suitable antineoplastic target. *Nat Rev Cancer* 4, 349-360.
- Adams, J., Behnke, M., Chen, S., Cruickshank, A.A., Dick, L.R., Grenier, L., Klunder, J.M., Ma, Y.-T., Plamondon, L., and Stein, R.L. (1998). Potent and selective inhibitors of the proteasome: Dipeptidyl boronic acids. *Bioorganic & Medicinal Chemistry Letters* 8, 333-338.
- Adhikary, S., and Eilers, M. (2005). Transcriptional regulation and transformation by Myc proteins. *Nat Rev Mol Cell Biol* 6, 635-645.
- Aoki, K., Yoshida, T., Matsumoto, N., Ide, H., Sugimura, T., and Terada, M. (1997). Suppression of Ki-ras p21 levels leading to growth inhibition of pancreatic cancer cell lines with Ki-ras mutation but not those without Ki-ras mutation. *Mol Carcinog* 20, 251-258.
- Au, W.-Y., Tam, S., Fong, B.M., and Kwong, Y.-L. (2006). Elemental arsenic entered the cerebrospinal fluid during oral arsenic trioxide treatment of meningeal relapse of acute promyelocytic leukemia. *Blood* 107, 3012-3013.
- Ayton, P.M., and Cleary, M.L. (2001). Molecular mechanisms of leukemogenesis mediated by MLL fusion proteins. *Oncogene* 20, 5695-5707.
- Azmin, M.N., Stuart, J.F., and Florence, A.T. (1985). The distribution and elimination of methotrexate in mouse blood and brain after concurrent administration of polysorbate 80. *Cancer Chemother Pharmacol* 14, 238-242.
- Barna, M., Pusic, A., Zollo, O., Costa, M., Kondrashov, N., Rego, E., Rao, P.H., and Ruggero, D. (2008). Suppression of Myc oncogenic activity by ribosomal protein haploinsufficiency. *Nature* 456, 971-975.
- Besson, A., Dowdy, S.F., and Roberts, J.M. (2008). CDK inhibitors: cell cycle regulators and beyond. *Dev Cell* 14, 159-169.
- Beverly, L.J., and Varmus, H.E. (2009). MYC-induced myeloid leukemogenesis is accelerated by all six members of the antiapoptotic BCL family. *Oncogene* 28, 1274-1279.
- Bishop, J.M. (1983). Cellular oncogenes and retroviruses. *Annu Rev Biochem* 52, 301-354.
- Blum, G., Gazit, A., and Levitzki, A. (2000). Substrate competitive inhibitors of IGF-1 receptor kinase. *Biochemistry* 39, 15705-15712.
- Bos, J.L. (1989). ras oncogenes in human cancer: a review. *Cancer Res* 49, 4682-4689.
- Boxer, R.B., Jang, J.W., Sintasath, L., and Chodosh, L.A. (2004). Lack of sustained regression of c-MYC-induced mammary adenocarcinomas following brief or prolonged MYC inactivation. *Cancer Cell* 6, 577-586.
- Braig, M., Lee, S., Loddenkemper, C., Rudolph, C., Peters, A.H.F.M., Schlegelberger, B., Stein, H., Dorken, B., Jenuwein, T., and Schmitt, C.A. (2005). Oncogene-induced senescence as an initial barrier in lymphoma development. *Nature* 436, 660-665.
- Broadwell, R.D., Salzman, M., and Kaplan, R.S. (1982). Morphologic Effect of Dimethyl Sulfoxide on the Blood-Brain Barrier. *Science* 217, 164-166.

Brunet, A., Bonni, A., Zigmond, M.J., Lin, M.Z., Juo, P., Hu, L.S., Anderson, M.J., Arden, K.C., Blenis, J., and Greenberg, M.E. (1999). Akt promotes cell survival by phosphorylating and inhibiting a Forkhead transcription factor. *Cell* 96, 857-868.

Calabretta, B., and Perrotti, D. (2004). The biology of CML blast crisis. *Blood* 103, 4010-4022.

Capotosti, F., Hsieh, J.J., and Herr, W. (2007). Species selectivity of Mixed Lineage Leukemia/Trithorax and HCF proteolytic maturation pathways. *Mol Cell Biol* 27, 7063-7072.

Carrano, A.C., Eytan, E., Hershko, A., and Pagano, M. (1999). SKP2 is required for ubiquitin-mediated degradation of the CDK inhibitor p27. *Nat Cell Biol* 1, 193-199.

Chang, L.-W., Nagarajan, R., Magee, J.A., Milbrandt, J., and Stormo, G.D. (2006). A systematic model to predict transcriptional regulatory mechanisms based on overrepresentation of transcription factor binding profiles. *Genome Research* 16, 405-413.

Chen, L., Willis, S.N., Wei, A., Smith, B.J., Fletcher, J.I., Hinds, M.G., Colman, P.M., Day, C.L., Adams, J.M., and Huang, D.C. (2005a). Differential targeting of prosurvival Bcl-2 proteins by their BH3-only ligands allows complementary apoptotic function. *Mol Cell* 17, 393-403.

Chen, Z., Trotman, L.C., Shaffer, D., Lin, H.-K., Dotan, Z.A., Niki, M., Koutcher, J.A., Scher, H.I., Ludwig, T., Gerald, W., *et al.* (2005b). Crucial role of p53-dependent cellular senescence in suppression of Pten-deficient tumorigenesis. *Nature* 436, 725-730.

Cheng, E.H., Wei, M.C., Weiler, S., Flavell, R.A., Mak, T.W., Lindsten, T., and Korsmeyer, S.J. (2001). BCL-2, BCL-X(L) sequester BH3 domain-only molecules preventing BAX- and BAK-mediated mitochondrial apoptosis. *Mol Cell* 8, 705-711.

Chin, L., Tam, A., Pomerantz, J., Wong, M., Holash, J., Bardeesy, N., Shen, Q., O'Hagan, R., Pantginis, J., Zhou, H., *et al.* (1999). Essential role for oncogenic Ras in tumour maintenance. *Nature* 400, 468-472.

Chu, I., Sun, J., Arnaout, A., Kahn, H., Hanna, W., Narod, S., Sun, P., Tan, C.-K., Hengst, L., and Slingerland, J. (2007). p27 Phosphorylation by Src Regulates Inhibition of Cyclin E-Cdk2. *128*, 281-294.

Colomer, R., Lupu, R., Bacus, S.S., and Gelmann, E.P. (1994). erbB-2 antisense oligonucleotides inhibit the proliferation of breast carcinoma cells with erbB-2 oncogene amplification. *Br J Cancer* 70, 819-825.

Contos, J.J.A., Ishii, I., and Chun, J. (2000). Lysophosphatidic Acid Receptors. *Molecular Pharmacology* 58, 1188-1196.

Dai, C., Whitesell, L., Rogers, A.B., and Lindquist, S. (2007a). Heat shock factor 1 is a powerful multifaceted modifier of carcinogenesis. *Cell* 130, 1005-1018.

Dai, M.S., Arnold, H., Sun, X.X., Sears, R., and Lu, H. (2007b). Inhibition of c-Myc activity by ribosomal protein L11. *EMBO J* 26, 3332-3345.

Danial, N.N., and Korsmeyer, S.J. (2004). Cell Death: Critical Control Points. *116*, 205-219.

Dash, A.B., Williams, I.R., Kutok, J.L., Tomasson, M.H., Anastasiadou, E., Lindahl, K., Li, S., Van Etten, R.A., Borrow, J., Housman, D., *et al.* (2002). A murine model of CML blast crisis induced by cooperation between BCR/ABL and NUP98/HOXA9. *Proc Natl Acad Sci U S A* 99, 7622-7627.

Demo, S.D., Kirk, C.J., Aujay, M.A., Buchholz, T.J., Dajee, M., Ho, M.N., Jiang, J., Laidig, G.J., Lewis, E.R., Parlati, F., *et al.* (2007). Antitumor Activity of PR-171, a Novel Irreversible Inhibitor of the Proteasome. *Cancer Res* 67, 6383-6391.

Der, C.J., Krontiris, T.G., and Cooper, G.M. (1982). Transforming genes of human bladder and lung carcinoma cell lines are homologous to the ras genes of Harvey and Kirsten sarcoma viruses. *Proc Natl Acad Sci U S A* 79, 3637-3640.

Di Fiore, P.P., Pierce, J.H., Kraus, M.H., Segatto, O., King, C.R., and Aaronson, S.A. (1987). erbB-2 is a potent oncogene when overexpressed in NIH/3T3 cells. *Science* 237, 178-182.

Dijkers, P.F., Medema, R.H., Pals, C., Banerji, L., Thomas, N.S., Lam, E.W., Burgering, B.M., Raaijmakers, J.A., Lammers, J.W., Koenderman, L., *et al.* (2000). Forkhead transcription factor FKHR-L1 modulates cytokine-dependent transcriptional regulation of p27(KIP1). *Mol Cell Biol* 20, 9138-9148.

Dimartino, J.F., and Cleary, M.L. (1999). Mll rearrangements in haematological malignancies: lessons from clinical and biological studies. *British journal of haematology* 106, 614-626.

Ding, L., Ellis, M.J., Li, S., Larson, D.E., Chen, K., Wallis, J.W., Harris, C.C., McLellan, M.D., Fulton, R.S., Fulton, L.L., *et al.* (2010). Genome remodelling in a basal-like breast cancer metastasis and xenograft. *Nature* 464, 999-1005.

Ding, L., Getz, G., Wheeler, D.A., Mardis, E.R., McLellan, M.D., Cibulskis, K., Sougnez, C., Greulich, H., Muzny, D.M., Morgan, M.B., *et al.* (2008). Somatic mutations affect key pathways in lung adenocarcinoma. *Nature* 455, 1069-1075.

Ding, Q., He, X., Hsu, J.M., Xia, W., Chen, C.T., Li, L.Y., Lee, D.F., Liu, J.C., Zhong, Q., Wang, X., *et al.* (2007). Degradation of Mcl-1 by beta-TrCP mediates glycogen synthase kinase 3-induced tumor suppression and chemosensitization. *Mol Cell Biol* 27, 4006-4017.

Dobson, C.L., Warren, A.J., Pannell, R., Forster, A., and Rabbitts, T.H. (2000). Tumorigenesis in mice with a fusion of the leukaemia oncogene Mll and the bacterial lacZ gene. *The EMBO journal* 19, 843-851.

Domina, A.M., Vrana, J.A., Gregory, M.A., Hann, S.R., and Craig, R.W. (2004). MCL1 is phosphorylated in the PEST region and stabilized upon ERK activation in viable cells, and at additional sites with cytotoxic okadaic acid or taxol. *Oncogene* 23, 5301-5315.

Downward, J. (2003). Targeting RAS signalling pathways in cancer therapy. *Nat Rev Cancer* 3, 11-22.

Eischen, C.M., Weber, J.D., Roussel, M.F., Sherr, C.J., and Cleveland, J.L. (1999). Disruption of the ARF-Mdm2-p53 tumor suppressor pathway in Myc-induced lymphomagenesis. *Genes Dev* 13, 2658-2669.

Elofsson, M., Splittgerber, U., Myung, J., Mohan, R., and Crews, C.M. (1999). Towards subunit-specific proteasome inhibitors: synthesis and evaluation of peptide alpha',beta'-epoxyketones. *Chem Biol* 6, 811-822.

Evan, G.I., Wyllie, A.H., Gilbert, C.S., Littlewood, T.D., Land, H., Brooks, M., Waters, C.M., Penn, L.Z., and Hancock, D.C. (1992). Induction of apoptosis in fibroblasts by c-myc protein. *Cell* 69, 119-128.

- Fanidi, A., Harrington, E.A., and Evan, G.I. (1992). Cooperative interaction between c-myc and bcl-2 proto-oncogenes. *Nature* 359, 554-556.
- Felsher, D.W., and Bishop, J.M. (1999). Reversible tumorigenesis by MYC in hematopoietic lineages. *Molecular Cell* 4, 199-207.
- Fomchenko, E.I., and Holland, E.C. (2006). Mouse Models of Brain Tumors and Their Applications in Preclinical Trials. *Clinical Cancer Research* 12, 5288-5297.
- Frisch, S., and Francis, H. (1994). Disruption of epithelial cell-matrix interactions induces apoptosis. *The Journal of Cell Biology* 124, 619-626.
- Garraway, L.A., and Sellers, W.R. (2006). Lineage dependency and lineage-survival oncogenes in human cancer. *Nat Rev Cancer* 6, 593-602.
- Geng, Y., Yu, Q., Sicinska, E., Das, M., Schneider, J.E., Bhattacharya, S., Rideout, W.M., Bronson, R.T., Gardner, H., and Sicinski, P. (2003). Cyclin E ablation in the mouse. *Cell* 114, 431-443.
- Gesbert, F., Sellers, W.R., Signoretti, S., Loda, M., and Griffin, J.D. (2000). BCR/ABL regulates expression of the cyclin-dependent kinase inhibitor p27Kip1 through the phosphatidylinositol 3-Kinase/AKT pathway. *J Biol Chem* 275, 39223-39230.
- Grimmler, M., Wang, Y., Mund, T., Cilensek, Z., Keidel, E.M., Waddell, M.B., Jakel, H., Kullmann, M., Kriwacki, R.W., and Hengst, L. (2007). Cdk-inhibitory activity and stability of p27Kip1 are directly regulated by oncogenic tyrosine kinases. *Cell* 128, 269-280.
- Groll, M., Kim, K.B., Kairies, N., Huber, R., and Crews, C.M. (2000). Crystal Structure of Epoxomicin:20S Proteasome Reveals a Molecular Basis for Selectivity of α' , β' -Epoxyketone Proteasome Inhibitors. *Journal of the American Chemical Society* 122, 1237-1238.
- Gupta, G.P., Nguyen, D.X., Chiang, A.C., Bos, P.D., Kim, J.Y., Nadal, C., Gomis, R.R., Manova-Todorova, K., and Massague, J. (2007). Mediators of vascular remodelling co-opted for sequential steps in lung metastasis. *Nature* 446, 765-770.
- Hahn, W.C., Counter, C.M., Lundberg, A.S., Beijersbergen, R.L., Brooks, M.W., and Weinberg, R.A. (1999). Creation of human tumour cells with defined genetic elements. *Nature* 400, 464-468.
- Hahn, W.C., and Weinberg, R.A. (2002). Modelling the molecular circuitry of cancer. *Nat Rev Cancer* 2, 331-341.
- Hanahan, D., and Weinberg, R.A. (2000). The hallmarks of cancer. *Cell* 100, 57-70.
- Hara, T., Kamura, T., Kotoshiba, S., Takahashi, H., Fujiwara, K., Onoyama, I., Shirakawa, M., Mizushima, N., and Nakayama, K.I. (2005). Role of the UBL-UBA protein KPC2 in degradation of p27 at G1 phase of the cell cycle. *Mol Cell Biol* 25, 9292-9303.
- Harris, H. (2008). Concerning the origin of malignant tumours by Theodor Boveri. Translated and annotated by Henry Harris. Preface. *J Cell Sci* 121 Suppl 1, v-vi.
- Hemann, M.T., Bric, A., Teruya-Feldstein, J., Herbst, A., Nilsson, J.A., Cordon-Cardo, C., Cleveland, J.L., Tansey, W.P., and Lowe, S.W. (2005). Evasion of the p53 tumour surveillance network by tumour-derived MYC mutants. *Nature* 436, 807-811.

Hideshima, T., Richardson, P., Chauhan, D., Palombella, V.J., Elliott, P.J., Adams, J., and Anderson, K.C. (2001). The Proteasome Inhibitor PS-341 Inhibits Growth, Induces Apoptosis, and Overcomes Drug Resistance in Human Multiple Myeloma Cells. *Cancer Res* 61, 3071-3076.

Hoeglund, A.B., Howard, A.L., Wanjala, I.W., Pham, T.C.T., Parrill, A.L., and Baker, D.L. (2010). Characterization of non-lipid autotaxin inhibitors. *Bioorganic & Medicinal Chemistry* 18, 769-776.

Hoiby, T., Mitsiou, D.J., Zhou, H., Erdjument-Bromage, H., Tempst, P., and Stunnenberg, H.G. (2004). Cleavage and proteasome-mediated degradation of the basal transcription factor TFIIA. *The EMBO journal* 23, 3083-3091.

Hoiby, T., Zhou, H., Mitsiou, D.J., and Stunnenberg, H.G. (2007). A facelift for the general transcription factor TFIIA. *Biochim Biophys Acta* 1769, 429-436.

Hsieh, J.J., Cheng, E.H., and Korsmeyer, S.J. (2003a). Taspase1: a threonine aspartase required for cleavage of MLL and proper HOX gene expression. *Cell* 115, 293-303.

Hsieh, J.J., Ernst, P., Erdjument-Bromage, H., Tempst, P., and Korsmeyer, S.J. (2003b). Proteolytic cleavage of MLL generates a complex of N- and C-terminal fragments that confers protein stability and subnuclear localization. *Mol Cell Biol* 23, 186-194.

Hudziak, R.M., Schlessinger, J., and Ullrich, A. (1987). Increased expression of the putative growth factor receptor p185HER2 causes transformation and tumorigenesis of NIH 3T3 cells. *Proc Natl Acad Sci U S A* 84, 7159-7163.

Jacobs, J.J., Kieboom, K., Marino, S., DePinho, R.A., and van Lohuizen, M. (1999). The oncogene and Polycomb-group gene bmi-1 regulates cell proliferation and senescence through the ink4a locus. *Nature* 397, 164-168.

Jones, S., Zhang, X., Parsons, D.W., Lin, J.C., Leary, R.J., Angenendt, P., Mankoo, P., Carter, H., Kamiyama, H., Jimeno, A., *et al.* (2008). Core signaling pathways in human pancreatic cancers revealed by global genomic analyses. *Science* 321, 1801-1806.

Julien, E., and Herr, W. (2003). Proteolytic processing is necessary to separate and ensure proper cell growth and cytokinesis functions of HCF-1. *Embo J* 22, 2360-2369.

Kalaany, N.Y., and Sabatini, D.M. (2009). Tumours with PI3K activation are resistant to dietary restriction. *Nature* 458, 725-731.

Kamata, T., and Feramisco, J.R. (1984). Epidermal growth factor stimulates guanine nucleotide binding activity and phosphorylation of ras oncogene proteins. *Nature* 310, 147-150.

Kauffman-Zeh, A., Rodriguez-Viciana, P., Ulrich, E., Gilbert, C., Coffey, P., Downward, J., and Evan, G. (1997). Suppression of c-Myc-induced apoptosis by Ras signalling through PI(3)K and PKB. *Nature* 385, 544-548.

Khan, J.A., Dunn, B.M., and Tong, L. (2005). Crystal structure of human Taspase1, a crucial protease regulating the function of MLL. *Structure* 13, 1443-1452.

Kim, H., Rafiuddin-Shah, M., Tu, H.C., Jeffers, J.R., Zambetti, G.P., Hsieh, J.J., and Cheng, E.H. (2006). Hierarchical regulation of mitochondrion-dependent apoptosis by BCL-2 subfamilies. *Nat Cell Biol* 8, 1348-1358.

- Kim, H., Tu, H.C., Ren, D., Takeuchi, O., Jeffers, J.R., Zambetti, G.P., Hsieh, J.J., and Cheng, E.H. (2009). Stepwise activation of BAX and BAK by tBID, BIM, and PUMA initiates mitochondrial apoptosis. *Mol Cell* 36, 487-499.
- Konopleva, M., Contractor, R., Tsao, T., Samudio, I., Ruvolo, P.P., Kitada, S., Deng, X., Zhai, D., Shi, Y.X., Sneed, T., *et al.* (2006). Mechanisms of apoptosis sensitivity and resistance to the BH3 mimetic ABT-737 in acute myeloid leukemia. *Cancer Cell* 10, 375-388.
- Kotake, Y., Zeng, Y., and Xiong, Y. (2009). DDB1-CUL4 and MLL1 mediate oncogene-induced p16INK4a activation. *Cancer Res* 69, 1809-1814.
- Kotoshiba, S., Kamura, T., Hara, T., Ishida, N., and Nakayama, K.I. (2005). Molecular dissection of the interaction between p27 and Kip1 ubiquitylation-promoting complex, the ubiquitin ligase that regulates proteolysis of p27 in G1 phase. *J Biol Chem* 280, 17694-17700.
- Kozar, K., Ciemerych, M.A., Rebel, V.I., Shigematsu, H., Zagozdzon, A., Sicinska, E., Geng, Y., Yu, Q., Bhattacharya, S., Bronson, R.T., *et al.* (2004). Mouse development and cell proliferation in the absence of D-cyclins. *Cell* 118, 477-491.
- Krivtsov, A.V., and Armstrong, S.A. (2007). MLL translocations, histone modifications and leukaemia stem-cell development. *Nat Rev Cancer* 7, 823-833.
- Land, H., Parada, L.F., and Weinberg, R.A. (1983). Tumorigenic conversion of primary embryo fibroblasts requires at least two cooperating oncogenes. *Nature* 304, 596-602.
- Lee, J.T., Chen, D.Y., Yang, Z., Ramos, A.D., Hsieh, J.J., and Bogoy, M. (2009). Design, syntheses, and evaluation of Taspase1 inhibitors. *Bioorg Med Chem Lett* 19, 5086-5090.
- Leone, G., DeGregori, J., Sears, R., Jakoi, L., and Nevins, J.R. (1997). Myc and Ras collaborate in inducing accumulation of active cyclin E/Cdk2 and E2F. *Nature* 387, 422-426.
- Letai, A., Bassik, M.C., Walensky, L.D., Sorcinelli, M.D., Weiler, S., and Korsmeyer, S.J. (2002). Distinct BH3 domains either sensitize or activate mitochondrial apoptosis, serving as prototype cancer therapeutics. *Cancer Cell* 2, 183-192.
- Ley, T.J., Mardis, E.R., Ding, L., Fulton, B., McLellan, M.D., Chen, K., Dooling, D., Dunford-Shore, B.H., McGrath, S., Hickenbotham, M., *et al.* (2008). DNA sequencing of a cytogenetically normal acute myeloid leukaemia genome. *Nature* 456, 66-72.
- Liang, J., Zubovitz, J., Petrocelli, T., Kotchetkov, R., Connor, M.K., Han, K., Lee, J.H., Ciarallo, S., Catzavelos, C., Beniston, R., *et al.* (2002). PKB/Akt phosphorylates p27, impairs nuclear import of p27 and opposes p27-mediated G1 arrest. *Nat Med* 8, 1153-1160.
- Lim, K.H., and Counter, C.M. (2005). Reduction in the requirement of oncogenic Ras signaling to activation of PI3K/AKT pathway during tumor maintenance. *Cancer Cell* 8, 381-392.
- Liu, H., Cheng, E.H., and Hsieh, J.J. (2007). Bimodal degradation of MLL by SCF^{Skp2} and APC^{Cdc20} assures cell cycle execution: a critical regulatory circuit lost in leukemogenic MLL fusions. *Genes Dev* 21, 2385-2398.
- Liu, H., Peng, H.W., Cheng, Y.S., Yuan, H.S., and Yang-Yen, H.F. (2005). Stabilization and enhancement of the antiapoptotic activity of mcl-1 by TCTP. *Mol Cell Biol* 25, 3117-3126.

- Loonstra, A., Vooijs, M., Beverloo, H.B., Allak, B.A., van Drunen, E., Kanaar, R., Berns, A., and Jonkers, J. (2001). Growth inhibition and DNA damage induced by Cre recombinase in mammalian cells. *Proc Natl Acad Sci U S A* 98, 9209-9214.
- Lopez-Otin, C., and Hunter, T. (2010). The regulatory crosstalk between kinases and proteases in cancer. *Nat Rev Cancer* 10, 278-292.
- Lowe, S.W., Cepero, E., and Evan, G. (2004). Intrinsic tumour suppression. *Nature* 432, 307-315.
- Luo, J., Solimini, N.L., and Elledge, S.J. (2009). Principles of cancer therapy: oncogene and non-oncogene addiction. *Cell* 136, 823-837.
- Malumbres, M., and Barbacid, M. (2003). RAS oncogenes: the first 30 years. *Nat Rev Cancer* 3, 459-465.
- Martins, C.P., Brown-Swigart, L., and Evan, G.I. (2006). Modeling the therapeutic efficacy of p53 restoration in tumors. *Cell* 127, 1323-1334.
- Maurer, U., Charvet, C., Wagman, A.S., Dejardin, E., and Green, D.R. (2006). Glycogen synthase kinase-3 regulates mitochondrial outer membrane permeabilization and apoptosis by destabilization of MCL-1. *Mol Cell* 21, 749-760.
- Medema, R.H., Kops, G.J., Bos, J.L., and Burgering, B.M. (2000). AFX-like Forkhead transcription factors mediate cell-cycle regulation by Ras and PKB through p27kip1. *Nature* 404, 782-787.
- Merlo, L.M.F., Pepper, J.W., Reid, B.J., and Maley, C.C. (2006). Cancer as an evolutionary and ecological process. *Nat Rev Cancer* 6, 924-935.
- Michaloglou, C., Vredeveld, L.C.W., Soengas, M.S., Denoyelle, C., Kuilman, T., van der Horst, C.M.A.M., Majoor, D.M., Shay, J.W., Mooi, W.J., and Peeper, D.S. (2005). BRAF^{V600E}-associated senescence-like cell cycle arrest of human naevi. *Nature* 436, 720-724.
- Milne, T.A., Briggs, S.D., Brock, H.W., Martin, M.E., Gibbs, D., Allis, C.D., and Hess, J.L. (2002). MLL targets SET domain methyltransferase activity to Hox gene promoters. *Mol Cell* 10, 1107-1117.
- Mulcahy, L.S., Smith, M.R., and Stacey, D.W. (1985). Requirement for ras proto-oncogene function during serum-stimulated growth of NIH 3T3 cells. *Nature* 313, 241-243.
- Neering, S.J., Bushnell, T., Sozer, S., Ashton, J., Rossi, R.M., Wang, P.Y., Bell, D.R., Heinrich, D., Bottaro, A., and Jordan, C.T. (2007). Leukemia stem cells in a genetically defined murine model of blast-crisis CML. *Blood* 110, 2578-2585.
- Network, T.C.G.A.R. (2008). Comprehensive genomic characterization defines human glioblastoma genes and core pathways. *Nature* 455, 1061-1068.
- Nickeleit, I., Zender, S., Sasse, F., Geffers, R., Brandes, G., Sörensen, I., Steinmetz, H., Kubicka, S., Carlomagno, T., Menche, D., *et al.* (2008). Argyrin A Reveals a Critical Role for the Tumor Suppressor Protein p27kip1 in Mediating Antitumor Activities in Response to Proteasome Inhibition. *14*, 23-35.
- Niehof, M., and Borlak, J. (2008). EPS15R, TASP1, and PRPF3 are novel disease candidate genes targeted by HNF4alpha splice variants in hepatocellular carcinomas. *Gastroenterology* 134, 1191-1202.

Oltersdorf, T., Elmore, S.W., Shoemaker, A.R., Armstrong, R.C., Augeri, D.J., Belli, B.A., Bruncko, M., Deckwerth, T.L., Dinges, J., Hajduk, P.J., *et al.* (2005). An inhibitor of Bcl-2 family proteins induces regression of solid tumours. *Nature* 435, 677-681.

Opferman, J.T. (2006). Unraveling MCL-1 degradation. *Cell Death Differ* 13, 1260-1262.

Pagano, M., Tam, S.W., Theodoras, A.M., Beer-Romero, P., Del Sal, G., Chau, V., Yew, P.R., Draetta, G.F., and Rolfe, M. (1995). Role of the ubiquitin-proteasome pathway in regulating abundance of the cyclin-dependent kinase inhibitor p27. *Science* 269, 682-685.

Palomero, T., Lim, W.K., Odom, D.T., Sulis, M.L., Real, P.J., Margolin, A., Barnes, K.C., O'Neil, J., Neuberg, D., Weng, A.P., *et al.* (2006). NOTCH1 directly regulates c-MYC and activates a feed-forward-loop transcriptional network promoting leukemic cell growth. *Proceedings of the National Academy of Sciences* 103, 18261-18266.

Parada, L.F., Tabin, C.J., Shih, C., and Weinberg, R.A. (1982). Human EJ bladder carcinoma oncogene is homologue of Harvey sarcoma virus ras gene. *Nature* 297, 474-478.

Pardridge, W.M. (2005). The Blood-Brain Barrier: Bottleneck in Brain Drug Development. *NeuroRX* 2, 3-14.

Parsons, D.W., Jones, S., Zhang, X., Lin, J.C., Leary, R.J., Angenendt, P., Mankoo, P., Carter, H., Siu, I.M., Gallia, G.L., *et al.* (2008). An integrated genomic analysis of human glioblastoma multiforme. *Science* 321, 1807-1812.

Pelengaris, S., Khan, M., and Evan, G. (2002a). c-MYC: more than just a matter of life and death. *Nat Rev Cancer* 2, 764-776.

Pelengaris, S., Khan, M., and Evan, G.I. (2002b). Suppression of Myc-induced apoptosis in beta cells exposes multiple oncogenic properties of Myc and triggers carcinogenic progression. *Cell* 109, 321-334.

Pelengaris, S., Littlewood, T., Khan, M., Elia, G., and Evan, G. (1999). Reversible activation of c-Myc in skin: induction of a complex neoplastic phenotype by a single oncogenic lesion. *Mol Cell* 3, 565-577.

Pershouse, M.A., Stubblefield, E., Hadi, A., Killary, A.M., Yung, W.K., and Steck, P.A. (1993). Analysis of the functional role of chromosome 10 loss in human glioblastomas. *Cancer Res* 53, 5043-5050.

Pleasance, E.D., Cheetham, R.K., Stephens, P.J., McBride, D.J., Humphray, S.J., Greenman, C.D., Varela, I., Lin, M.-L., Ordonez, G.R., Bignell, G.R., *et al.* (2010a). A comprehensive catalogue of somatic mutations from a human cancer genome. *Nature* 463, 191-196.

Pleasance, E.D., Cheetham, R.K., Stephens, P.J., McBride, D.J., Humphray, S.J., Greenman, C.D., Varela, I., Lin, M.L., Ordonez, G.R., Bignell, G.R., *et al.* (2010b). A comprehensive catalogue of somatic mutations from a human cancer genome. *Nature* 463, 191-196.

Radich, J.P., Dai, H., Mao, M., Oehler, V., Schelter, J., Druker, B., Sawyers, C., Shah, N., Stock, W., Willman, C.L., *et al.* (2006). Gene expression changes associated with progression and response in chronic myeloid leukemia. *Proceedings of the National Academy of Sciences of the United States of America* 103, 2794-2799.

Rodriguez-Viciano, P., Warne, P.H., Dhand, R., Vanhaesebroeck, B., Gout, I., Fry, M.J., Waterfield, M.D., and Downward, J. (1994). Phosphatidylinositol-3-OH kinase as a direct target of Ras. *Nature* 370, 527-532.

Ruggero, D., and Pandolfi, P.P. (2003). Does the ribosome translate cancer? *Nat Rev Cancer* 3, 179-192.

Saarela, J., Oinonen, C., Jalanko, A., Rouvinen, J., and Peltonen, L. (2004). Autoproteolytic activation of human aspartylglucosaminidase. *Biochem J* 378, 363-371.

Samadi, N., Gaetano, C., Goping, I.S., and Brindley, D.N. (2009). Autotaxin protects MCF-7 breast cancer and MDA-MB-435 melanoma cells against Taxol-induced apoptosis. *Oncogene* 28, 1028-1039.

Santos, E., Tronick, S.R., Aaronson, S.A., Pulciani, S., and Barbacid, M. (1982). T24 human bladder carcinoma oncogene is an activated form of the normal human homologue of BALB- and Harvey-MSV transforming genes. *Nature* 298, 343-347.

Sarkisian, C.J., Keister, B.A., Stairs, D.B., Boxer, R.B., Moody, S.E., and Chodosh, L.A. (2007). Dose-dependent oncogene-induced senescence in vivo and its evasion during mammary tumorigenesis. *Nat Cell Biol* 9, 493-505.

Saunders, L.P., Ouellette, A., Bandle, R., Chang, W.C., Zhou, H., Misra, R.N., De La Cruz, E.M., and Braddock, D.T. (2008a). Identification of small-molecule inhibitors of autotaxin that inhibit melanoma cell migration and invasion. *Mol Cancer Ther* 7, 3352-3362.

Saunders, L.P., Ouellette, A., Bandle, R., Chang, W.C., Zhou, H., Misra, R.N., De La Cruz, E.M., and Braddock, D.T. (2008b). Identification of small-molecule inhibitors of autotaxin that inhibit melanoma cell migration and invasion. *Molecular Cancer Therapeutics* 7, 3352-3362.

Schwickart, M., Huang, X., Lill, J.R., Liu, J., Ferrando, R., French, D.M., Maecker, H., O'Rourke, K., Bazan, F., Eastham-Anderson, J., *et al.* (2010). Deubiquitinase USP9X stabilizes MCL1 and promotes tumour cell survival. *Nature* 463, 103-107.

Scrideli, C.A., Carlotti, C.G., Jr., Okamoto, O.K., Andrade, V.S., Cortez, M.A., Motta, F.J., Lucio-Eterovic, A.K., Neder, L., Rosemberg, S., Oba-Shinjo, S.M., *et al.* (2008). Gene expression profile analysis of primary glioblastomas and non-neoplastic brain tissue: identification of potential target genes by oligonucleotide microarray and real-time quantitative PCR. *J Neurooncol* 88, 281-291.

Sears, R., Leone, G., DeGregori, J., and Nevins, J.R. (1999). Ras enhances Myc protein stability. *Mol Cell* 3, 169-179.

Sears, R., Nuckolls, F., Haura, E., Taya, Y., Tamai, K., and Nevins, J.R. (2000). Multiple Ras-dependent phosphorylation pathways regulate Myc protein stability. *Genes Dev* 14, 2501-2514.

Serrano, M., Lin, A.W., McCurrach, M.E., Beach, D., and Lowe, S.W. (1997). Oncogenic ras provokes premature cell senescence associated with accumulation of p53 and p16INK4a. *Cell* 88, 593-602.

Shaffer, A.L., Emre, N.C., Lamy, L., Ngo, V.N., Wright, G., Xiao, W., Powell, J., Dave, S., Yu, X., Zhao, H., *et al.* (2008). IRF4 addiction in multiple myeloma. *Nature* 454, 226-231.

Shah, J.J., and Orlowski, R.Z. (2009). Proteasome inhibitors in the treatment of multiple myeloma. *Leukemia* 23, 1964-1979.

- Shaughnessy, J.D. (2008). Cancer: An unexpected addiction. *Nature* 454, 172-173.
- Sherr, C.J. (1996). Cancer Cell Cycles. *Science* 274, 1672-1677.
- Sherr, C.J., and Roberts, J.M. (1995). Inhibitors of mammalian G1 cyclin-dependent kinases. *Genes & Development* 9, 1149-1163.
- Shih, C., and Weinberg, R.A. (1982). Isolation of a transforming sequence from a human bladder carcinoma cell line. *Cell* 29, 161-169.
- Shin, I., Yakes, F.M., Rojo, F., Shin, N.Y., Bakin, A.V., Baselga, J., and Arteaga, C.L. (2002). PKB/Akt mediates cell-cycle progression by phosphorylation of p27(Kip1) at threonine 157 and modulation of its cellular localization. *Nat Med* 8, 1145-1152.
- Shoemaker, R.H. (2006). The NCI60 human tumour cell line anticancer drug screen. *Nat Rev Cancer* 6, 813-823.
- Sicinski, P., Donaher, J.L., Parker, S.B., Li, T., Fazeli, A., Gardner, H., Haslam, S.Z., Bronson, R.T., Elledge, S.J., and Weinberg, R.A. (1995). Cyclin D1 provides a link between development and oncogenesis in the retina and breast. *Cell* 82, 621-630.
- Sin, N., Kim, K.B., Elofsson, M., Meng, L., Auth, H., Kwok, B.H.B., and Crews, C.M. (1999). Total synthesis of the-potent proteasome inhibitor epoxomicin: a useful tool for understanding proteasome biology. *Bioorganic & Medicinal Chemistry Letters* 9, 2283-2288.
- Sjolander, A., Yamamoto, K., Huber, B.E., and Lapetina, E.G. (1991). Association of p21ras with phosphatidylinositol 3-kinase. *Proc Natl Acad Sci U S A* 88, 7908-7912.
- Slany, R.K., Lavau, C., and Cleary, M.L. (1998). The oncogenic capacity of HRX-ENL requires the transcriptional transactivation activity of ENL and the DNA binding motifs of HRX. *Mol Cell Biol* 18, 122-129.
- Solimini, N.L., Luo, J., and Elledge, S.J. (2007). Non-oncogene addiction and the stress phenotype of cancer cells. *Cell* 130, 986-988.
- Stratton, M.R., Campbell, P.J., and Futreal, P.A. (2009). The cancer genome. *Nature* 458, 719-724.
- Takeda, A., Goolsby, C., and Yaseen, N.R. (2006a). NUP98-HOXA9 induces long-term proliferation and blocks differentiation of primary human CD34+ hematopoietic cells. *Cancer Res* 66, 6628-6637.
- Takeda, S., Chen, D.Y., Westergard, T.D., Fisher, J.K., Rubens, J.A., Sasagawa, S., Kan, J.T., Korsmeyer, S.J., Cheng, E.H., and Hsieh, J.J. (2006b). Proteolysis of MLL family proteins is essential for *taspase1*-orchestrated cell cycle progression. *Genes Dev* 20, 2397-2409.
- Tyagi, S., Chabes, A.L., Wysocka, J., and Herr, W. (2007). E2F activation of S phase promoters via association with HCF-1 and the MLL family of histone H3K4 methyltransferases. *Mol Cell* 27, 107-119.
- van Delft, M.F., Wei, A.H., Mason, K.D., Vandenberg, C.J., Chen, L., Czabotar, P.E., Willis, S.N., Scott, C.L., Day, C.L., Cory, S., *et al.* (2006). The BH3 mimetic ABT-737 targets selective Bcl-2 proteins and efficiently induces apoptosis via Bak/Bax if Mcl-1 is neutralized. *Cancer Cell* 10, 389-399.

- Vassilev, L.T., Vu, B.T., Graves, B., Carvajal, D., Podlaski, F., Filipovic, Z., Kong, N., Kammlott, U., Lukacs, C., Klein, C., *et al.* (2004). In vivo activation of the p53 pathway by small-molecule antagonists of MDM2. *Science* 303, 844-848.
- Velu, T.J., Beguinot, L., Vass, W.C., Willingham, M.C., Merlino, G.T., Pastan, I., and Lowy, D.R. (1987). Epidermal-growth-factor-dependent transformation by a human EGF receptor proto-oncogene. *Science* 238, 1408-1410.
- Ventura, A., Kirsch, D.G., McLaughlin, M.E., Tuveson, D.A., Grimm, J., Lintault, L., Newman, J., Reczek, E.E., Weissleder, R., and Jacks, T. (2007). Restoration of p53 function leads to tumour regression in vivo. *Nature* 445, 661-665.
- Viglietto, G., Motti, M.L., Bruni, P., Melillo, R.M., D'Alessio, A., Califano, D., Vinci, F., Chiappetta, G., Tschlis, P., Bellacosa, A., *et al.* (2002). Cytoplasmic relocalization and inhibition of the cyclin-dependent kinase inhibitor p27(Kip1) by PKB/Akt-mediated phosphorylation in breast cancer. *Nat Med* 8, 1136-1144.
- Vogelstein, B., and Kinzler, K.W. (2004). Cancer genes and the pathways they control. *Nat Med* 10, 789-799.
- Vong, Q.P., Cao, K., Li, H.Y., Iglesias, P.A., and Zheng, Y. (2005). Chromosome Alignment and Segregation Regulated by Ubiquitination of Survivin. *Science* 310, 1499-1504.
- Vousden, K.H., and Lu, X. (2002). Live or let die: the cell's response to p53. *Nat Rev Cancer* 2, 594-604.
- Wei, M.C., Zong, W.X., Cheng, E.H., Lindsten, T., Panoutsakopoulou, V., Ross, A.J., Roth, K.A., MacGregor, G.R., Thompson, C.B., and Korsmeyer, S.J. (2001). Proapoptotic BAX and BAK: a requisite gateway to mitochondrial dysfunction and death. *Science* 292, 727-730.
- Weinstein, I.B. (2000). Disorders in cell circuitry during multistage carcinogenesis: the role of homeostasis. *Carcinogenesis* 21, 857-864.
- Weinstein, I.B. (2002). Cancer. Addiction to oncogenes--the Achilles heel of cancer. *Science* 297, 63-64.
- Weinstein, I.B., and Joe, A. (2008). Oncogene addiction. *Cancer Research* 68, 3077-3080.
- Woods, D., Parry, D., Cherwinski, H., Bosch, E., Lees, E., and McMahon, M. (1997). Raf-induced proliferation or cell cycle arrest is determined by the level of Raf activity with arrest mediated by p21Cip1. *Mol Cell Biol* 17, 5598-5611.
- Xia, Z.B., Anderson, M., Diaz, M.O., and Zeleznik-Le, N.J. (2003). MLL repression domain interacts with histone deacetylases, the polycomb group proteins HPC2 and BMI-1, and the corepressor C-terminal-binding protein. *Proc Natl Acad Sci U S A* 100, 8342-8347.
- Xue, W., Zender, L., Miething, C., Dickins, R.A., Hernando, E., Krizhanovskiy, V., Cordon-Cardo, C., and Lowe, S.W. (2007). Senescence and tumour clearance is triggered by p53 restoration in murine liver carcinomas. *Nature* 445, 656-660.
- Yokoyama, A., Kitabayashi, I., Ayton, P.M., Cleary, M.L., and Ohki, M. (2002). Leukemia proto-oncoprotein MLL is proteolytically processed into 2 fragments with opposite transcriptional properties. *Blood* 100, 3710-3718.

Yu, B.D., Hess, J.L., Horning, S.E., Brown, G.A., and Korsmeyer, S.J. (1995). Altered Hox expression and segmental identity in Mll-mutant mice. *Nature* 378, 505-508.

Zha, J., Weiler, S., Oh, K.J., Wei, M.C., and Korsmeyer, S.J. (2000). Posttranslational N-myristoylation of BID as a molecular switch for targeting mitochondria and apoptosis. *Science* 290, 1761-1765.

Zhang, J., Yang, P.L., and Gray, N.S. (2009). Targeting cancer with small molecule kinase inhibitors. *Nat Rev Cancer* 9, 28-39.

Zhong, Q., Gao, W., Du, F., and Wang, X. (2005). Mule/ARF-BP1, a BH3-only E3 ubiquitin ligase, catalyzes the polyubiquitination of Mcl-1 and regulates apoptosis. *Cell* 121, 1085-1095.

Zhou, H., Spicuglia, S., Hsieh, J.J., Mitsiou, D.J., Hoiby, T., Veenstra, G.J., Korsmeyer, S.J., and Stunnenberg, H.G. (2006). Uncleaved TFIIA is a substrate for taspase 1 and active in transcription. *Mol Cell Biol* 26, 2728-2735.

CURRICULUM VITAE

David Y. Chen

Medical Scientist Training Program
Washington University in Saint Louis
660 South Euclid Avenue
Saint Louis, MO 63110
chenda@wusm.wustl.edu

EDUCATION

August, 2003 – present *Washington University School of Medicine, Saint Louis, Missouri*

Doctor of Medicine (M.D., expected May 2012)

Doctor of Philosophy (Ph.D., expected May 2012), Molecular Cell Biology

Thesis: Taspase1 is a non-oncogene mediator of tumorigenesis and maintenance

Advisor: James J.-D. Hsieh, M.D., Ph.D.

September, 1999 – May 2003 *The University of Michigan, Ann Arbor, Michigan*

Bachelor of Science (B.S.), Cellular and Molecular Biology, with Distinction and High Honors

Thesis: Investigations on the mechanism underlying E-cadherin repression in breast cancer

Advisor: Eric R. Fearon, M.D., Ph.D.

Minor: Moral and Political Philosophy

RESEARCH EXPERIENCE

October, 2005 – May 2010 *Washington University School of Medicine, Saint Louis, Missouri*

Department of Medicine, Division of Molecular Oncology

Principal Investigator: James J.-D. Hsieh, M.D., Ph.D.

March 2000 – August 2003 *The University of Michigan, Ann Arbor, Michigan*

Department of Internal Medicine

Principal Investigator: Eric R. Fearon, M.D., Ph.D.

June 1999 – August 1999 *Karmanos Cancer Institute, Detroit, Michigan*

Department of Pharmacology

Principal Investigator: Ralph E. Parchment, Ph.D.

TEACHING EXPERIENCE

Fall 2006 *Washington University School of Medicine, Saint Louis, Missouri*

Philosophers in Medicine selective, curriculum development

Fall 2005 *Washington University School of Medicine, Saint Louis, Missouri*

M05 AnatNeuro 501A: "Human Anatomy and Development", teaching assistant

Summer 2002 *The University of Michigan, Ann Arbor, Michigan*

Michigan Math and Science Scholars: "A Journey through Modern Molecular Science,"
lecturer and curriculum development

Fall 2002 *The University of Michigan, Ann Arbor, Michigan*
UC260: "Law, Ethics, and the Life Sciences", teaching assistant

Fall 2001 *The University of Michigan, Ann Arbor, Michigan*
UC260: "Law, Ethics, and the Life Sciences", teaching assistant

ACADEMIC SERVICE

May 2005 - August 2008 *Washington University in Saint Louis, Saint Louis, Missouri*
Center for the Study of Ethics and Human Values, student fellow

January 2005 - June 2005 *Washington University in Saint Louis, Saint Louis, Missouri*
The Practice of Medicine II, course liason

January 2005 - June 2005 *Washington University in Saint Louis, Saint Louis, Missouri*
Lowry-Moore Academic Society, student organizer

January 2002 – May 2003 *The University of Michigan, Ann Arbor, Michigan*
Students Exploring the Life Sciences and Society (SELSS), founding president

CLINICAL EXPERIENCE

June 2005-July 2005 *Chang-Gung Memorial Hospital, Kaohsiung, Taiwan*
Departments of Cardiology and Oncology, visiting student

March 2005 *International Service Learning, Managua, Nicaragua*
Forum for International Health and Tropical Medicine service trip, volunteer

PUBLICATIONS

Chen, D.Y., Lee, Y., Van Tine, B.A., Searleman, A.C., Westergard, T., Liu, H., Tu, H.-C., Takeda, S., Lu, D., Piwnica-Worms, D.R., Oh, K.J., Hermone, A., Gussio, R., Shoemaker, R.H., Cheng, E.H., and Hsieh, J.J. A Small Molecule Inhibitor of Taspase1 Disrupts Breast and Brain Tumor Growth. *Manuscript in preparation.*

Chen, D.Y., Liu, H., Takeda, S., Tu, H.C., Sasagawa, S., Van Tine, B.A., Lu, D., Cheng, E.H., and Hsieh, J.J. (2010). Taspase1 Functions as a Non-oncogene Addiction Protease that Coordinates Cancer Cell Proliferation and Apoptosis. *Cancer Res* **70**, 5358-67.

Lee, J.T., **Chen, D.Y.**, Yang, Z., Ramos, A.D., Hsieh, J.J., and Bogyo, M. (2009). Design, syntheses, and evaluation of Taspase1 inhibitors. *Bioorg Med Chem Lett* **19**, 5086-5090.

Chen, D.Y. (2009) O Doctor Where Art Thou? Why Fewer Students Pursue Internal Medicine. *Virtual Mentor* **11**, 378-382.

Tu, H.C., Ren, D., Wang, G.X., **Chen, D.Y.**, Westergard, T.D., Kim, H., Sasagawa, S., Hsieh, J.J., and Cheng, E.H. (2009). The p53-cathepsin axis cooperates with ROS to activate programmed necrotic death upon DNA damage. *Proc Natl Acad Sci U S A* **106**, 1093-1098.

Takeda, S., **Chen, D.Y.**, Westergard, T.D., Fisher, J.K., Rubens, J.A., Sasagawa, S., Kan, J.T., Korsmeyer, S.J., Cheng, E.H., and Hsieh, J.J. (2006). Proteolysis of MLL family proteins is essential for taspase1-orchestrated cell cycle progression. *Genes Dev* **20**, 2397-2409.

Dasgupta, B., Yi, Y., **Chen, D.Y.**, Weber, J.D., and Gutmann, D.H. (2005). Proteomic analysis reveals hyperactivation of the mammalian target of rapamycin pathway in neurofibromatosis 1-associated human and mouse brain tumors. *Cancer Res* 65, 2755-2760.

Hajra, K.M., **Chen, D.Y.**, and Fearon, E.R. (2002). The SLUG zinc-finger protein represses E-cadherin in breast cancer. *Cancer Res* 62, 1613-1618.